Cape Peninsula
University of Technology

Performance of zeolite ZSM-5 synthesised from South African fly ash in the conversion of methanol to hydrocarbons

By

Leo Folifac

Thesis submitted in fulfilment of the requirements for the degree

Master of Engineering: **Chemical Engineering**

In the Faculty of Engineering

At the Cape Peninsula University of Technology

Supervisor: Prof. Tunde, V. Ojumu

Co-supervisor: Prof Leslie, F. Petrik

Bellville Campus

September 2018

DECLARATION

I, Leo Folifac, declare that the contents of this thesis represent my own unaided work, and that the thesis has not previously been submitted for academic examination towards any qualification. Furthermore, it represents my own opinions and not necessarily those of the Cape Peninsula University of Technology.

Signed **Date**

ABSTRACT

Zeolites have found applications as heterogeneous or solid catalyst in the petrochemical and refining industries. Zeolite ZSM-5 in particular is a highly siliceous solid catalyst with a porous network that consists of medium pore structure (pore openings 5-5.5 A). The solid catalyst (ZSM-5) is well known for its high temperature stability and strong acidity, which makes it an established catalyst used for different petrochemical processes such as Methanol-To-Gasoline (MTG), isomerisation, disproportionation, and cracking. Unlike in the past, the synthesis of zeolite ZSM-5 from other sources that contains silica (Si) and alumina (Al) with the addition of a template (TPBr) as a structure-directing agent is eminent. Its synthesis can be achievable from coal fly ash that is a waste material and a cheap source of Si and Al. Coal fly ash is a waste material that is produced during the combustion of coal to generate electricity. The elemental composition of coal fly ash consists of mostly SiO_2 and Al_2O_3 together with other significant and trace elements. Zeolite ZSM-5 catalyst synthesised from coal fly ash by previous authors required an excessive amount of additional source of silica even though the XRD spectra still show the presence of quartz and mullite phase in the final products. These phases prevented the use of fly ash (solid) as a precursor to synthesise zeolite ZSM-5 products. However, the synthesis of high purity zeolite ZSM-5 products by extracting silica and alumina from South African fly ash and then using it with small amounts of fumed silica was investigated

This aim was achieved by fusing fly ash (FA) with sodium hydroxide (NaOH) under hydrothermal condition set at 550 ^oC for 1 hour 30 minutes. The quartz and mullite phase observed by previous authors was digested by the fusion process. Thereafter, the treatment of fused fly ash filtrate (FFAF) with concentrated H_2SO_4 (98-99%), precipitated silica and removed Al that therefore increased the Si/Al ratio from 1.97 in fly ash (FA) to 9.5 in the silica extract (named fused fly ash extract). This route was designed to improve the quality of the final products and reduced the amount of fumed silica added to the synthesis mixture prior to hydrothermal synthesis. In this line of investigation, the process of adding fumed silica to the hydrothermal gel was optimised. H-FF1 with a Si/Al ratio of 9.5 was synthesised using the silica extract without the addition of fumed silica. Its XRD, SEM and relative crystallinity results proved that H-FF1 was inactive and hence was not further characterised and utilised in the conversion of methanol to hydrocarbons (MTH). Purer phase zeolite ZSM-5 products (H-FF2 and H-FF3) that were synthesised from silica extract with the addition of small amounts of fumed silica were characterised and successfully used in the methanol to hydrocarbons (MTH) reaction. The synthesised ZSM-5 products had different Si/Al ratio, different morphology, crystal size, BET surface area, and relative crystallinity as well as different trends in the MTH

reaction. It was also observed that H-FF2 and H-FF3 (pure phase) solid catalyst deactivated faster than the commercial H-ZSM-5 in the MTH reaction. However, the MTH conversion over H-FF2 competed with that of the commercial H-ZSM-5 within 3 hours of time on stream (TOS) but later deactivated at a faster rate. This was caused by the large crystal size and reduced BET surface area of H-FF2 when compared to the commercial H-ZSM-5. However, H-FF2 performed better than H-FF3 on stream (MTH reaction) due to its smaller crystal size and higher BET.

This study has successfully utilised a route that synthesised high purity zeolite ZSM-5 products from the South African fused fly ash extract (FFAE) with the addition of small amounts of fumed silica. The properties of the synthesised zeolite ZSM-5 products (H-FF2 and H-FF3) were similar to that of the commercial H-ZSM-5 as well as active in the MTH reaction. This promoted the utilisation of a waste material (coal fly ash) to synthesise highly siliceous zeolite ZSM-5 products that avoided the presence of mineral phases from fly ash in the final products.

KEY WORDS

Coal fly ash
Acid treatment
Zeolite ZSM-5
Fusion
Fused fly ash extract
Tetrapropylammonium bromide
Methanol-to-hydrocarbons (MTH) reaction

DEDICATION

This thesis is dedicated to my closest family members for their tremendous support throughout the course of this study:

- Simon Leo Folifac (Late Father)
- Juliana Ngimdou Folifac (Late Mother)
- Vivian Ngune Folifac (Late Sister)
- Wilson Tatianu Folifac (Brother)
- Quinta Tshafac Folifac (Sister)
- Christina Nzondia Folifac (sister)
- Bella-Rose Folifac (child)
- Perpetua Muchuchu Folifac (Fiancé)
- Anthonio Manuel Domingos (Family Friend)

ACKNOWLEDGEMENTS

I would like to thank the almighty God for the gift of life, protection, and strength throughout this study.

I would like to thank:

- My supervisor Prof T.V Ojumu for offering me the opportunity to accomplish my postgraduate studies under his supervision. I thank him for his guidance, advice, support, and patience and most importantly for believing in me. May God bless you Prof.

- My Co-supervisor Prof L.F Petrik for her tremendous support, encouragement, love, advice, financial support and the opportunity to complete my masters study through the ENS research group. For always listening to my problems and look for ways to solve them. May the almighty God continue to bless and protect you Prof.

- Dr Roland Missengue for his supportive advice and motivation towards my lab work

- Mrs Ilse Wells, Mrs Vanessa Kellerman, Mr Ralston Richards, and generally to my friends and colleagues at the Environmental Nano Science research group (ENS) for their technical and physical assistance that jointly make my research work comfortable.

- Dr Edith Beukes (University of the Western Cape), Mr Adrian Joseph (University of Western Cape), Mr David Kok (Cape Peninsular University of Technology), Mr Nicholas Laidler (University of Cape Town), Mrs Ilse Wells (university of western cape), for their help in carrying out the following analysis: NMR, SEM, FTIR, XRD, ICP and BET respectively.

- My closest family for their prayers, love and support especially my brother (Wilson Tatianu Folifac) for his tremendous financial support, love, care and guidance. May our good God always protect and bless you.

- My brothers and sister in Christ for their spiritual interference

TABLE OF CONTENT

LIST OF FIGURES

LIST OF TABLES

LIST OF ABBREVIATIONS

Abbreviations	Meaning
LGC	Low-grade coal
TPBr	Tetrapropylammonium bromide
FA	Fly ash
CFA	Coal fly ash
FFA	Fused fly ash
FFAE	Fused fly ash extract
XRD	X-ray diffraction spectroscopy
SEM	Scanning Electron Microscope
NMR	Nuclear Magnetic Resonance spectroscopy
XRF	X-ray Fluorescent Spectroscopy
BET	Brunauer Emmett-Teller
FT-IR	Fourier Transformed-Infrared Spectroscopy
ICP-OES	Inductive Coupled Plasma-Optical Emission Spectroscopy
EDS	Energy Dispersive Spectroscopy
FCC	Fluid catalytic cracking
MTH	Methanol to Hydrocarbons
C2	Ethene
C3	propene
C4	Butane
FID	Flame Ionisation Detector
GC	Gas Chromatography
H	Hematite
M	Mullite
Q	Quartz
I	Inert
IUPAC	International Union of Pure and Applied Chemistry
LOI	Loss of Ignition
SBU’s	Sub Building Units
WHSV	Weight per Hourly Space Velocity
OSDA’s	Organic Structure Directing Agents
TOS	Time On Stream
PPM	Parts per million

Na	Sodium
NaOH	Sodium Hydroxide
Si	Silicon
Al	Aluminium
Mg	Magnesium
H_2SO_4	Sulphuric acid
FID	Flame ionisation detector
FFAF	Fused fly ash filtrate
FFAE	Fused fly ash extract
Comm	Commercial

CHAPTER 1
GENERAL INTRODUCTION

1.1. Introduction

Chapter one of the present study feature the general introduction and lays down a purview of the research topic. It will also sequentially present the research problem statement, aim of the research, objectives of the research, research questions, study approach, importance of the study, and the structure of the present study.

1.2. Background

Coal fly ash is a by-product that is produced during the combustion of coal to produce energy in the form of electricity. In this line of investigation, Ahmaruzzaman, (2010) reported that about 500 million tonnes of coal fly ash is annually generated around the world. In South Africa, Eskom generated about 36.22 million tonnes of fly ash in the year 2011 due to the combustion of low grade coal in their coal-fired plants for the generation of electricity (Eskom, 2011). Above 90% of the generated fly ash is disposed in dumping sites such as fields and dumps. The increasing dumping of huge quantities of coal fly ash in dumping sites is becoming a pressing issue around the world. The by-product of coal (fly ash) contains a reasonable amount of Si, Al and Fe that is locked up in the fly ash mineral phases. Fly ash also contains toxic elements that can be pollutants to our ecosystem and ground water. Due to these disposal problems and threats caused by fly ash in our ecosystem, researchers have carried out intensive studies on how fly ash can be applicable to other processes in order to reduce the effects of dumbing on our environment. Fly ash has been used in wastewater purification (Gupta and Torres, 1998), adsorbent of flue gasses (Tsuchiai et al., 1995), construction of materials (Ahmaruzzaman, 2010), synthesis of zeolites (Babajide et al., 2012, Musyoka et al., 2012, Musyoka, 2009, Chareonpanich et al., 2004, Petrik et al., 2003, Kalyankar et al., 2011), and the treatment of acid coal mine drainage (Petrik et al., 2003). The Si and Al content in fly ash can be used as a cheap source of Si and Al towards the synthesis of zeolites since fly ash is readily available in dumps. Musyoka et al. (2009) reported the synthesis of zeolite Na-P1 while in 2010, the author reported the synthesis of zeolite A and X all from the South African fly ash. The synthesis of highly siliceous zeolite ZSM-5 from different fly ashes has also been reported. Chareonpanich et al. (2004) reported the synthesis of a cubic fly ash based zeolite ZSM-5 using the mae-moh fly ash with an excessive additional source of silica extracted from rice husk while Kalyankar et al. (2011) reported the synthesis of a fly ash based zeolite ZSM-5 product using a lignite Indian fly ash with an excessive additional source of silica from silica sol. The current study will focus on the extraction of Si and Al from fly ash that would inturn minimise the amount of silica added to the synthesis gel prior to hydrothermal crystallisation

and how the elemental composition of the hydrothermal gel would tailor the morphology of the synthesised crystals as well as their catalytic performance in the MTH reaction. Studies have reported the conventional use of different types of structure directing agent in the synthesis of high silica content zeolite ZSM-5. Petrik et al. (1995) reported the synthesis of zeolite ZSM-5 using tetrapropylamonium bromide (TPBr) as a structure-directing agent. However, Narayanan et al. (1995) reported the synthesis of zeolite ZSM-5 without utilising any form of a structure directing agent to facilitate formation. Petrik (2009) further reported that even though a structure directing agent greatly affects the formation of zeolite ZSM-5, other ions such as Na^+, K^+ etc including water can also affect the formation of zeolites and their pore size distribution. In this study, the structure-directing agent (or templating agent) that was used to aid the formation of the synthesised zeolite ZSM-5 crystals and their pore size distribution was tetrapropylammonium bromide (TPBr). This is because the level of purity of zeolite ZSM-5 crystals synthesised using a structure-directing agent increases as follows: alcohols < amines < tetrapropylammonium halide (Van der Gaag, 1987). Highly siliceous zeolite ZSM-5 has found wide application as a solid catalyst because it has strong acidity, high temperature stability as well as high silica content (Bleken et al., 2012). The pore system of zeolite ZSM-5 (made up of micropores and mesopores) plays an important role during catalysis, however they are some limitations to their pore size in allowing bigger reactants in reaching their active sites or for products to diffuse out from their active sites (Moliner, 2012). To minimise the diffusional constraints caused by restricted pore size in zeolite ZSM-5, the heterogeneous catalyst can be synthesised or modified such that a secondary pore system is generated. This will greatly enhance the activity of the catalyst especially in the petrochemical sector where a large amount of feed is processed each day to synthesise new valuable hydrocarbons from crude oil. A secondary pore network system in zeolites can be achieved using the correct cation/anion pairs (Petrik, 2009).

1.3. Research problem statement

The generation of electricity by Eskom using South African (SA) coal has resulted in about 36.22 million tonnes of fly ash (FA) produced per annum. However only a fraction of the fly ash generated has been beneficially used as intermediate or raw materials in industrial processes (5-10%). The remaining fly ash is disposed in dumps and contains traces of toxic elements that are not environmentally friendly. Most dumping sites occupy a large amount of land and require proper handling; this has raised the concern of high economic costs for their maintenance**.** Over the past 50 years, intensive investigation by researchers on the utilisation of fly ash in various processes (such as construction etc) has been conducted to minimise its effect on the environment. In this line of investigation, the synthesis of fly ash based zeolitic catalysts that can be applied in other processes such as the synthesis of hydrocarbons from alcohol will help to reduce some of the ash disposal problems. Fly ash can be used in the

synthesis of solid catalysts such as low silica zeolites (Si/Al = 1-2 = X, Y) due to its compositional similarity to natural occurring zeolites. Nonetheless in order synthesis highly siliceous fly ash based zeolites such as ZSM-5, a Si/Al ratio above 10 is required and therefore an extra source of silica is also required. Since fly ash is readily available in dumps, this by-product of coal is regarded as one of the cheapest raw materials (contains Si and Al) that can be used as a starting material in the synthesis of zeolites. Despite the potential application of fly ash in the synthesis of zeolites, the performance of the heterogeneous catalyst in some processes may be affected by undigested phases (quartz and mullite) or elements coming from fly ash. This study aims to synthesis high purity zeolite ZSM-5 products from the South African fused fly ash extract with the addition of small amounts of fumed silica as well as test the performance of the synthesised ZSM-5 catalyst in the methanol to hydrocarbons(MTH) reaction.

1.4. Aim of the research

The main aim of this study is to synthesise pure phase zeolite ZSM-5 products from the South African fly ash with the addition of small amounts of fumed silica and use the synthesised zeolite ZSM-5 catalyst to test its performance in the conversion of methanol to hydrocarbons (MTH).

1.5. Objectives of the study

- ✓ To determine the elemental composition of fly ash (starting material) so that the Si/Al ratio obtained in the fused fly ash extract can be monitored and adjusted in the synthesis mixture by adding small amounts of fumed silica.
- ✓ To synthesise high purity zeolite ZSM-5 products from the South African fused fly ash extract (FFAE) having different Si/Al ratios, different morphologies, crystal size, and BET surface area.
- ✓ Comparing the physical and chemical properties of the synthesised zeolite ZSM-5 products with that of the commercial zeolite ZSM-5
- ✓ To investigate the performance of the synthesised zeolite ZSM-5 products in the conversion of methanol to hydrocarbons.

1.6. Research questions

In order to achieve the goals (aims and objectives) of this study, the following research questions needs to find answers in the course of the current study.

- ✓ Can high purity siliceous zeolite ZSM-5 products be synthesised from fused fly ash extract (FFAE) with the addition of small amounts of fumed silica?

- ✓ What is the smallest amount of silica source (fumed silica) that can be added to the synthesis mixture of fused fly ash extract to synthesise high purity zeolite ZSM-5

- ✓ Can the Si/Al ratio or elemental composition of the hydrothermal gel play a role in tailoring the physico-chemical properties of ZSM-5 products during hydrothermal crystallisation?

- ✓ What process conditions will achieve optimum methanol to hydrocarbons conversion over the synthesised zeolite ZSM-5 catalysts?

- ✓ Can the conversion of methanol to hydrocarbons using the synthesised zeolite ZSM-5 catalyst be comparable to that of a commercial zeolite ZSM-5?

1.7. Study approach

The research approach of the current study was established after an intensive literature review of related studies from articles, thesis, books etc. By so doing, a suitable methodology of the present study was coined so that the research questions laid down in section 1.6 will be answered and the research objectives laid down in section 1.5 will be achieved. The raw material (as-received fly ash) that was utilised in order to synthesise zeolite ZSM-5 products was characterised using the following characterisation methods that include: X-ray diffraction spectroscopy (XRD), Scanning electron Microscopy (SEM), X-ray fluorescence spectroscopy (XRF), and Fourier Transformed Infrared Spectroscopy (FT-IR).

Thereafter, the analysed as-received fly ash was fused with NaOH (to form fused fly ash) in order to convert the insoluble mineral phases of the as-received fly ash to soluble mineral phases of fly ash. The fused fly ash was analysed using X-ray diffraction spectroscopy (XRD), Scanning electron Microscopy (SEM), and Fourier Transformed Infrared Spectroscopy (FT-IR). The analysed fused fly ash was mixed with distilled water at a ratio of 1 g: 4 mL for 1 hour 30 minutes followed by filtration to obtain fused fly ash filtrate (FFAF). The filtrate was then treated with concentrated H_2SO_4 (98-99 %) to precipitate silica in solution so as to remove Al and Fe that will inturn boost up the Si/Al ratio of the extract. The precipitated silica (named fused fly ash extract) was analysed using X-ray diffraction spectroscopy (XRD), Scanning electron Microscopy (SEM), Fourier Transformed Infrared Spectroscopy (FT-IR) and plasma-optical emission spectroscopy (ICP-OES). The ICP-OES results of fused fly ash extract (FFAE) provides an indication of the elemental composition or the Si/Al ratio in the extract as well as what quantity of fumed silica is required to adjust the Si/Al ratio of the synthesis gel. Thereafter,

fused fly ash extract (FFAE) was mixed with distilled water, small amounts of fumed silica (varied parameter), and tetrapropylamonium bromide as a structure directing agent. The synthesis mixture was then poured into sealed Teflon cup placed inside a steel synthesis vessel prior to hydrothermal synthesis set at 165 ^{o}C for 72 hours. Thereafter hydrothermal crystallisation, the crystallised ZSM-5 samples were then washed, dried, detemplated, ion exchanged followed by calcination in order to obtain the acid form (H-form).

In this line of investigation, the synthesised zeolite H-ZSM-5 samples were then characterised and compared with the physico-chemical properties of the commercial H-ZSM-5. The characterisation techniques include: X-ray diffraction spectroscopy analysis (XRD), Scanning Electron Microscopy (SEM), Fourier Transformed Infrared Spectroscopy (FT-IR), Brunauer-Emmett-Teller (BET) and Nuclear Magnetic resonance (NMR)

The analysed H-ZSM-5 catalysts (synthesised and commercial) were used in the conversion of methanol to hydrocarbons so that the performance of the synthesised zeolite ZSM-5 catalysts can be benchmarked against the commercial H-ZSM-5.

1.8. Importance of the study

This research aims at utilising a South African class F coal fly ash from the Arnot coal power station to synthesise highly siliceous zeolite ZSM-5 that will be applicable in the conversion of methanol to hydrocarbons. In this study, the Arnot class F fly ash was used as an initial cheap source of silica and alumina prior to the addition of fumed silica to synthesise zeolite ZSM-5 products. The synthesis of zeolite ZSM-5 from the South African fly ash by the current study was motivated by the fact that fly ash is a waste material that contains reasonable amount of Si and Al (building blocks of ZSM-5). Moreover, zeolite ZSM-5 is considered one of the most important catalyst in the chemical and petrochemical sector. During the synthesis of zeolite ZSM-5, a silica source and an alumina source is usually required. In this study, the effect of adjusting the initial source of silica and alumina (fused fly ash extract) on the elemental composition and morphology of the crystal particles was investigated. Many authors have utilised Zeolite ZSM-5 samples synthesised from pure chemicals in a series of reactions, however, the present study used zeolite ZSM-5 products synthesised from the South African fly ash (SAFA) as a solid or heterogeneous catalyst in the conversion of methanol to valuable hydrocarbons.

1.9. Structure of the present study

This study is divided into six separate chapters and that include:

- ✓ Chapter one (which is the present chapter)

- ✓ Chapter two (Literature review)
- ✓ Chapter three (experimental and analytical techniques)
- ✓ Chapter four (Characterisation of the synthesised zeolite ZSM-5 samples using the method described in chapter 3)
- ✓ Chapter five (Application of the synthesised zeolite ZSM-5 products in the conversion of methanol to hydrocarbons)
- ✓ Chapter six (conclusion and recommendations)

Chapter 1: Current chapter

The present chapter provides information on the general idea or introduction of the study

Chapter 2: Literature review related to the present study

Chapter two provides a general literature review on coal, coal fly ash, and zeolites as well as their applications. Logical ways in which zeolite ZSM-5 can be synthesised from fly ash have been thoroughly reviewed including the fusion step that can be the basis for zeolite ZSM-5 synthesis in this study. Analytical techniques used to characterise fly ash, zeolites and their synthesised products have been highlighted.

Chapter 3: Experimental and analytical techniques

This chapter provides a description on the way the starting raw material (fly ash) was handled and stored. It will also provide detailed information on the list of equipment, and the list of chemicals that were utilised during this study. It will further lay down the experimental methods that were used in the synthesis of the fly ash based zeolite ZSM-5. It will also describe the fixed bed reactor system that was used during the conversion of methanol to hydrocarbons over the synthesised ZSM-5 samples. Finally, the analytical techniques used to characterise coal fly ash, Silica extract (named fused fly ash extract), and synthesised zeolite ZSM-5 products, as well as products coming from the methanol to hydrocarbons reaction over the synthesised zeolite ZSM-5 catalysts will be discussed.

Chapter 4: Characterisation of fly ash based zeolite ZSM-5

The Characterisation results of coal fly ash (CFA), fused fly ash (FFA), fused fly ash extract (FFAE), and the synthesised fly ash based zeolite ZSM-5 products was highlighted in this chapter. The results obtained after standardising the GC used to analyse products from the MTH reaction was also presented in this chapter.

Chapter 5: Application of the synthesised zeolite ZSM-5 in the methanol to hydrocarbons (MTH) reaction.

In this chapter, the activity of the synthesised zeolite ZSM-5 products in the conversion of methanol to other valuable hydrocarbons will be compared to that of the commercial H-ZSM-5 purchased from zeolyst in order to investigate their performance.

Chapter 6: Conclusion and recommendation

This chapter draws the conclusion of this study based on the obtained results and will also recommend future work based on the results.

CHAPTER 2
LITERATURE REVIEW

2.1. Introduction

This chapter will lay down an overview of coal fly ash and its application. It will also present literature on zeolites in general and zeolite ZSM-5 in particular. Thereafter, it will present the different methods or characterisation techniques used to investigate the properties of coal fly ash and zeolites together with their applications as solid catalysts.

2.2. Coal fly ash

Coal fly ash is a waste material generated as a result of burning coal to produce electricity. Fly ash has different colours from light grey to black based on the amount of unburned carbon in the fly ash (Speight, 2015). This colour changes highlights the fact that fly ash from different sources can vary in properties and composition. Fly ash consist of fine grains that are made up of spherical glassy particles derived from the dressing method of coal before combustion or from the minerals buried in coal (Ahmaruzzaman, 2010, Kutchko and Kim, 2006). The specific gravity and specific surface area of coal fly ash ranges from 2 to 3 m^2/g and 170 to 1000 m^2/g (Crelling et al., 1986). Fly ash also has particle sizes that range from 0.5 to 200 microns (Scheetz and Earle, 1998) and contains both amorphous and crystalline components. The collection methods of fly ash as they escape from flue gas are by means of electrostatic precipitators or mechanical devices such as cyclones. Wang and Wu (2006) reported that the major elements found in coal fly ash are silica (SiO_2), alumina (Al_2O_3), and iron (Fe_2O_3).

According to Eskom, coal fired power plants generate more than 36.22 Mt/annum of fly ash with just a tiny fraction put into constructive use with the remaining dumped in fields. Fly ash is abrasive, alkaline and refractory in nature (Madzivire et al., 2010). The alkalinity and toxic elements such as Hg, U, Y, V and Sr found in fly ash causes land, water and air pollution. Akinyemi (2011) also reported that the large volumes of fly ash generated together with its leaching potential, causes huge disposal problems. Because of all the listed environmental problems caused by fly ash, researchers have carried out intensive studies on ways to improve its constructive reuse.

2.3. By products of coal combustion

The burning of coal generates by-products that are usually called coal combustion by-products (CCPs). These by-products are composed of non-combustible, inorganic residues and organics that are incompletely combusted. This depends on the mineralogy of the coal together with the physical and chemical changes during the process of combustion (Speight, 2015,

Querol et al., 2002). Some resultant by-products of coal combustion are wet bottom boiler slag, dry bottom ash, fly ash, and flue gas desulphurisation materials (Kalyoncu and Olson, 2001, Scheetz and Earle, 1998).

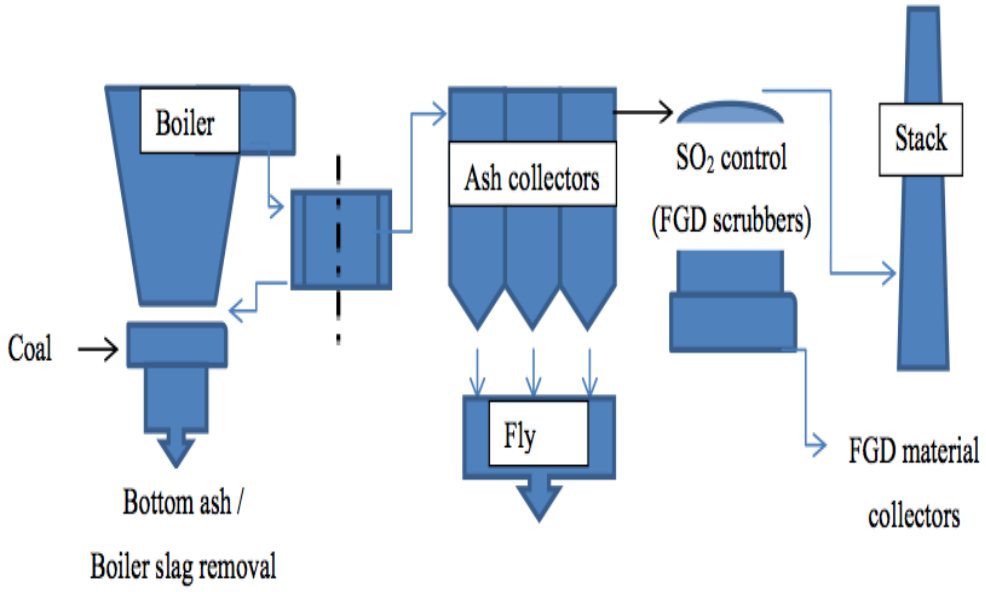

Figure 2. 1: Schematic of coal combustion by-products collection (Musyoka. 2012)

The combustion of coal in a dry bottom boiler leads to the formation of 20 % bottom ash, which is heavier, coarser and granular while 80% is fly ash (fine granular powder) that is collected by electrostatic precipitators. The boiler slag generated during coal combustion results from cyclones or slag type boilers and is made up of coarse, dense, black, glassy particles that accounts for only 2.5 % of the total amount of coal combustion by-products (CCPs). Flue gas desulphurisation materials are generated because of the process that is used to remove SO_2 from the exhaust gas of coal-fired boiler.

2.4. Coal fly ash formation

During coal combustion, one of the most abundant by-products generated is called coal fly ash. The mechanism of formation of coal fly ash is influenced by the conditions of combustion together with parameters such as the chemical composition of the coal, intrinsic reactivity, particle size, mineral matter, porosity, volatiles and ash content (Crelling et al., 1986). Coal fly ash is made up of the inorganic materials found in coal that have been fused in the process of combusting coal. These inorganic materials present in coal undergoes a physical and chemical transformation at high temperatures (1400- 1700 ^{0}C) during the thermal process to form coal fly ash (Madzivire et al., 2010) . Some of the physical transformations of the inorganic contents in coal are as follows: coalescence of individual mineral grains within a char particle, incomplete coalescence due to disintegration of the char, fragmentations of the inorganic mineral particles, and formation of cenospheres.

2.5. Physical and chemical properties of coal fly ash

The physico-chemical properties of coal fly ash together with their mineralogical composition depends on the following: type or source of coal, composition of the coal that undergo combustion, combustion system, and finally the combustion process (Bhanarkar et al., 2008, Eary et al., 1990). Before fly ash is utilised in any form of application, the fly ash has to undergo characterisation in terms of its composition, the mineral content, surface chemistry and reactivity. The composition of fly ash that is affected by the properties of the coal type and the method employed in handling and storage, plays an important role in potential recycling (Murphy et al., 1984). Table 2.1 presents chemical constituents of burning different rank of coal.

Table 2. 1: Comparison of the ranges of chemical constituents of fly ash produced from burning different ranks of coals (Adriano et al., 1980).

Components	Bituminous (mass %)	Sub-bituminous (mass %)	Lignite (mass %)
SiO_2	20-60	40-60	25-45
Al_2O_3	5-35	20-30	10-25
Fe_2O_3	10-40	4-10	4-15
CaO	1-12	5-30	15-40
MgO	0-5	1-6	3-30
SO_3	0-4	0-2	0-6
Na_2O	0-4	0-2	0-4
K_2O	0-3	0-4	0-4
LOI	0-15	0-3	0-5

The measurement of the LOI (Loss of Ignition) after coal combustion by the coal power plant is of great importance because it reports on the amount of carbon that was not burnt during the process of combustion (Koukouzas et al., 2007). The LOI result indicates if there was a complete or partial combustion of the coal and also provides enough information about the suitability of the fly ash in cement replacement in concrete. Foner et al. (1999) reported that the LOI in fly ash ranges from a value of 4 to12 %. The American Society for Testing Materials Standards (ASTM C618) categorise fly ash either as a class F or C depending on its content

of the major elements (Si, Al, and Fe). Fly ash is in the class F category when the weight percent (Wt %) of the major elements SiO_2, Al_2O_3, and Fe_2O_3 is above 70 while fly ash is classified as a class C (fly ash) when the weight percent (Wt %) of the major elements SiO_2, Al_2O_3, and Fe_2O_3 lies between 50 and 70 with a high lime content.

Table 2. 2: Fly ash classification according to chemical composition (ASTM C 618 – 95) (Scheetz and Earle, 1998).

Chemical components	**Class F fly ash**	**Class C fly ash**
Silicon dioxide (SiO_2) + Aluminium oxide (Al_2O_3) + Iron oxide (Fe_2O_3), min. %	70	50
Sulphur trioxide (SO_3), max. %	5	5
Moisture content, max. %	3	3
Loss of Ignition, max, %	6	6
Available alkali (as Na_2O)	1.5	1.5

As the percentage of CaO (lime) is not mentioned in Table 2.2, the class F fly ash has been reported to contain about 5 % CaO while the class C fly ash contains a higher proportion of CaO that ranges from 10-35 % (Ahmaruzzaman, 2010, Koukouzas et al., 2007). When a poor-quality coal, namely lignite or sub-bituminous coal undergoes a process of combustion, a class C fly ash is generated, while when a high quality coal, namely bituminous or anthracite coal, undergoes a process of combustion, a class F fly ash is generated (Adriano et al., 1980). Fly ash either has a pozzolanic or cementitious property. A class F fly ash hardens up when it reacts with $Ca(OH)_2$ and H_2O (pozzolanic in nature), meanwhile a class C fly ash exhibits a self-hardening property when it reacts with water (cementitious in nature) (Manz, 1999, Adriano et al., 1980). Putting aside the difference between a class F and C fly ash in terms of their major elements (Si, Al, Fe, and Ca), another significant difference between both of them is their percentage of alkalis and sulphates that are higher in class C fly ash than in

class F fly ash. Somerset et al. (2004) reported that South African coal fly ash has a high percentage of Si, Al, and CaO.

2.6. Application of coal fly ash

As previously stated, millions of tonnes of fly ash are generated each year and that causes serious ecological and health problems with poor management. Researchers have been looking for different ways in which this vast waste called fly ash can be utilised. According to Wang and Wu (2006), fly ash can have positive applications in different sectors. Fly ash is suitable for a particular application based on its physico-chemical properties. Fly ash has been reported to be used in the backfilling of mine voids (Skousen and Ziemkiewicz, 1995), treatment of acid mine drainage (Madzivire et al., 2011, Petrik et al., 2003), synthesis of geopolymer (Nyale et al., 2013), zeolites synthesis (Babajide et al., 2012, Musyoka et al., 2012, Chareonpanich et al., 2004, Somerset et al., 2004). Gupta et al. (2012) reported that fly ash can be utilised as soil amendment in agriculture due to its physical properties (pH, texture, holding capacity of water, bulk density together with the fact that fly ash contains essential nutrients for plants). Fly ash can be utilised in the treatment of wastewater by removing heavy metal, organic matters and colour (Viraraghavan, 1993). The extraction of alumina with the use of sulphuric acid from fly ash has been reported (Nyale et al., 2013) . Shcherban et al., 1995 also reported the extraction of Al, Fe, and Si from the fly ash waste. In the construction sector, fly ash has been used for construction due to its pozzolanic property at ordinary temperature (fly ash + $Ca(OH)_2$ + H_2O). This process saves costs since fly ash is abundant in dumping fields (Foner et al., 1999). Davini (1996) reported the removal of SO_2 and NO_X from flue gases. Even though fly ash has been utilised in a significant number of applications, it is still a major problem in our ecosystem and health. Therefore, researchers are still looking for other beneficial routes in which fly ash can be applicable. In this line of investigation, this study focuses on the synthesis of zeolite ZSM-5 from the South African fly ash (source of Al and Si) and its application as solid catalyst in the methanol to hydrocarbons (MTH) reaction. Zeolite ZSM-5 is one of the most important solid acid catalysts in the petrochemical industry in cracking hydrocarbons and has also been used in the synthesis of hydrocarbons from alcohol. Figure 2.2 summarises the applications of fly ash in different sectors (Wang and Wu, 2006).

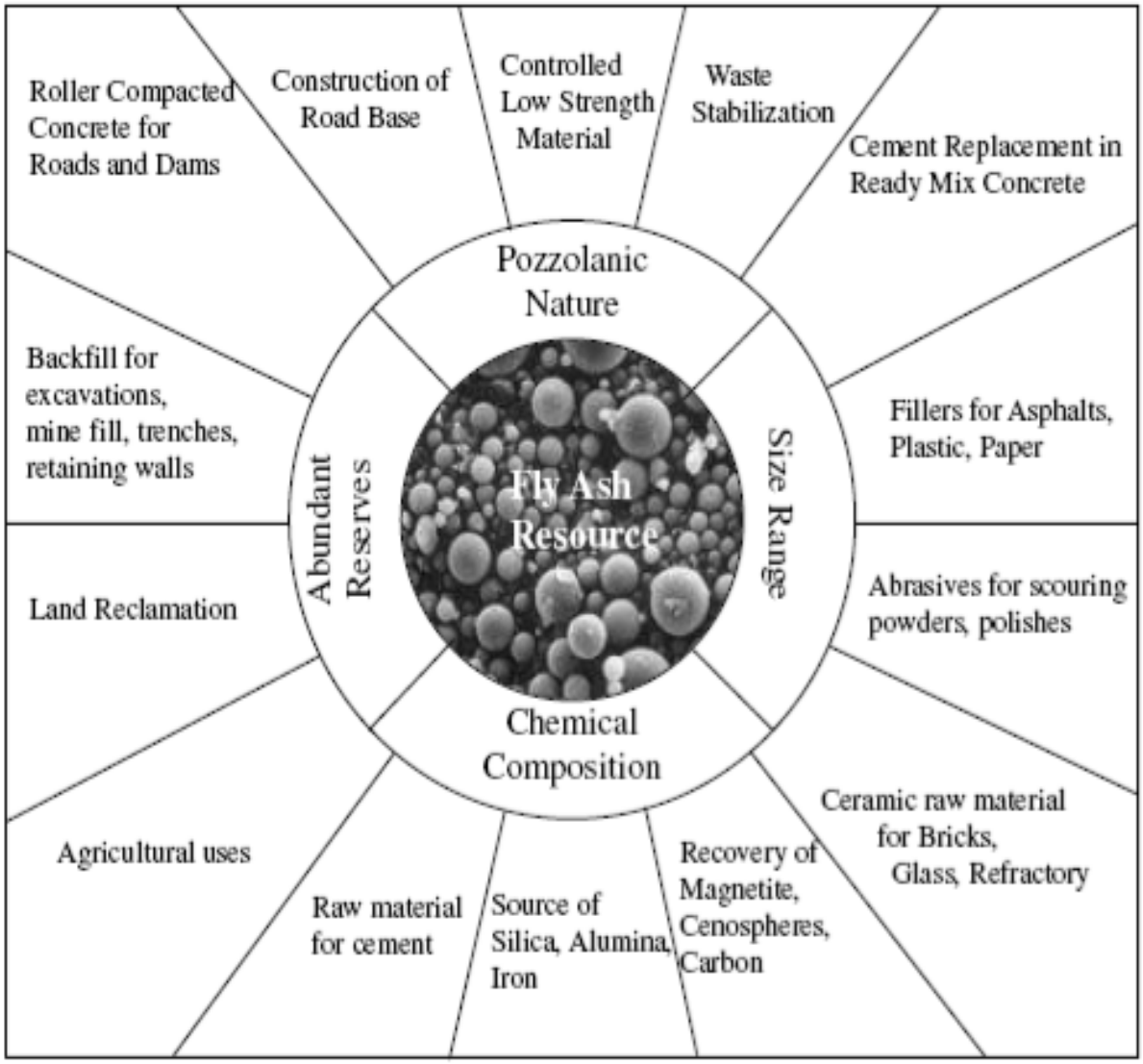

Figure 2. 2: Summary of the possible applications of fly ash (Wang and Wu, 2006)

2.7. Zeolites

The science of zeolites is a vast area of research by many scientists with published patents and articles. In this section, the general aspects of zeolites and the use of fly ash in the synthesis of zeolites will be discussed together with their application as a solid acid catalyst.

2.7.1. History of zeolites

In 1756, a Swedish mineralogist, AF Crönstedt, brought into existence the word zeolite when he discovered a porous mineral that had boiling effects upon heating it in a blowpipe flame (Crönstedt, 1756: referenced in, (Colella and Gualtieri, 2007). The meaning of the word zeolite comes from a combined Greek word, with “zeo” meaning to boil and “lithos” meaning a stone (Byrappa and Yoshimura, 2001). After the discovery of the porous mineral termed zeolite between 1777 and 1800, many scientists further investigated other unique properties of the

mineral such as adsorption, dehydration and reversible cation exchange. In this same line of investigation, St Claire Deville in the year 1862 succeeded to hydrothermally synthesised the first zeolite named levynite (Flanigen et al., 2010). It was reported by Friedel (1896) and Grandjean (1910) that dehydrated zeolites were able to adsorb liquids and gases such as alcohols, benzene, and chloroform as well as gases such as air, hydrogen and ammonia. The authors finally concluded that dehydrated zeolites have an open framework. Further exploring the properties of zeolites, Weigel and Steinhoff (1925) reported the first molecular selectivity within the open framework of zeolites. They reported that the open framework of chabazite was selective to adsorb H_2O, methanol, formic acid and ethanol while the open framework of chabazite was selective to neither acetone nor benzene. Akinyemi (2011) reported the single crystal structure of analcite while Barrer (1945) reported the molecular size of zeolites in order classify zeolites for the first time. Different zeolites that have commercial applications such as zeolite A, X, and Y came into existence between 1949 and 1954 and their first applications were in the drying of refrigerator gas and natural gas. In the year 1962 and 1969 zeolite X was used as a heterogeneous catalyst for hydrocarbon cracking by Exxon Mobil (Flanigen et al., 2010). Finally, Barrer and Denny reported the synthesis of highly siliceous zeolites such as ZSM-5 and beta by introducing an organic templating agent (tetra-ammonium cations). From there on in the late 1960s Mobil oil used this templating agent in the synthesis of zeolites such as ZSM-5, ZSM-12, ZSM-11 (Cejka, 2007). Most of the very first synthetic zeolites were synthesised by the early authors using chemical reactants, some of the late researchers have proven that zeolites can be synthesised from a feedstock that contains silica and alumina. Kuwahara et al. (2010) succeeded to synthesise both zeolite A and X from a furnace slag having a mass percent (%) of 34.58 of SiO_2 and 14.78 % of Al_2O_3 while Atta et al. (2007) synthesised zeolite X and Y from kaolin clay having a mass % of 47.30 % of SiO_2 and 36.80 % of Al_2O_3.

2.7.2. Zeolites structure

Zeolites can be defined as highly porous crystalline aluminosilicates with a three-dimensional structural framework of SiO_4 and AlO_4 that are tetrahedrally bonded at the corners by sharing an oxygen atom (Auerbach et al., 2003, Weitkamp et al., 1999). In the context of the zeolite structure, T is the tetrahedrally coordinated atom where T can be either Si or Al, making up a network that is three dimensional with voids and open spaces. When Al (III) replaces Si (IV) in the structure, the +3 charge of the Al causes the framework to have a negative charge that needs to be counter-balanced by extra-framework cations in order to maintain an overall neutral structure. The extra-framework cations can be exchanged by an acid solution through a process known as ion exchange. The AlO^-_4 tetrahedral can also be substituted by other elements having 3 or 4 valence ions namely B, Ga, Fe, Ge, Ti, etc. (Chester and Derouane, 2009). Zhao et al. (1997) reported that the three dimensional structure of zeolites are formed

when SiO_4 and AlO_4 are combined according to Lowenstein's rule which states that two like tetrahedra such as AlO_4 experience the same electrostatic repulsions due to negative charges and therefore cannot be linked by an oxygen bridge (Zhao et al., 1997). Figure 2.3 presents the manner in which the primary building blocks combine to form a zeolite structure.

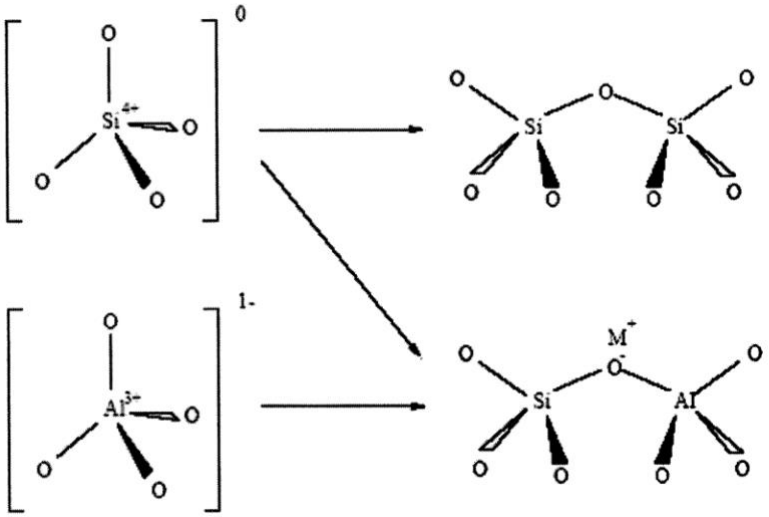

Figure 2. 3: Primary building block of zeolites (Musyoka et al., 2012)

The formula that represents the proportions of elements for a zeolite without representing the arrangement or the number of atoms is represented in equation 2.1

$$M^{n+}_{x/n}\ Al_x\ Si_{1-x}\ O_2.\ yH_2O \quad \text{..... Equation 2.1}$$

Where x = 0 to 0.5, M^n+= compensating exchangeable cation (such as alkali, alkali earth metals or alkylammonium cation (Wright and Lozinska, 2011), y= number of H_2O molecules. Metal ions with three or four valence electrons such as B, Ga, Fe, Ge, and Ti etc. can be used to replace Al^{3+} in the zeolite structure (Chester and Derouane, 2009). In zeolites, the primary building units (PBUs) are made up of silicate and aluminate tetrahedra that later link up to form the secondary-building units (SBUs) that lead to the formation of the zeolite framework structure. The black dots at the corner of the polyhedral in Figure 2.4 show the positions of the tetrahedral atoms (Wright and Lozinska, 2011).

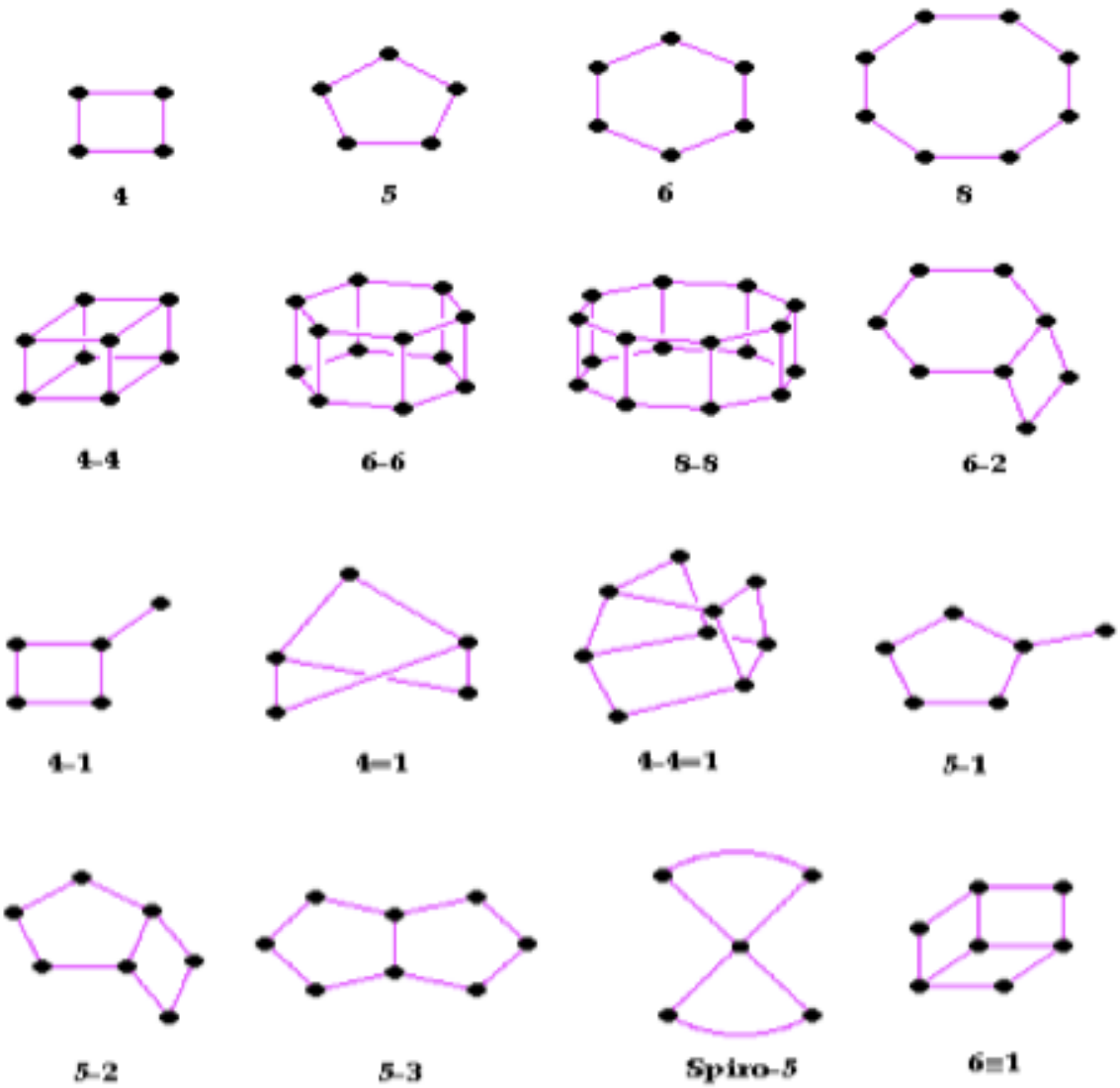

Figure 2. 4: Secondary-building units: the corners of the polyhedra represent tetrahedral atoms (Nagy et al., 1998)

2.7.3. Properties of zeolites

The ion exchanging ability in zeolites is one of the most important properties that comes from the presence of extra framework charge balancing cations. These cations (extra framework cation) may vary from one structure to the next structure. Zeolites such as A, X or chabazite with low silica value, can be completely ion exchanged (Wright and Lozinska, 2011). When zeolites are ion exchanged (protonated), they become acidic because of the presence of Brönsted acid sites that can become Lewis acid sites in the course of losing a molecule of H_2O as shown in Figure 2.5.

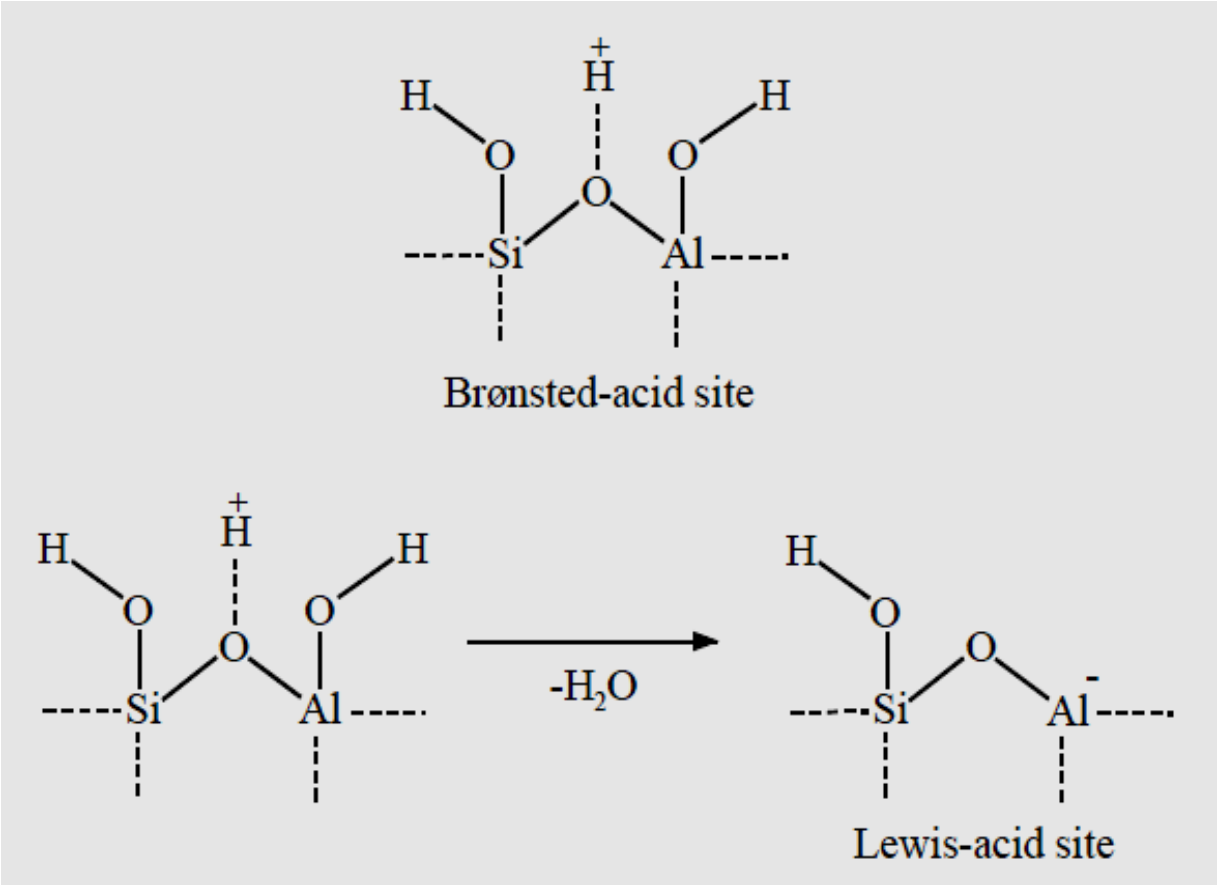

Figure 2. 5: Schematic of Brönsted and Lewis acid sites (Barzetti et al., 1996)

The open framework in zeolites allows zeolites to be subjected to reversible hydration and dehydration. When zeolites are dehydrated, the manner in which the cations are coordinated is greatly reduced and therefore favours the coordination of oxygen atoms with silica and aluminium at the corners of the structure (Wright and Lozinska, 2011). Electrical conductivity in zeolites is as a result of the possible migration of cations through the zeolite framework (Nagy et al., 1998). Zeolites have different pore sizes and shapes that are interconnected with the help of cages and channels (build up by SiO_2 and Al_2O_3) that allow zeolites to selectively adsorb some molecules (Davis, 2002)

2.7.4. Formation of zeolites

There are many different types of natural occurring zeolites as well as synthetic zeolites (synthesised in the laboratory). Scientists have discovered about 40 zeolites that occur naturally on the earth crust while more than 140 synthetic zeolites have been synthesised in the laboratory (Amber et al., 2013). Due to intensive research carried out by scientists in the field of synthetic zeolites, more zeolites have been identified especially after aluminophosphate zeolites were synthesised by Wilson et al., (1982).

a) Natural zeolites and their formation

Zeolites that occur naturally are usually formed at high temperature in the presence of H_2O. They are also usually found in an environment where magmatic activity has taken place or is still taken place. Some of the possible routes that synthetic zeolites can be formed are listed in this section (Chester and Derouane, 2009): Formations which are due to the results of low grade burial metamorphism, deposits as a result of hydrothermal or low-temperature alteration of marine sediments, crystals resulting from hydrothermal or hot-spring activity that involves reactions of solutions and basaltic lava flows, deposits that are formed from volcanic sediments in closed alkaline and saline lake systems, formation from open lake or ground water systems that acts on volcanic sediments. Chester and Derouane (2009) reported that the mentioned routes that lead to the formation of naturally occurring zeolites operate in systems that are open and are dependent on variables such as temperature, pressure, and time. Nevertheless, naturally occurring zeolites are hardly suitable for commercial purposes due to the fact they are most of the time contaminated by other minerals.

b) Synthetic zeolites

When scientists investigated how naturally occurring zeolites were formed, they were inspired to duplicate the conditions of formation and synthesise other zeolites in the laboratory. The only factor scientists could not duplicate was time, since it took so many years in nature (Chester and Derouane, 2009). All synthetic zeolites were synthesised under hydrothermal conditions with temperature that ranges between 45 ^{o}C and 200 ^{o}C (Musyoka et al., 2012, Moliner, 2012).

The general routes by which synthetic zeolites are made are presented in Table 2.3 (Chester and Derouane, 2009)

Table 2. 3: Preparatory processes of zeolites (Chester and Derouane, 2009)

Synthesis	Reactants	Products
Hydrogel	Reactive oxides, soluble silicates,	High purity powder preforms zeolites in the gel mix
Clay conversion	Raw kaolin, metakaolin, calcined Kaolin, soluble silicate, caustic Sodium, chloride	Low high purity powder binderless, preform zeolite in clay, derived matrix
Others	Natural SIO_2, acid treated clay, Amorphous mineral, volcanic glass, Caustic, $Al_2O_3.3H_2O$	Low to high purity powder, zeolite on ceramic support. Binderless preforms

Zeolitisation is a very complex chemical process that is used in the synthesis of zeolites (Hay and Sheppard, 2001). Barrer et al. (1959) Was the one who reported the first proposed mechanism on the Zeolitisation process. Porous zeolites are formed from the secondary-building units with the addition of either silica or alumina tetrahedra. After the proposed mechanism by Barrer et al. (1959), it was later reported that these mechanisms deal with the conversion of reactants in the amorphous form to crystalline products (Martínez and Pérez-Pariente, 2011). Until date the precise mechanism of Zeolitisation has not been reported (Cubillas and Anderson, 2010).

The formation of zeolites involves mechanisms that are very complex. This can be attributed to the plethora of chemical reactions, equilibria, and solubility variations that happens during the crystallisation process (Byrappa and Yoshimura, 2001). They are three main processes that are involved during the synthesis of zeolites, namely, induction, nucleation and crystal growth.

Figure 2.6 displays a schematic that shows the various steps involved during the synthesis of zeolites

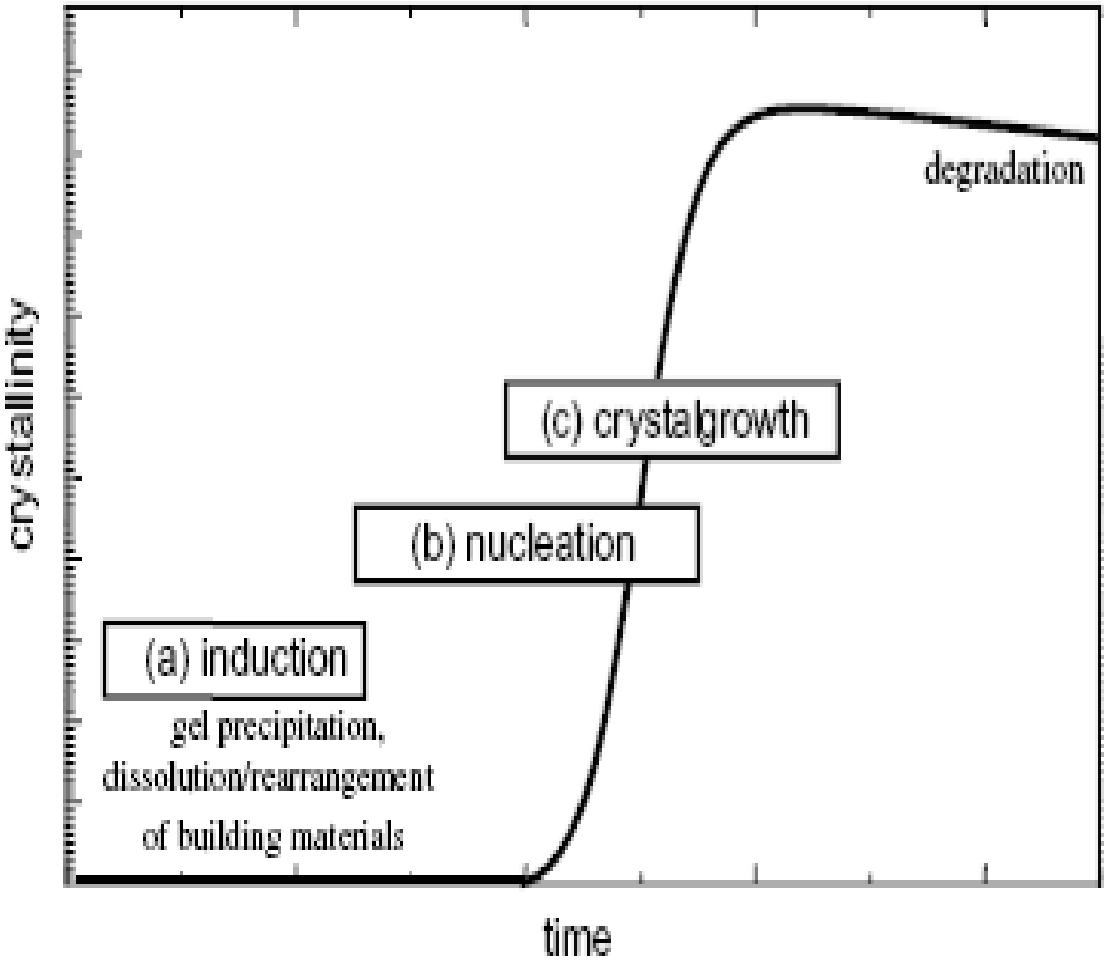

Figure 2. 6: the various steps involved during the formation of zeolites (Herrmann et al., 2005)

The Induction step involves the precipitation of gel, dissolution and rearrangement of the building materials (Herrmann et al., 2005)

The Nucleation step involves the rearrangement of atoms and molecules of the reactant phase to form a cluster of the product phase that can irreversibly grow into a large macroscopic size.

The Crystal growth step involves the growth of the nuclei into a full-grown crystal either by addition or condensation (Hay and Sheppard, 2001)

Zeolites that are synthesised in the laboratory are known to be metastable and may be converted to other zeolites or denser phases that are thermodynamically more stable under certain conditions. The degradation process follows the Ostwald law of successive transformation (Hay and Sheppard, 2001).

2.7.5. Chemical variables that affects the synthesis of zeolites

During zeolites synthesis, one of the important factors that govern the outcome of the crystals from the slurry or gel is the composition of the slurry or gel from which the crystals will emerge. The composition of the synthesis slurry or gel can be made up of a variety of organic and inorganic components that can tailor the crystallisation process (Marcilly, 1986). Figure 2.7 displays a scheme of zeolite synthesis.

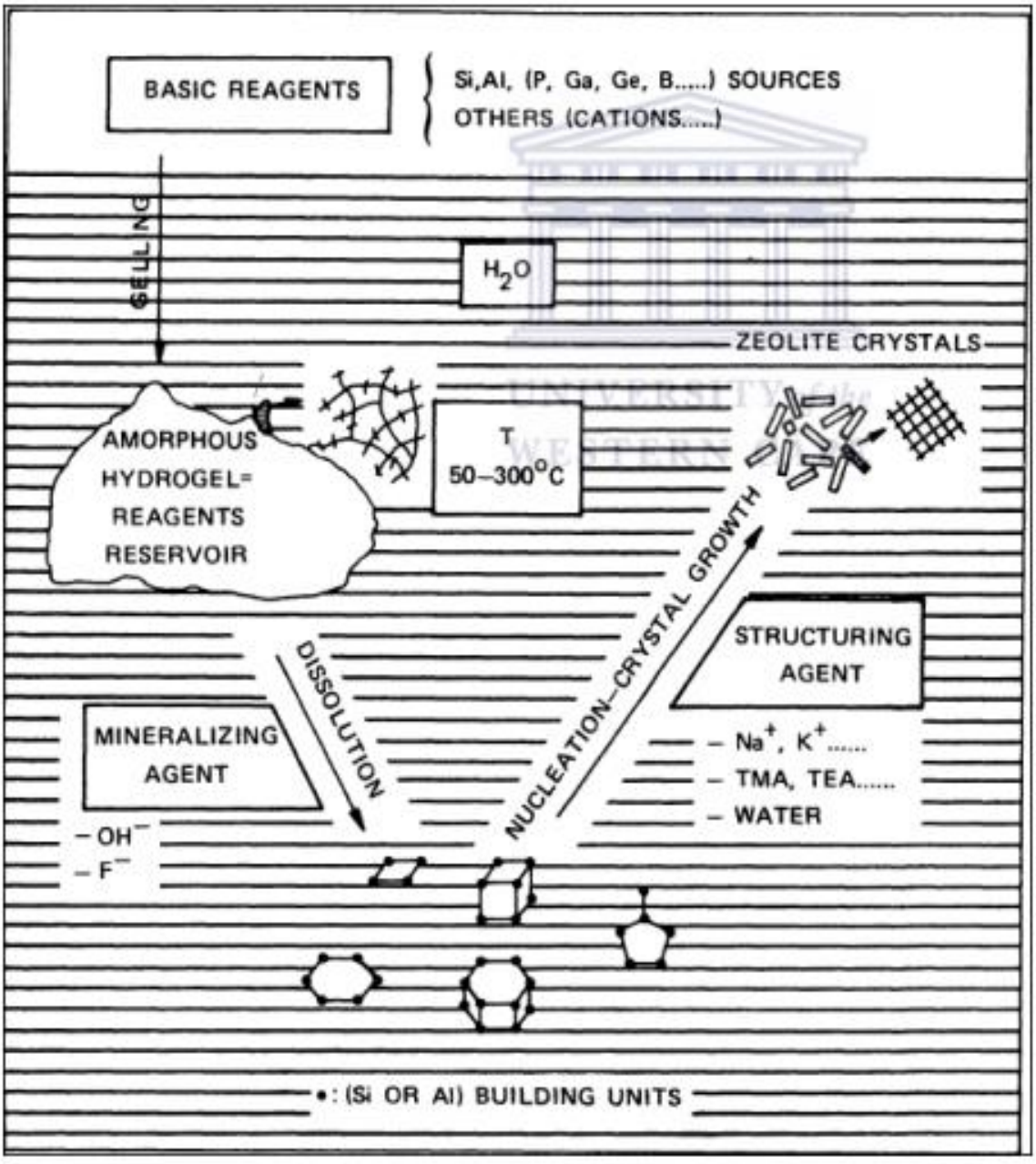

Figure 2. 7: Scheme of zeolite synthesis (Marcilly, 1986)

a) Solvents

During the synthesis of zeolites, different solvents have been used namely distilled water, ethanolamine, propanol, and ethylene glycol (Bibby and Dale, 1985). H_2O is the most

commonly used solvent in the synthesis of zeolites that allows organic and inorganic components to go into solution and also acts as a template (Guth and Kessler, 1999).

b) Mineralisation agent

The chemical specie that precipitates silicate and aluminosilicate in the synthesis mixture of zeolite is termed the Mineralisation agent. This specie (Mineralisation agent) acts as a catalyst during the synthesis of zeolites, where it is consumed during dissolution and recovered after crystallisation (Guth and Kessler, 1999). The commonly used Mineralisation specie is the hydroxyl ion that promotes the solubility of sources that contain silica and alumina. It also functions in directing the formation of soluble silicate and aluminate ion, which are $[Si(OH)_{4-n}O_n^{n-}]$ and $[Al(OH)_4^-]$ (Milton, 1956). Zeolites that are rich in aluminium can be directed by hydroxyl anion during synthesis (Milton, 1956). The mineralisation specie (hydroxyl ion) causes thermal stability problems (during synthesis) at high temperature and pressure due to Hoffman degradation on the structure directing agent. The use of F^- as a mineralisation agent during zeolite synthesis came as a breakthrough since this route could lower the pH towards neutral and prevent the degradation of the organic structure-directing agent. Flanigen et al., 1978 are the authors who first described the fluoride route of synthesis that favours the synthesis of highly siliceous zeolites (Flanigen et al., 2010)

C) Structure directing agent

There are 2 types of structure directing agents, namely the inorganic cations such as Na^+, K^+, Ca^{2+}, Mg^{2+}, and the quaternary ammonium cations such as tetraethylammonium and tetrapropylammonium (TEA^+ and TPA^+). The inorganic cations are mostly used to synthesise high aluminium zeolites such as A, X, and Y. This is because many of the exchangeable cations will occupy the pore space of the zeolites that will compensate the zeolites charge (Wright and Lozinska, 2011). The quaternary ammonium structure directing agents are used to synthesis new zeolite phases with high silica values such as zeolite Beta and ZSM-5. This is because the organic structure directing agents are bulky and less will be included in the zeolite pores as compared to smaller inorganic cations, therefore decreasing the negative charge density of the framework and thus the aluminium content (Wright and Lozinska, 2011). Zeolites structure are formed by the linkage of tetrahedral groups (AlO_4 and SiO_4 tetrahedra) through their shared oxygen atoms at the corners of the framework (Wright and Lozinska, 2011). One of the criteria used in establishing the identity of a zeolite framework is the number of the tetrahedrally coordinated atoms per nm^3. (Kirov and Filizova, 2012) reported the influence of cations such as Na^+, K^+, Ca^{2+}, Mg^{2+}, during zeolitisation. In this study, TPA template was used to facilitate the formation of ZSM-5 crystals due to its advantages mentioned in this section.

d) Elemental composition

Zeolites framework is built from silicon and aluminium that are coordinated by an oxygen atom (Wright and Lozinska, 2011). The source and purity of these elements (Si, Al and O_2) can affect the physico-chemical properties and catalytic efficiency of the solid catalyst (Karge and Robson, 2001). Zeolites synthesised from pure chemicals often have better physico-chemical properties and catalytic efficiency than zeolites synthesised from other sources (Losch et al., 2016). To account for cheap synthesis of zeolites, cheap sources of silica, aluminium and oxygen such as from clay and fly ash have been utilised in this process (Musyoka et al., 2014, Kuwahara et al., 2010)

2.7.6. Modification of zeolites

To name a few, zeolites have found application as heterogeneous catalysts, adsorbents, and as ion exchangers. In order to tailor the properties of the microporous materials so as to suit a particular application, a post synthetic modification may be very necessary. In zeolites, the post synthetic treatment begins with the regular process of drying, detemplating and ion exchanging to a broad spectrum of treatments that can tailor their properties for a particular application. Yan et al. (2003) reported that a post-synthetic treatment can include introduction, dislodgement or replacement of framework atoms or charge balancing cations. When a different atom is introduced to the zeolite structure, an excellent compatibility of the element is required with the TO_4 tetrahedral framework as well as when elements of neither low nor high oxidation state are introduced into the structure of the zeolites a balance charge is required (Moliner et al., 2011). Both Si and Al^{3+} in the zeolite framework can be replaced by compatible cations. Common cations that can successfully replace Si in the zeolite structure includes: Be, Zn, Mg, Al, B, Ga, Ge, Sn, Ti, P (Moliner et al., 2011) while some common trivalent ions that can successfully replace Al^{3+} atom in the zeolite tetrahedral structure includes: Ga^{3+}, Fe^{3+} or B^{3+}. The substitution of these trivalent cations into the zeolite framework structure to replace Al^{3+} atoms can have the following effects: Introduce charges and change the acidic property of the zeolite, Change the size and shape of the zeolite pore, and finally affects the stability of the zeolite framework (Moliner et al., 2011). Valtchev et al. (2013) reported the effects of replacing an atom in zeolites while Kitaev et al., (2013) reported the modification of the acid characteristic in H-ZSM-5 by introducing to the zeolite structure S and Ti from sufuryl chloride and titanium tetrachloride respectively. In this line of investigation, Maier et al. (2011) reported the modified acidity in BEA zeolite through a treatment of steaming. Zhang et al. (2014) reported the conversion of the sodium form of ZSM-5 to its H-form using the following conditions: treatment with oxalic acid followed with the calcination of the sample set at 550^0C for 4 hours. The synthesised catalyst by the author has found application as a support to synthesise TiO_2/H-ZSM-5 composite photocatalyst. Zeolites have found application as

heterogeneous catalysts since their discovery some decades ago, however, the orientation of their pore size have been reported to induce some diffusional constraint in terms of selectivity towards some molecules (especially bulky molecules) (Moliner, 2012). Some researchers are looking for ways to solve the problem of diffusional constraints in zeolites by trying to synthesise mesoporous and microporous zeolites. The synthesis of zeolites can be constructive or destructive and can create mesopores in the zeolite catalysts (Chal et al., 2011, Louis et al., 2010).

2.7.7. Synthesis of zeolites from coal fly ash

Fly ash is well known to contain silica and alumina locked up in their mineral phases that can be used in the synthesis of different fly ash based zeolites (Holler and Wirsching 1985 cited Belviso et al., 2010). During the synthesis of zeolites from fly ash, some authors have reported different methods that vary in their molarity, alkaline solution, alkaline agents, time, temperature, type of incubation and solution, solid ratio (Belviso et al., 2009). Typically fly ash based zeolites such as sodalite, Analcime, erionite, X, P, A, L ZSM-18 have been synthesised using the hydrothermal process reported by Holler and Wirsching (1985) without the fly ash being activated. The activation process in this context is the heat treatment of the starting material (fly ash) with alkaline in order to dissolve the amorphous aluminosilicate glass material (Vadapalli et al., 2010, Adamczyk and Bialecka, 2005). Therefore zeolites typically synthesised without the activation process normally have undissolved quartz and mullite coming from fly ash (Musyoka et al., 2012). When both the hydrothermal process and the fusion step were combined to synthesise zeolites from fly ash, the authors observed that the zeolitisation process was enhanced and the apparent non-reacted mineral phases in the end product was greatly reduce due to the fusion process (Musyoka et al., 2012, Ojha et al., 2004). The fusion process is a process whereby NaOH and fly ash are reacted in the presence of heat. The reported range of values on temperature and time during the fusion process is as follows: temperature (between 450°C to 650°C) and time (between 1 to 3 hours) (Musyoka et al., 2012, Klamrassamee et al., 2010). Purer form of fly ash based zeolites can be synthesised by extracting amorphous silica and alumina from the fused fly ash. With a higher siliceous zeolite such as ZSM-5, an excessive additional source of silica is normally required during its synthesis from fly ash. Chareonpanich et al. (2004) reported the synthesis of ZSM-5 from the Mae-Moh fly ash with the addition of silica extracted from rice husk while Kalyankar et al (2011) also reported the synthesis of zeolite ZSM-5 from the Indian fly ash with the addition of silica sol into the synthesis mixture in order to raise the Si/Al ratio from 3 to 37.5. Van der Gaag (1987) suggested that in order to synthesise zeolite ZSM-5, a Si/Al ratio above 10 is required unlike the synthesis of high alumina zeolites such as X, Y etc that require a Si/Al ratio that is less than 10.

2.7.8. Classification of zeolites

Table 2.4, 2.5, and 2.6 reported the classification of zeolites based on the following characteristics: morphology, crystal structure, effective pore diameter, and chemical composition. The classification of zeolites based on their crystalline nature, classification of natural zeolites based on their morphology, and classification of zeolites based on their Si/Al ratio are presented in Table 2.4, 2.5, and 2.6. Natrolite, solecite, mesolite, thomsonite, and edingtonite (fibrous zeolites) form needle-like or fibrous aggregates. Heulandite, brewsterte, mordenite, wellsite, and phillipsite (platy and lamellar zeolites) are characterised due to their cleavage or lamellar habbit and finally faujasite, chabazite, gmelinite and levyne (cubic or robust zeolites) are characterised based on their sorptive properties and their 4- to 6- rings.

Table 2. 4: Classification of natural zeolites based on their morphological characteristics (Szostak, 1998)

Fibrous zeolites	Platy or lamellar zeolites	Cubic or robust zeolites
Natrolite, solecite, mesolite, thomsonite, edingtonite	Heulandite, brewsterite, mordenite, wellsite, phillipsite	Faujasite, chabazite, gmelinite, levyne

Table 2. 5: Classification of zeolites based on their Si/Al ratio (Jacob, 1998)

Class	Si/Al ratio	Typical example
Low silica zeolites	1 to1.5	A, and X
Intermediate silica zeolites	2 to 5	Erionite, chabazite, clinoptilolite, mordenite, L, Y, omega.
High silica zeolites	10 to several thousands	ZSM-5, ZSM-11, EU-1, EU-2, beta, mordenite, erionite, Y

Zeolites can also be classified based on their small, medium or large ring openings as represented in Table 2.6

Table 2. 6: Classification of zeolites based on their small, medium, or large ring openings (Jacob, 1998)

8-membered ring (small pore)	10-membered ring (medium pore)	12-membered ring (large pore)
Linde A, ZK-5, chabazite, gismondine, etc	Heulandite, ZSM-5, RU-1, EU-2, ZSM-11, etc	Faujasite, mordenite, beta, omega, etc.

Despite the different methods that have been reported in the classification of zeolites, the IUPAC and IZA communities have set different rules in classifying zeolites using a code consisting of 3 capital letters as represented in Table 2.7 (Auerbach et al., 2003).

Table 2.7 presents IUPAC mnemonic codes of zeolites and their framework density (FD) (Meier and Baerlocher, 1999)

Table 2. 7: IUPAC mnemonic codes of zeolites and their framework density (FD) (Meier and Baerlocher, 1999)

Code structure	Type of material	Isotypes	FD
ABW	Li-A (BW)	BePO-ABW, ZnAsO-ABW	17.6
AFI	AlPO-5	SSZ-24, CoAPO-5, SAPO-5	16.9
ANA	Analcime	Leucite, Wairakite, AlPO-24	19.2
BEA	Beta	Tschernichite, Borosilicate-BEA	15.3
CAN	Cancrinite	Tiptopite, basic CAN, ECR-5	16.9
CHA	Chabazite	AlPO-34, MeAPO-37, Phi	15.1
ERI	Erionite	AlPO-17, LZ220	16.1
FAU	Faujasite	X, Y, SAPO-37, ZnPO-X	13.3
GIS	Gismodine	Garronite, Na-P, MAPO-43	16.4
HEU	Heulandite	Clinoptilolite, LZ219	17.5
LTA	Linde type A	SAPO-42, ZK-4, GaPO-LTA	14.2
MEL	ZSM-11	Silicalite-2, Borolite-D, TS-2	17.4
MFI	ZSM-5	Silicalite-1, Borolite-C, TS-1	18.4
SOD	Sodalite	Tugtupite, basic SOD, AlPO-20	16.7

The framework density can also be used in the classification of zeolites

2.8. Applications of zeolites

Zeolites have found different applications and each application is a function of their properties. Both natural and synthetic zeolites are annually consumed in great quantities. Jha and Singh (2011) and Yilmaz and Müller (2009) reported that about 250,000 tons of natural zeolites are consumed annually in the treatment of waste water or in the improvement of soil while 300,000 tons of synthetic zeolites are being used annually as heterogeneous catalysts and adsorbents. The following supporting factors are the reasons why zeolites have uniquely found so many different applications and that include: their Ion exchange capacity and adsorption, the presence of active sites (Brönsted, Lewis, basic, and redox active sites) that are different depending on the nature of their physico-chemical properties and can independently or collectively speed up multifunctional processes. Lastly, the ability of shape selectivity that can have positive outcomes during a chemical reaction (Byrappa and Yoshimura, 2001)

2.8.1. Ion exchange capacity

Scientists have found different industrial applications where zeolites are effectively used as ion exchangers. Some of the processes include: the use of zeolite Na-A as a water softener by

simply replacing the group (I) metal ion (Na^+) of the zeolite A with the group (II) metal ion such as Ca^{2+} and Mg^{2+} in the H_2O (Jha and Singh, 2011). Ismail et al. (2013) reported the removal of toxic metals in the treatment of waste water and in the solution of soil chemistry. Ismail et al. (2013) also reported the main factors affecting the ion exchanging process during the removal of toxic metals such as the pH, ionic strength, concentration of the ion of the initial metal. Some microporous materials with very high ion exchange capacity such as zeolite A, faujasite, chabazite, P, etc. have been reported by Ismail et al. (2013) to be used in the decontamination of industrial effluents, waste water and sludge by simply removing toxic metals such as Pb^{2+}, Cd^{2+}, Cu^{2+}, Zn^{2+}. In this same line of investigation, Ismail et al. (2013) reported that the LTA zeolite have the capacity to remove about 99.99% of the cation Pb^{2+} and 95.56% of Zn^{2+} from solution. Somerset et al. (2008) reported the removal of Hg and Pd in waste water with the fly ash based-zeolite having linde A, sodalite and faujasite phases. Lastly it has also been reported that radioactive elements such as Cs, Sr and Ba can be removed from drinking water using either synthetic zeolites or natural zeolites (Eisler, 2012) .

2.8.2. Adsorption

Jha and Singh., (2011) reported that the presence of a rigid structure containing cages and channels has a positive effect when zeolites undergo a process of adsorption/desorption. Roland and Kleinschmidt. (2005) also reported that zeolites can be used in the adsorption of both gasses and liquids. The adsorption characteristic of zeolites has found a role to play in soils and that include: soil additives, toxic metal adsorption, carrier of pesticides, herbicides and fungicides. Zeolites can be used to absorb water from a stream of gas and to remove SO_2 and NH_3 either from water or gaseous emissions. They have also found application in the adsorption of hydrogen, sulphides, and NH_4 from animal faeces and also to control odour (Jha and Singh, 2011). Chunfeng et al. (2009) reported that zeolite A and X have also been used in dye and methylene blue removal from wastewater.

2.8.3. Catalysis

Zeolites have been reported to be used as heterogeneous catalysts especially in the chemical sector (Yilmaz and Müller, 2009). The availability of Brönsted acid sites together with other unique properties that includes thermal stability, porosity and ion exchange capability in line with the ability to be modified amorphously by replacing Al, Fe, Ga, B, and Ti has led to an increase use of zeolites in catalysis and also in the replacement of mineral acids in catalysis (Nagy et al., 1998, Bekkum et al., 1991). Byrappa and Yoshimura (2010) have reported that zeolites are far less corrosive and can almost be fully recovered after a chemical reaction unlike $AlCl_3$, $ZnCl_2$, and H_2SO_4 that were initially used. The key factors that have made zeolites an ideal catalyst in different industrial processes includes the presence of Brönsted acid sites,

Lewis acid sites, porosity, shape and size selectivity. The concept of shape selectivity in zeolites allows product selectivity to be shifted from the equilibrium mixture. Despite the fact that a wide range of zeolites have been reported, only a handful have been applied as heterogeneous catalysts in industrial processes. These include ZSM-5, ZSM-22, faujasite, beta, mordenite, and ferrierite (Lercher and Jentys, 2011). 27% of zeolites have been accounted as heterogeneous catalysts based on their value on world zeolite markets. Some of the applicable processes in the chemical and petrochemical sector where zeolites are being utilised as heterogeneous catalyst are fluid catalytic cracking, hydroxylation, oximation, epoxidation, akylation, and methanol to gasoline (Millini, 2011, Yilmaz and Müller, 2009). Gilson et al. (2011) reported that zeolite applications linked to cleaner energy are still emerging. Hudec (2011) also reported that 95% of zeolite ZSM-5 and Y are utilised as heterogeneous catalysts in fluid catalytic cracking, CO_2 conversion and NO_X etc.

2.8.4. Shape selectivity of zeolite catalysts

The concept of shape selectivity in zeolites is one of the most important factors in catalysis. The chemical transformation of feed molecules by microporous catalysts to selectively synthesise hydrocarbon products is as a result of the size of the catalyst pores and cavities, and the strength of Lewis and BrÖnsted acid site (Csicsery, 1983). The application of shape selectivity by zeolite catalysts is practically used in petroleum companies and other related companies. Shape selectivity is sub-divided into three groups.

a) Reactant shape selectivity: Reactant shape selectivity is applicable to both bulkier and smaller reacting molecules. Large or bulkier reactant molecules are rejected by a smaller opening or pore sites from reaching the active sites (Csicsery, 1983), on the other hand smaller molecules or medium molecules passes through the opening or pore to the active sites for catalytic conversion to products.

b) Restricted transition state selectivity: Restricted transition selectivity occurs only when the transition state of the chemical reaction is larger than the zeolite pores such that the pore sites become pregnant with transition state molecules. When this happens, molecules in the pore adjust to form products with intermediates that can suite the pore size of the catalysts (Csicsery, 1986).

c) Product selectivity: Product selectivity occurs when the products formed in the zeolite pores are bigger or bulkier such that they cannot diffuse out of the zeolite pores. Although some zeolites pores can allow the formation of both bulkier and smaller molecules, their aperture cannot allow the diffusion of the bulkier products out, by so doing a further chemical reaction is undergone by the bulkier molecules in order to leave the active sites.

The concept of mass limitations in zeolite catalysts is as a result of both product and reactant selectivities by the catalysts. When molecules in reactant selectivity diffuses faster to their destined active sites, these get converted faster, however, in product selectivity, molecules with high mass transport limitations require a longer time for reaction while that of low mass limitation are diffused out of the active sites (Csicsery, 1986) .

d) Advantages of shape selective catalysis

The advantages of shape selectivity in zeolites include: low by-products formed, develop a friendly environment, more economically viable process, and limits the costs for separation and disposal of by-products. Figure 2.8 presents the different types of shape selectivity in zeolites

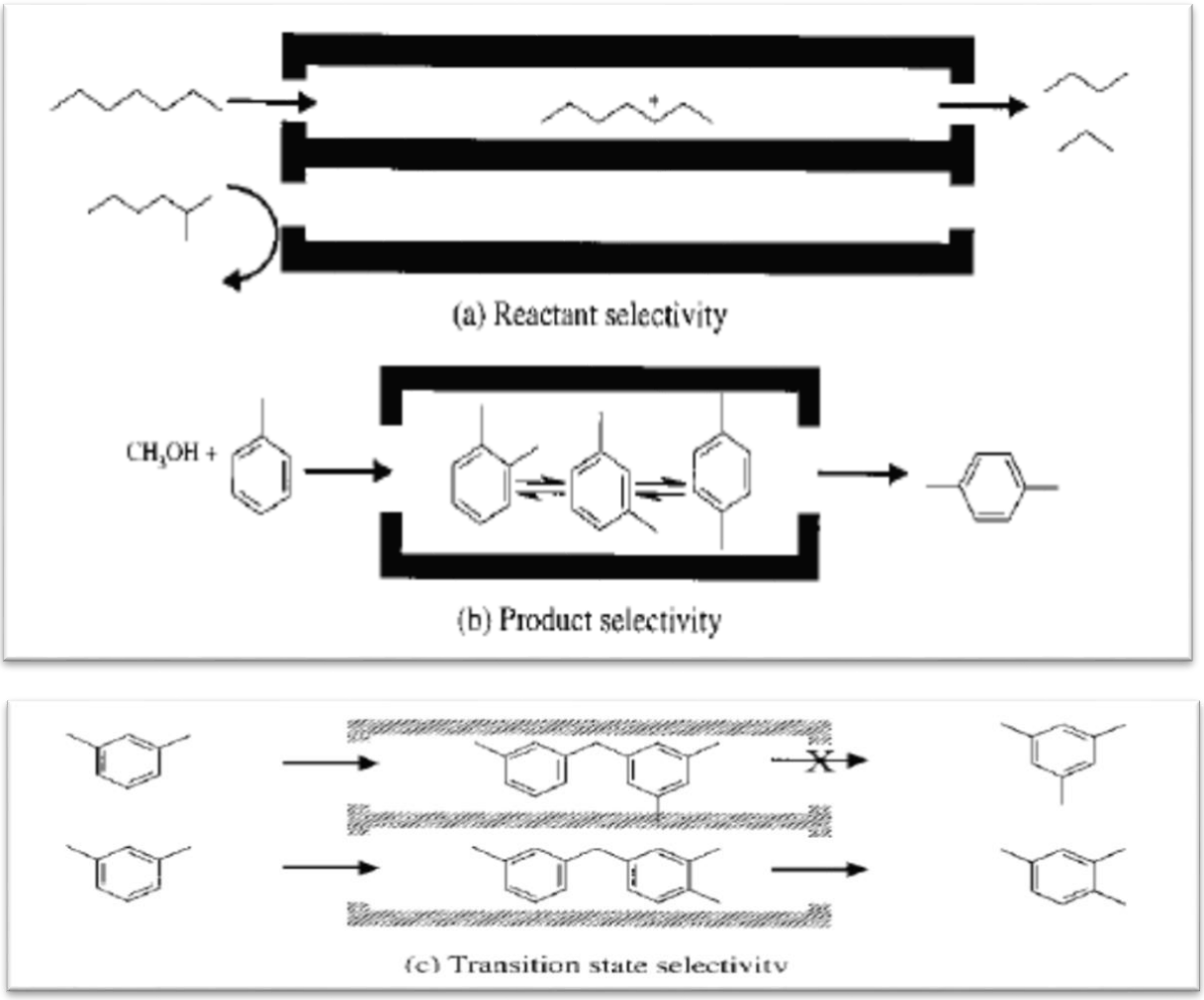

Figure 2. 8: (a) Reactant Selectivity; (b) Product Selectivity; (c) Transition-state Selectivity (Attfield, 2002)

2.9. Zeolite ZSM-5

Zeolite ZSM-5 is a highly siliceous medium pore solid catalyst that is three dimensional in shape. It is known for its high temperature stability, high content of silica, and strong acidity making it a suitable catalyst in petrochemical applications that include: Methanol to gasoline processes, Cracking, Aromatic akylation (Yilmaz and Müller, 2009, Öhrman, 2005).

2.9.1 Formation of zeolite ZSM-5

The formation of zeolite ZSM-5 is as a result of the 5-5-1 secondary pentasil units joining up to form chains that consequently link up to form sheets in the presence of a template (commonly used tetrapropylammoniumbromide) (Wright and Lozinska, 2011, Bonilla et al., 2004)

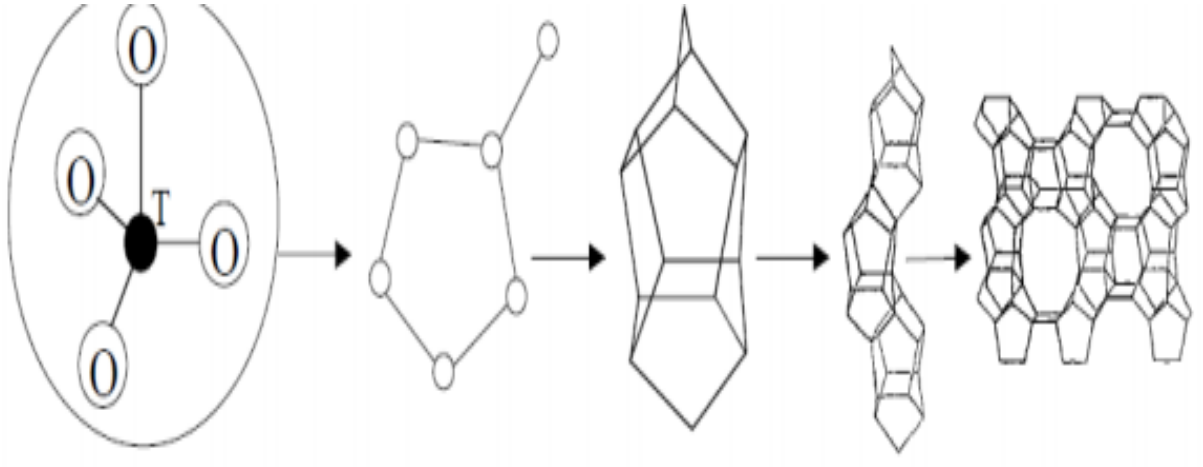

Figure 2. 9: Three-dimensional structure of ZSM-5 zeolite (Devadas, 2006)

Zeolite ZSM-5 catalyst belongs to the MFI family having pore windows that consist of 10 membered rings. The pore systems in zeolite ZSM-5 are in the b or a direction (that is straight channels of elliptical shape or circular cross sections respectively). ZSM-5 is a highly siliceous zeolite with a Si/Al ratio ranging from 10 to thousands (Jacob, 1998). The most common morphology of zeolite ZSM-5 crystals belonging to the MFI family is the coffin shape that occur as a result of the fast growth in the C direction (Öhrman, 2005). In this same line of investigation, Petrik et al. (1995) reported that the morphology of zeolite ZSM-5 crystals can be changed by changing some synthetic parameters such as the structure directing agent etc, and that the catalytic activity and deactivation was affected by the crystal habbit.

2.9.2. Synthesis of zeolite ZSM-5

The synthesis of zeolite ZSM-5 is basically from a hydrothermal solution containing Si and Al from their respective sources in the presence of a structure-directing agent (Van der Gaag, 1987). They are different types of structure directing agent that can be use during the synthesis

of zeolite ZSM-5 with tetrapropylammonium bromide being the most common type (Bonilla et al., 2004, Narayanan et al., 1995) . Table 2.8 presents a list of other structure-directing agents that can be used in the synthesis of zeolite ZSM-5

Table 2. 8: Organic structure directing agents reported for the synthesis of zeolite ZSM-5 (Van der Gaag, 1987).

Tetrapropylammonium halide	Methylquinuclidine
Tetraethylammonium halide	Morpholine
Tripropylamine	Ethylenediamine
Dipropylamine	Diethylenetetraamine
Propylamine	Triethylenetriamine
1,6-diaminohexane	Dipropylenetriamine
1,6-hexanediol	Dihexamethylenetriamine
1,5-diaminopentane	Di-n-butylamine
Ethanolamine	Ethanol
Propanolamine	Ethanol+ammonia
Pentaerythritol	Glycerol

In this study, tetrapropylammonium bromide as a structure-directing agent was selected for the synthesis of zeolite ZSM-5 from fly ash. This is because its synthesised ZSM-5 crystals have a higher level of purity than ZSM-5 crystals synthesised by other organic structure directing agents (Van der Gaag, 1987). In general, Structure-directing agents have the following advantages and that include: directs the formation of the ZSM-5 morphology, prevents already formed crystals to go into solution, and prevent recrystallisation of the already formed crystals (Van der Gaag, 1987). Despite the advantages of using a structure directing agent during the synthesis of zeolite ZSM-5, Narayanan et al. (1995) reported that zeolite ZSM-5 can be synthesised without the addition of a template into the hydrothermal gel. The morphologies of zeolite ZSM-5 can be coffin, and or cuboidal shaped crystals etc. The morphology of zeolite ZSM-5 can be tailored under the influence of the following and that include: template/Si ratio, Al content, Polymerisation of silica, the type of metal present, Alkalinity and the synthesis conditions of the hydrothermal gel (Bleken et al., 2012, Wang et al., 2008, Petrik et al., 1995).

Some researchers have studied possibility of synthesising high siliceous zeolite ZSM-5 from fly ash and they concluded that zeolite ZSM-5 can be synthesised from fly ash with the addition of excessive silica source into the hydrothermal gel (Kalyankar et al., 2011, Reanvattana, 2005, Chareonpanich et al., 2004). In this same line of investigation, Chareonpanich et al. (2004) reported the synthesis of zeolite ZSM-5 from Thailand lignite fly ash with Si extract from rice

husk and tetrapropylammonium bromide as a structure-directing agent. Adjusting the Si/Al ratio and varying the hydrothermal synthesis conditions optimised the process. The recorded phase purity of the synthesised zeolite ZSM-5 samples by these authors was 43 % and 20 % of Al_2O_3 did not take part during ZSM-5 synthesis. However, the current study aims at extracting silica from a South African class F fly ash, and then using it with small amounts of fumed silica to synthesise zeolite ZSM-5. This will reduce the amount of silica used by previous authors as well as improve phase purity and crystallinity of zeolite ZSM-5 recorded by previous authors. This study will further use the synthesised zeolite ZSM-5 catalyst from fly ash in the conversion of methanol to hydrocarbons and that will be benchmarked against the commercial ZSM-5.

2.9.3. Applications

Zeolite ZSM-5 has been reported as a solid acid catalyst with one of the highest function especially in the chemical and petrochemical sector (Lercher and Jentys, 2011). Triantafillidis et al. (1999) reported that since the discovery of zeolite ZSM-5 in 1983, the acid catalyst has been used as a route to increase the octane number of gasoline in the fluid catalytic unit (FCC) and have been used in large number of industrial units. Bleken et al. (2012) and Ramasamy and Wan (2013) reported the conversion of alcohols to hydrocarbons using zeolite ZSM-5 as a solid catalyst. Sani-Souna-Sido et al. (2008) reported that zeolite ZSM-5 has been used in Nazrov cyclisation reaction. The chlorination of aromatics by ZSM-5 has also been reported by Boltz et al., (2014). Despite the high catalytic performance of zeolite ZSM-5 in the various chemical processes, the formation of coke during a chemical reaction has limited its lifetimes ability as a heterogeneous catalyst. In order to minimise the formation of coke or deactivation of zeolite ZSM-5 catalysts, some authors have gone as far as performing a post synthetic modification on the catalyst usually by loading metals (Inaba et al., 2006). This study will limit itself to the synthesis of highly siliceous zeolite ZSM-5 from the South African class F fly ash and its application as solid catalyst in the conversion of methanol to hydrocarbons.

2.10. Characterisation of fly ash, zeolites, and catalytic products

This section will lay down detailed information from literature concerning the characterisation methods that were used in characterising the starting material (fly ash), fused fly ash (FFA) fused fly ash extract (FFAE), synthesised zeolite ZSM-5 products from fly ash and the methanol to hydrocarbons products.

2.10.1. X-ray diffraction spectroscopy

The X-ray diffraction (XRD) technique is one of the most important methods used in identifying and characterising zeolites be it at synthesis, post-synthesis, modification and catalysis (Cundy and Cox, 2005). This technique allows the exploration of crystalline materials in a wide range of the atomic structure thereby determining the identity and level of purity of the identified phase during synthesis or of the synthesised products (Subotic and Bronic, 2003). Szostak (1998) reported that the most important information obtained by the XRD technique gives an indication of how successfully a crystalline material was formed or how unsuccessful the process was. Typically, XRD patterns are usually recorded in the form of scattered intensity as a function of the Bragg angle (Pecharsky and Zavalij, 2009). The diffraction pattern provides unique fingerprint peaks of the mineral phases present and this makes it easier to follow crystallization mechanisms, modification processes, molecular sieve properties and catalytic behavior (Musyoka et al., 2012). The diffraction pattern of zeolites is usually compared with that of the standard pattern so that the known structure can be recognized (Subotic and Bronic, 2003). The most accepted database that is usually and commonly used is that of the Joint Committee for Powder Diffraction Files (JCPDF) with constant revision by the International Center for Diffraction data (ICD). With the application of the Scherrer equation that takes into consideration the peak width and the average crystallite dimension, the crystallite dimension can be interpreted.

$$\beta_s\,(2\theta) = \frac{K\lambda}{T\cos\theta}$$

Where; β_S = crystallite size contribution to the integral peak width in radians,

K = crystal shape constant near unity, and

T = average thickness of the crystal in a direction normal to the diffracting plane hkl.

Zeolite ZSM-5 can be identified using its characteristic fingerprint peaks.

2.10.2. Imaging Microscopy

Imaging analytical techniques have been used in obtaining useful information about the microstructure of a liquid and powder samples such as the morphology of the samples, particle size of the samples and lastly the particles shape of the samples (Byrappa and Yoshimura, 2001). In the early years dated back to 1930 two researchers by name Knoll and Ruska reported the use of electrons as a source of microscope illumination in order to investigate samples with the aim of bypassing the limitations set by light wavelength that was ~ 400 nm (Williams et al., 1998). The wavelength of light was used in the early days of optical microscopy before the introduction of electron as a microscope illumination source (Williams et al., 1998).

The scanning electron microscopy utilises secondary electrons during the analysis of zeolites and can also provide useful information with large zeolite particles that is ~ 1 µm.

2.10.3. Scanning Electron Microscopy (SEM)

The SEM technique is used solely to obtain information about the microstructure of samples especially that of zeolites. The formation of the particle's image is as result of an electron probe scanning the surface of the sample and the primary beam eventually interacts with the sample so that the image of the surface is recorded. Prior to the imaging of zeolites inside the SEM machine, zeolites undergo some simple preparation procedures. Since zeolites are not electrically conductive, the specimen is scattered on a conductive surface that can be a SEM stub, carbon tape or carbon paint for a better resolution of the image. Byrappa and Yoshimura (2001) reported that during the SEM imaging of the crystals of the zeolite sample, a low accelerating voltage is required that is ~5 kV

2.10.4. Infrared Spectroscopy

The infrared spectroscopy is globally utilised to investigate the chemistry of zeolites and also in catalysis. Different IR sampling techniques have been reported that include: Attenuation total reflectance, Diffuse reflectance, Photo Acoustic Fourier Transformed, and KBR wafer Technique. The as mentioned IR sampling techniques are arranged into 3 classes based on the type and nature of the instrumental design, and that includes:

Near-IR (>3000 cm^{-1}) gives information on adsorbed species such as water, organic molecules and small gas molecules, etc. in zeolite cavities or channels.

Mid-IR (4000 – 400 cm^{-1}) provides information on surface OH groups, adsorbed molecules and framework vibrations.

Far-IR (< 300 cm^{-1}) gives information on framework oxygen atoms and charge balancing cations in zeolite structures (Byrappa and Yoshimura, 2001).

The zeolitic framework vibrations are usually in the range of 1400 and 300 cm^{1} (Auerbach et al., 2003). The scanned spectra of zeolites can be complicated due to the following factors that include: the level of water in the zeolite, the presence and nature of the charge balancing cations and the elemental composition of the zeolitic material (Si/Al ratio). Shifts in zeolitic vibrational bands towards lower wavelength after a complete IR scan can be attributed to an increase in the Al content in the framework of the zeolite material having a longer Al-O (1.75 Å) bond than the Si-O (1.62 Å) bond (Byrappa and Yoshimura, 2001). The vibrational bands in the TO_4 tetrahedra are classified as internal or external vibrations that therefore represent the total vibration of the structural unit (Auerbach et al., 2003).

Table 2. 9: IR data of some zeolites containing 5-membered rings (Auerbach et al., 2003).

Zeolite types	Asymmetrical stretch		Symmetrical stretch		Double ring	T-O bend
	External	Internal	External	Internal		
Silicate	1225 (sh)	1093 (s)	790 (w)	-	550 (m)	450 (s)
ZSM-5	1225 (sh)	1093 (s)	790 (w)	-	550 (m)	450 (s)
Boralite	1228 (sh)	1096 (s)	800 (w)	-	550 (m)	450 (s)
ZSM-11	1225 (sh)	1093 (s)	790 (w)	-	550 (m)	450 (s)
Mordernite	1223 (sh)	1045 (s)	800 (w)	720 (w)	580, 560 (w)	450 (s)
Ferrierite	1218 (sh)	1060 (s)	780 (w)	695 (w)	563 (w)	455 (s)

2.10.5. X-Ray Fluorescence spectroscopy

The XRF analytical technique provides useful information about the matters elemental composition. The fundamental of the XRF technique is simply the interaction between the X-ray and the electrons of the atoms in the sample to create fluorescent spectra that will qualitatively and quantitatively identify the elemental composition of the bulk solid sample (Bekkum et al., 1991). Somerset et al. (2004) also reported that the XRF technique is useful in the qualitative and quantitative identification of elements during elemental analysis. Somerset et al. (2004) reported that the XRF technique is used to recognise trace and major elements in geological materials. The concentration of elements present in a sample can be calculated using the intensity of the fluorescent vibration. Two methods are normally used during sample preparation that include: pressed method and loose method.

Binders are normally used to aid samples that are difficult to be pressed into pellets meanwhile the loose powder method will require the samples reproducibility to be constantly checked. Finally, Takahashi (2015) reported that it is necessary to run a blank sample especially if the impurity in the sample needs to be monitored.

2.10.6. N_2 Brunauer-Emmett-Teller

The N_2 BET analytical method is a vital tool that is used to investigate the surface area of porous materials used in different applications. The surface area analysis informs researchers on how to optimise the surface area in zeolites for a particular application. The N_2 gas adsorption measures the total surface area as well as pore interiors and irregularities. There are three types of pore system in zeolites and the standard way of classifying them is through

their width size as proposed by the International Union of Pure and Applied Chemistry (IUPAC). Different pore systems in zeolites include: pore of internal width less than 2 nm (micropore), pore of internal width between 2 and 50 nm (mesopores), and pore of internal width greater than 50 nm (macropore) (Lowell et al., 2012). Macropores are found on the surface and their absorption and adsorption behavior is quite different from that of mesopores and micropores. There are six different types of isotherm that can describe the type of pores present.

- ✓ The type I isotherm: The steep slope at low pressure represents high uptake and this is characteristic of micropores in the material.

- ✓ Type II isotherm: The presence of a rounded knee serves as a sign and location of monolayer formation while the gentle slope found at the middle of the isotherm is an indication of the formation of a multilayer. The non-presence of a hysteresis loop finally indicates adsorption-desorption from a non-porous surface

- ✓ Type III isotherm: The non-presence of a knee shows the relative weakness of the attractive adsorbate-adsorbent

- ✓ Type IV isotherm: The remarkable characteristic feature that can be observed on this isotherm is the occurrence of a hysteresis loop that fully indicates the presence of mesopores.

- ✓ Type V isotherm: The non-presence of a knee just like in the type III isotherm indicates weak attractive interaction between the adsorbate and absorbent but there is the presence of hysteresis.

- ✓ Type VI isotherm: In this case there is a uniform, non-porous, surface multilayer adsorption (Lowell et al., 2004). Figure 2.10 presents the IUPAC classification of sorption isotherms (Lowell et al., 2012).

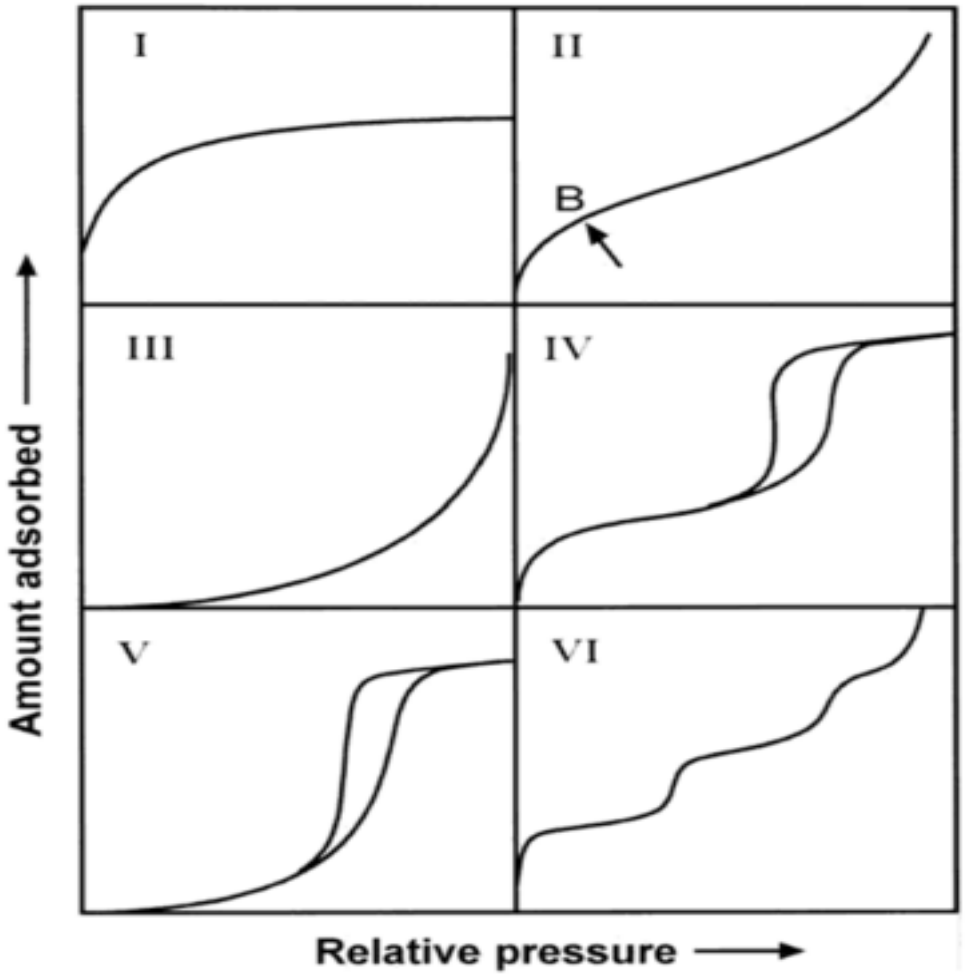

Figure 2. 10: Three-dimensional structure of ZSM-5 zeolite (Lowell et al., 2012)

The presence of a structure-directing agent in the pores of zeolite ZSM-5 affects the BET surface area of the catalyst. The BET surface area of zeolite ZSM-5 can be improved after detemplation followed by ion exchange with NH_4NO_3 and calcination (Zhang et al., 2014). Some authors have reported that the different BET surface area in ZSM-5 depends on the method of synthesis. The surface area of zeolite ZSM-5 synthesised by Zhang et al. (2014) was improved from 293.6 m^2 /g to 312.1 m^2 /g as the author varied and used different structure directing agent. In this study, the BET surface area of zeolite ZSM-5 would be monitored as the elemental composition in the synthesis mixture is adjusted. to synthesise zeolite ZSM-5.

2.10.7. Nuclear magnetic resonance

This analytical technique is sensitive in detecting chemical bonds in the structure that include: frame work atoms, extra-frame work species, surface site and adsorbate complexes (Hunger, 1997). Cubillas and Anderson (2010) reported that the solid-state NMR is complementary to the diffraction methods and are utilised to investigate the order of long-range crystals. Hunger (1997) reported that the zeolite properties that can be studied by the NMR technique includes: incorporation, coordination, and local structure of framework atoms in zeolites, distribution,

location, and coordination of extra-framework species; concentration, nature and the chemical behaviour of surface OH groups.

2.10.8. Gas chromatography (GC)

This technique (Gas chromatography) is used in the analysis of a complex mixture as it has the ability to separate, identify, and quantify volatalised components in the complex mixture. A typical GC consists of an injection port, a column (that contain a stationary and mobile phase), and a detector. During analysis, the sample is vapourised and then injected at the top of the temperature-controlled column. Thereafter the sample is made to flow in the column with the help of a stationary phase and a mobile phase. The complex mixture then interacts with the stationary phase of the column as it flows with the mobile phase. Their level of interaction depends on their polarity and boiling point (Jennings et al., 1997) hence generating different retention times for separation, identification, and quantification.

CHAPTER 3
EXPERIMENTAL AND ANALYTICAL TECHNIQUES

3.1 Introduction

This chapter presents detailed information on the type of materials and chemicals that were utilised during this research. It will also present detailed information on the study approach, experimental procedures and characterisation techniques employed in this study. Figure 3.1 schematically represents the experimental design and procedures so that the research questions laid down in Chapter 1 of this study can be addressed.

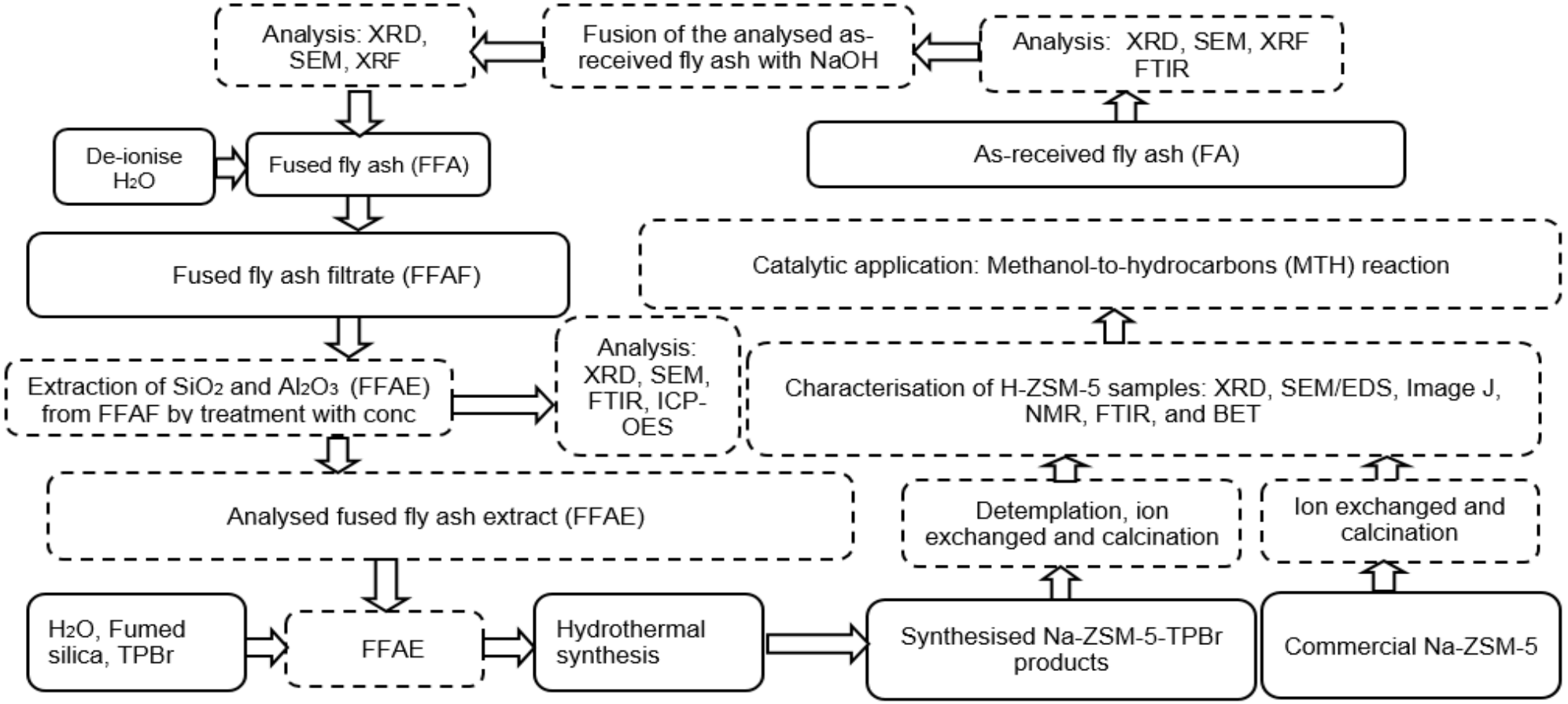

Figure: 3.1: Experimental approach used in this study (TPBr = template)

3.2. Material and chemicals

3.2.1. Source of South African fly ash

The raw material (fly ash) that was used in this study for the synthesis of zeolite ZSM-5 was obtained from the Arnot coal-power plant in the Mpumalanga province

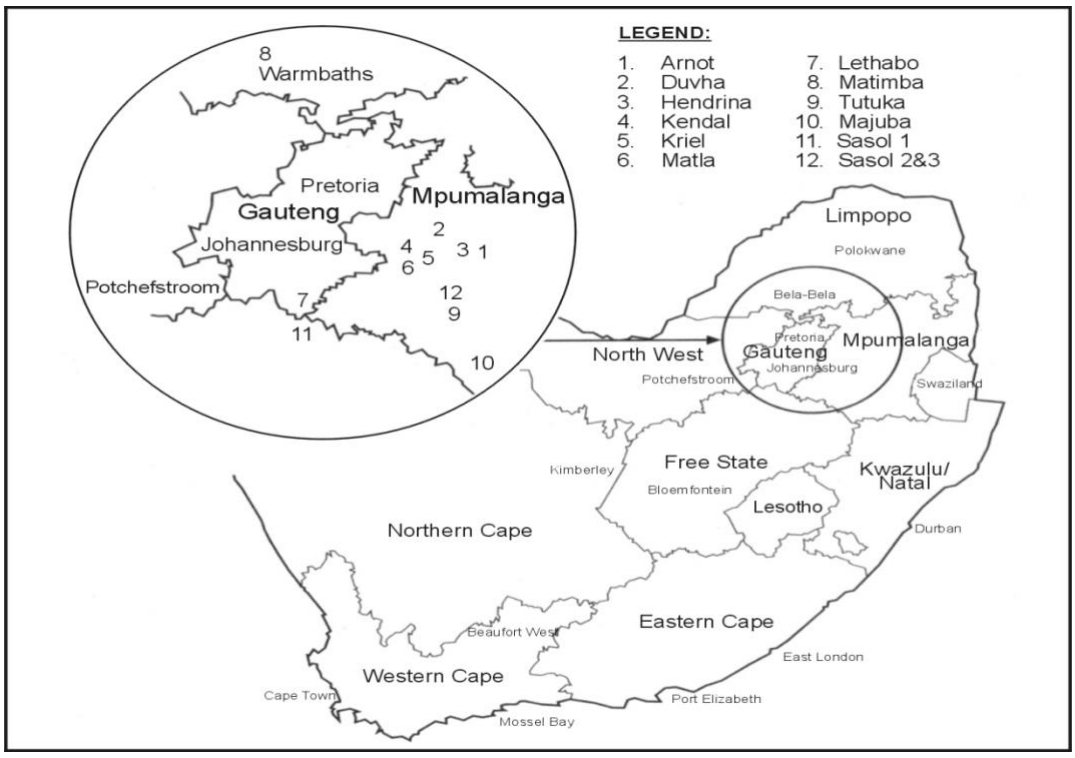

Figure 3. 1: Location of important pulverised coal-fired thermal power stations in the Republic of South Africa (Krüger, 2003)

3.2.2. Sample handling and storage

The fly ash sample collected from the Mpumalanga Arnot-coal power station was stored in an airtight sealed bag and was kept in a cool dry dark room. This was to prevent moisture, sunlight, and fluctuating temperature from altering with the composition of the fly ash by forming thermodynamically stable minerals that might affect the synthetic process of zeolite ZSM-5 products from fly ash. Tables 3.1 and 3.2 presents the list of chemicals and equipments that were utilised during this study as well as their source and purity.

3.2.3. Chemicals

Table 3. 1: List of chemicals

Chemicals	Source	Purity
Sulphuric acid (H_2SO_4)	Merck chemicals	98-99 %
Lithium bromide	Merck chemicals	98 %
Tetrapropylammonium bromide	Sigma-Aldrich	98 %
Sodium hydroxide (NaOH)	Kimix chemicals	97 %
Fumed Silica	Sigma-Aldrich	99.90 %
ZSM-5	Zeolyst	Commercial range
Methanol (CH_3OH) and dimethyl ether	Sigma-Aldrich	98 %
Nitric acid (HNO_3)	Sigma-Aldrich	98 %
Hydrocarbons (C2, C3, and C4)	Advance African Technology	
Hydrochloric acid	Sigma-Aldrich	99 %

3.2.4. Equipment

Table 3. 2: List of equipment

Equipments
Closed furnace
Stainless steel autoclaves
Oven (laboratory)
Freeze drying machine
Open ceramic tube furnace
Tedlar bags
Reactor furnace (FIBERCRAFT VF-3-12-V-S reactor furnace) and accessories
Reflux system with oil bath
Teflon lined Stainless autoclave

3.3. Methodology

The method that was used during the synthesis of zeolite ZSM-5 products from fused fly ash extract (FFAE) as well as their catalytic application is detailed in this section.

3.3.1. Synthesis of zeolite ZSM-5 products from South African fused fly ash extract (FFAE)

Zeolite ZSM-5 products used in this study were synthesised from Arnot fused fly ash extract (FFAE) that was obtained from fused fly ash filtrate (FFAF) after treatment with concentrated sulphuric acid (98-99%) followed by the addition of fumed silica (varied parameter), de-ionised water (H_2O) and tetrapropylammonium bromide (TPBr) as a structure directing agent.

After characterisation of the raw material (fly ash), the as-received Arnot fly ash was fused with NaOH in order to convert the insoluble mineral phases of fly ash to soluble phases of sodium aluminosilicate as proposed by Shigemoto et al. (1993). 50 g of the as-received fly ash was mixed with 60 g of NaOH in a porcelain crucible before fusion in a closed furnace at 550 ^{0}C for 1 hour 30 minutes. After the time elapsed, the furnace was switched off and the fused fly ash (FFA) was removed to allow cooling. Thereafter the fused material was ground and stored in a plastic container and termed fused fly ash (FFA) as shown in Figure 3.2.

Figure 3. 2: Experimental set up of the fusion process of the as-received fly ash with NaOH set at 550 ^{0}C for 1 hour 30 minutes (Refer to images in Figure 4.2 micrographs)

10 g of the powdered fused fly ash (FFA) was mixed with 50 mL of deionised water and the mixture was agitated for 2 hours using a magnetic stirrer. The slurry was then filtered (using a filtration set up) to obtain a clear solution of fused fly ash (named fused fly ash filtrate) that was green in colour. Under magnetic stirring of the filtrate, 2 mL of concentrated H_2SO_4 (98-99%) was added to the filtrate in a dropwise manner to precipitate silica so as to remove Al, Fe and other impurities. The silica precipitate named fused fly ash extract (FFAE) was white in colour with a pH of 11. The formed FFAE was washed with distilled H_2O and dried overnight in the oven set at 70 ^{0}C. After drying, the obtained fused fly ash extract (FFAE) was analysed to

determine its elemental composition using ICP-OES (inductive coupled-emission spectroscopy) technique as detailed in section 3.5.7. It was observed that the Si/Al ratio of the obtained FFAE was 9.5 and was higher than that of the as-received fly ash (1.97). However, the Si/Al ratio in the FFAE was still not deemed siliceous enough to synthesise crystalline zeolite ZSM-5 products since it was below 10 (refer to section 4.3 Figure 4.4). In this line of investigation, the effect of adding small amounts of fumed silica to the synthesis mixture in order to raise the Si/Al ratio above 10 was investigated (see Table 3.3).

2.5 g of the fused fly ash extract (FFAE) was mixed with 40 mL of deionised water for about 10 minutes. Thereafter, fumed silica (0.000 or 0.250 or 0.375 g) was added to the synthesis mixture together with 1 g of tetrapropylammonium bromide (TPBr) (see Table 3.3). Based on the amount of fumed silica added to the synthesis gel, the mixtures were coded FF1 (0.000 g of fumed silica), FF2 (0.250 g of fumed silica), and FF3 (0.375 g of fumed silica). The obtained mixtures were agitated with a magnetic stirrer for another 30 minutes before being poured into separate sealed Teflon cups each placed inside a steel synthesis vessel prior to hydrothermal synthesis at a condition of 165 ^{0}C for 72 hours. After crystallisation, the obtained crystals (Na-FF1-TPBr, Na-FF2-TPBr, and Na-FF3-TPBr) were washed and dried overnight at 70 ^{0}C. Finally, the samples were then detemplated, ion exchanged, and calcined in order to obtain their acidic form (H-form) as explained in the next sections.

During the synthesis of zeolite ZSM-5 products in this study, tetrapropylammonium bromide (TPBr) was used as a structure-directing agent to aid the formation of crystal particles as well as their pore size distribution.

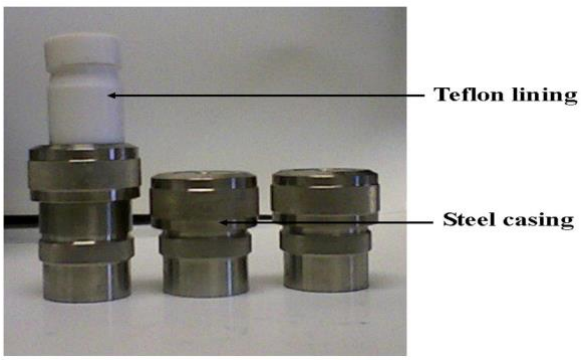

Figure 3. 3: Images of parr bombs and Teflon linings that were used during hydrothermal crystallisation of the fly ash based zeolite ZSM-5 products

Table 3.3. Presents the experimental conditions that were used to synthesise FF1, FF2, and FF3 from fused fly ash extract (FFAE).

Table 3. 3: Experimental conditions used for the synthesis of ZSM-5 products from fused fly ash extract (FFAE)

Code name	Variable parameter	Fixed parameters
	Fumed silica (g)	
FF1	0.000	• FFAE (2.5 g) • Volume of distilled H_2O (40 mL) • TPBr (1g) • Hydrothermal synthesis (165 ^{0}C, 72 hours)
FF2	0.250	• FFAE (2.5 g) • Volume of distilled H_2O (40 mL) • TPBr (1 g) • Hydrothermal synthesis (165 ^{0}C, 72 hours)
FF3	0.375	

The effect of small amounts of fumed silica (varied parameter) added to the initial source of Si and Al extracted from fly ash on the properties of the synthesised zeolite ZSM-5 products was discussed in chapter 4. Table 3.4 presents the molar regime of the synthesis mixture of H-FF1, H-FF2, and H-FF3

Table 3. 4: Code name of fly ash based zeolite ZSM-5 and molar regime

Code name	Molar regime				
FF1-TPBr	Al (1)	Si (9.1)	Na (37.9)	H_2O (2149)	TPBr (15.2)
FF2-TPBr	Al (1)	Si (38.1)	Na (37.9)	H_2O (2149)	TPBr (15.2)
FF3-TPBr	Al (1)	Si (49.5)	Na (37.9)	H_2O (2149)	TPBr (15.2)

3.3.2. Sample Detemplation

After hydrothermal crystallisation, the pores of the ZSM-5 products were occupied with tetrapropylammonium bromide (TPBr) that was used as a structure-directing agent during synthesis. In order to detemplate (drive away the structure directing agent) the synthesised zeolite ZSM-5 products, an open ceramic tube furnace was conditioned as presented in Table 3.5.

Table 3. 5: Experimental conditions used to detemplate synthesised Na-FF1-TPBr, Na-FF2-TPBr and Na-FF3-TPBr (TPBr = template or structure directing agent)

Temperature	Ramping temperature	Time
550 ^{0}C	15 ^{0}C/min	5 hours

Thereafter detemplation, Na-FF1-TPBr, Na-FF2-TPBr and Na-FF3-TPBr were converted to Na-FF1, Na-FF2, and Na-FF3. The obtained Na-form of the synthesised zeolite ZSM-5 samples were then ion exchanged and calcined to their acidic (H-form) or active form as detailed in section 3.3.3.

3.3.3. Experimental procedure used during ion exchanged and calcination of Na-FF1, Na-FF2, Na-FF3 and the commercial Na-ZSM-5

The non-acidic sodium form of the detemplated ZSM-5 samples Na-FF1, Na-FF2 and Na-FF3 were converted to their acidic form of H-FF1, H-FF2 and H-FF3 by ion exchange. The commercial Na-ZSM-5 was also converted to its acidic form (H-form) using the same ion exchange procedure. In this process, a 1 M NH_4NO_3 solution was prepared by mixing 8 g of NH_4NO_3 solid with 100 mL of distilled H_2O for about 15 minutes. 10 mL of the prepared acid solution was agitated with 1 g of the detemplated sample (ratio 1:10) at 80 ^{o}C for 3 hours. The mixture was filtered, and the process repeated three times with a freshly prepared acid solution (1M NH_4NO_3). The ion exchanged ammonium form (NH^+_4-ZSM-5) of the ZSM-5 products was filtered and dried overnight in the oven at 70 ^{o}C prior to calcination that was conducted at 550 ^{o}C for 5 hours with a ramping temperature of 15 ^{0}C/min to drive off NH_3 gas and form H-zeolite (H-FF1, H-FF2, H-FF3 and com H-ZSM-5).

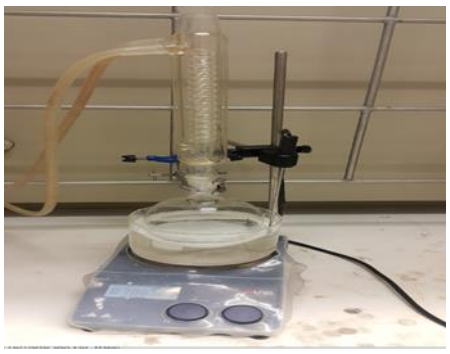

Figure 3. 4: Experimental set up showing the ion exchanging process of the synthesised Na-FF1, Na-FF1, Na-FF3 ZSM-5 and comm Na-H-FF1 to H-FF1, H-FF2, H-FF3 and the commercial H-ZSM-5

H-FF1, H-FF2, H-FF3 and commercial H-ZSM-5 were then characterised using the following analytical methods: XRD, SEM/EDS, Image J, NMR, FTIR and BET. The XRF technique was used to determine the elemental composition of the starting material (as-received fly ash) while the ICP-OES method was used to determine the elemental composition of fused fly ash extract (FFAE) and the concentration of cations in the ion exchanging solution of zeolite ZSM-5 samples.

3.3.4. Catalytic testing

After characterisation, the synthesised H-FF2, H-FF3 and the commercial H-ZSM-5 were used as heterogeneous catalyst in the methanol to hydrocarbons reaction (MTH) in a fixed bed reactor. The reason why H-FF1 was not used as a heterogeneous catalyst in the MTH reaction was explained in chapter 4 section 4.1.2.

3.3.5. Fixed-bed reactor system

The methanol to hydrocarbon (MTH) catalytic tests in this study was performed in a fixed bed quartz tube reactor. The reactor was enclosed with a furnace (FIBERCRAFT VF-3-12-v-s) equipped with GEFRAN 600 temperature controller for heat supply. The temperature of the furnace was monitored and regulated manually (by GEFRAN 600) in order to set the desired temperatures throughout different experimental runs. A constant atmospheric pressure of 1.01325 bars was also maintained throughout all experimental runs. An HLPC pump was used to pump and regulate the flow rate of methanol to the inlet of the reactor where it vaporises to produce a desired $WHSV^{-1}$ for all experimental runs. At the exit of the furnace enclosed fixed bed reactor system is attached a Tedlar bag (collector) that was used to collect gaseous hydrocarbon products. An attached bubble flow meter was used to measure the flow rate of the exiting gasses. Figure 3.6 presents a schematic of a fixed bed reactor system that was used in this study.

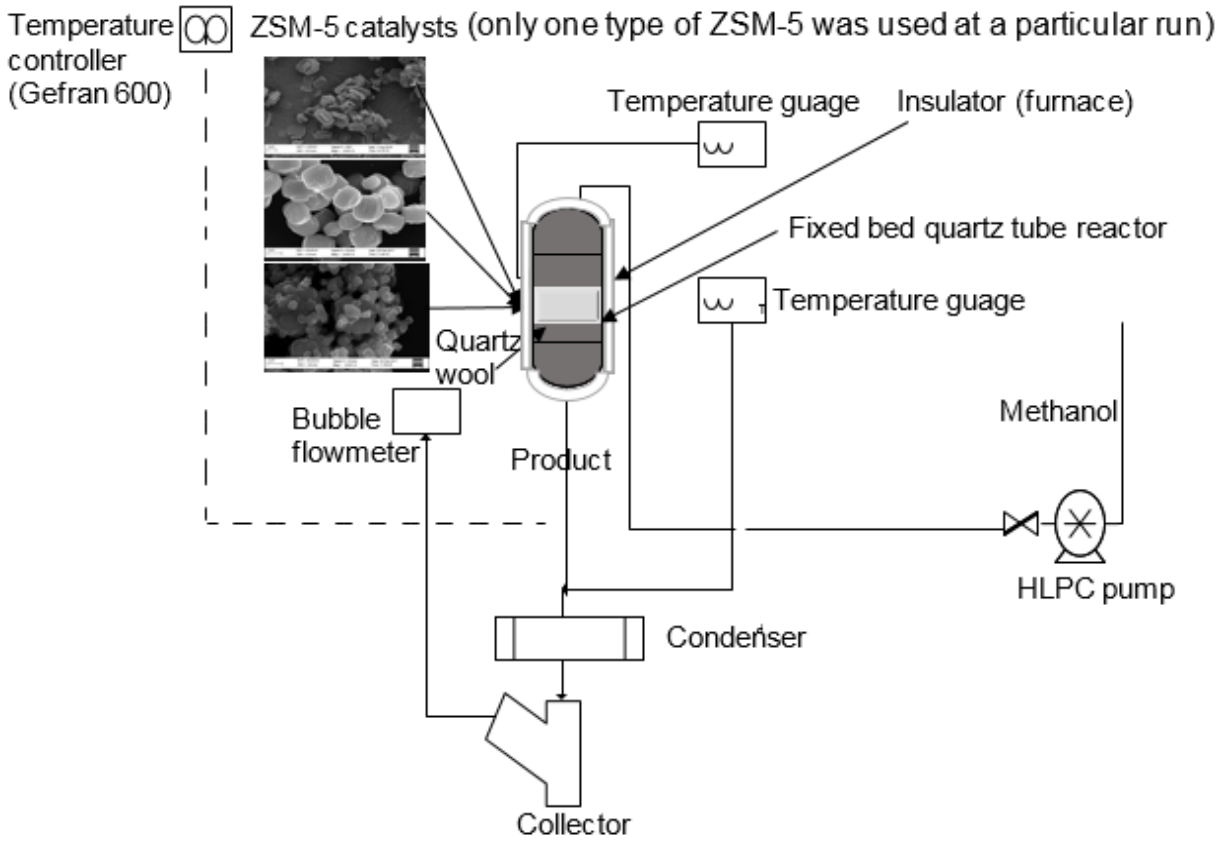

Figure 3. 5: Fixed-bed reactor system used in the conversion of methanol to hydrocarbons (MTH) reaction over H-FF2, H-FF3, and the commercial H-ZSM-5

The dimensions of the fixed bed reactor are as follows:

Length of reactor excluding external joints

L = 500 mm = 50 cm = 0.5 m

Diameter of reactor

D= 1mm = 0.1cm = 0.001 m

Internal diameter of reactor

I.D= 0.8 mm = 0.08 cm = 0.0008 m

Table 3.6 presents parameters investigated during the MTH reaction in the fixed bed reactor over H-FF2, H-FF3, and the commercial H-ZSM-5.

Table 3. 6: Parameters investigated during the methanol to hydrocarbon reaction runs

Weight per hourly space velocity ($WHSV^{-1}$)	Temperature	Contact time (hours)
2	350 and 400 ^{0}C	1-10

Before the catalytic testing, 0.5 g of the fly ash based H-ZSM-5 (either H-FF2 or H-FF3) catalyst was loaded into the fixed bed quartz tube reactor. The catalyst was securely held in position on the catalyst bed with a piece of glass wool. Immediately after the loading preparation, the reactor was then enclosed in a furnace furnished with a GERFRAN 600 controller. The furnace was switched on to a set point temperature or reaction temperature of 350^0 C or 400 ^{0}C required for that experimental run. It took about 30 minutes for the monitoring thermocouples of the reactor system to read the actual set point temperature. The reaction temperature was used to desorb water from the catalyst for an hour. Thereafter the feed (methanol = CH_3OH) was carried to the entrance of the fixed bed reactor with the help of a conditioned HLPC pump were it vapourised before reaching the catalyst on the bed. A weight per hourly space velocity (WHSV) of $2h^{-1}$ was used throughout the experimental runs. At this stage of the experimental preparation about 2 hours 30 minutes had elapsed before the time of the first data point collection for analysis. A Tedlar bag that was connected at the exit point of the fixed bed reactor was used to collect the gaseous products of the MTH reaction at an hourly interval for analysis by an offline GC. As the reaction proceeded, different Tedlar bags were used to collect gaseous products for up to 10 hours. In this study methanol and dimethyl ether were considered as reactants.

Equations

The equations below were used to calculate the percentage (%) conversion of methanol (CH_3OH) and selectivity towards ethylene (C2), propylene (C3), and butylene (C4).

Equation 3. 1

$$Concentration\ of\ product\ A = \frac{ppm\ of\ standard * peak\ area}{standard\ area}$$

Equation 3. 2

$$Methanol\ in(\frac{mol}{min}) = \frac{(Methanol\ flow\ rate * methanol\ density)}{M.W\ of\ methanol}$$

Equation 3. 3

$$Carbon\ in\ the\ fixed\ bed\ reactor\ \left(\frac{mol}{min}\right) = Methanol\ in(mol)$$

Equation 3. 4

$$Carbon\ out\left(\frac{mol}{min}\right) = Total\ mol\ of\ d/min$$

Equation 3. 5

$$Mass\ balance\ of\ Carbon = Carbon\ out\left(\frac{mol}{min}\right) - Carbon\ in\left(\frac{mol}{min}\right)$$

Equation 3. 6

$$MeOH(X) = \frac{n(methanol)in - [n(methanol)out - 2 * (DME)]}{n(methanol)in} * 100\%$$

Equation 3. 7

$$S(\%) = \frac{\sum x * n(ethylene)}{n(methanol)in - [n(methanol)out + 2 * n(DME)]} * 100$$

Equation 3. 8

$$S(\%) = \frac{\sum X * n(propylene)}{n(methanol)in - [n(methanol)out + 2 * n(DME)]} * 100$$

3.3.6. Analysis of hydrocarbon products synthesised from methanol

The composition of the gaseous products sampled hourly during each experimental run was analysed using a GC (Agilent 7890A) that was equipped with an FID detector using an RT-Q-BOND capillary column (RESTEK C/N: 19744, S/N: 1390468) with a column length of 30 m, internal diameter being 0.32 mm with a film thickness of 10 μm. The RT-Q-BOND column was coated with 100% divinyl benzene that was designed by RESTEK for hydrocarbons separation (olefins, paraffin's, oxygenates and solvents). During analysis, a manual injection (tight syringe) was used to extract the gaseous products that were collected in a Tedlar bag in an hourly basis before injection into the GC. The compounds in the product were identified using their separate characteristic retention times as detailed in section 4.1.4. At the end of the analysis, the data were then transferred into an excel sheet for further analysis.

The following section will present detailed information of the Gas Chromatography technique and the procedure used in standardising the GC for hydrocarbons detection after the methanol to hydrocarbon reaction (MTH reaction).

3.4. Characterisation techniques

This section lays down the different analytical techniques used during the characterisation of the as-received Arnot fly ash (AFA), fused fly ash (FFA), fused fly ash extract (FFAE), synthesised fly ash based zeolite ZSM-5 products (H-FF1, H-FF2, H-FF3), and the products coming from the methanol to hydrocarbon reaction (MTH). These methods include XRD, SEM, Image J software tool, FT-IR, NMR, ICP, and BET.

3.4.1. X-ray diffraction spectroscopy analysis

The mineralogical analysis of as-received Arnot fly ash (FA), fused fly ash (FFA), fused fly ash

extract (FFAE), and synthesised zeolite ZSM-5 products was performed using Phillip X-pert pro MPD X-ray diffractometer with Cu-K at 40 KV and 40 mA. In order to collect spectra results, the samples were ground to a fine powder and mounted onto rectangular polypropylene holders and scanned over a range of 4^0 to 60 ^{0} 2θ. Crystalline Mineral phases were then identified with the help of a High score Xpert software by comparing the collected patterns with the standard line patterns of the standard diffraction database supplied by International Centre for Diffraction Data (ICDD)

3.4.2. X-ray fluorescence spectroscopy analysis (XRF)

The XRF analytical technique was used to quantitatively and qualitatively analyse the elemental composition of the as-received fly ash by measuring the X-ray fluorescence that is released when the sample is excited by a primary X-ray source. The loss of ignition (LOI) was determined by conditioning 2 g of the fly ash at 900 ^{0}C for 4 hours that was subtracted from the overall percentage of the metal oxides. During analysis of the main elements contained in fly ash, the following procedure was used to prepare the sample.

The sample was dried overnight at 110^{0}C. 0.65 g of a flux together with 0.5% of LiBr were mixed and fused. The main elements in each fly ash sample were then determined on Philips PW 1480 X-ray spectrometer in the form of oxides as follows SiO_2, Al_2O_3, Fe_2O_3, CaO, MgO, TiO_2, K_2O, P_2O_5, MnO and together with some trace elements such as Cr_2O_3, K_2O, P_2O_5, Na_2O, MnO, and SO_3

3.4.3. Scanning electron microscopy-energy dispersive spectroscopy (SEM)

The SEM technique was performed to investigate the morphology of raw and fused fly ash as well as their synthesised zeolite ZSM-5 products. This technique was performed on a high-resolution Auriga field emission gun. During sample preparation, the as-received fly ash, fused fly ash, fly ash based zeolite ZSM-5 products, and the commercial H-ZSM-5 were sprinkled on adhesive carbon discs that were mounted on aluminium stubs before being coated by carbon on QUORUM Q150T ES metal coater. The coated samples were loaded into high-resolution SEM so that the surface of the specimens could be scanned in lines and frames by an electron beam to record an image. Records of the operating conditions used during this analysis were captured on each of the respective SEM micrographs. In order to determine the elemental compositions of the synthesised zeolite ZSM-5 samples using energy dispersive spectroscopy (EDS), six different areas of each sample was investigated for its elemental composition. This was done so that their respective Si/Al ratio could be established.

3.4.4. Image J software

The Image J software tool can be used to analyse the particle sizes of different images. In this study, the tool was used to analyse the mean crystal length and width of the synthesised zeolite

ZSM-5 products. During analysis, 20 crystal particles on each SEM micrographs were selected and measured using the image J software tool. The obtained results were then transferred to an excel sheet for further analysis with the mean equation. Finally, a bar chart containing an average crystal size of each zeolite ZSM-5 sample was constructed.

3.4.5. Fourier Transformed Infrared Spectroscopy (FT-IR)

The Fourier transformed infrared spectroscopy analytical technique was performed so as to investigate the structural coordination of the as-received fly ash and the synthesised zeolite ZSM-5 products from fused fly ash extract. This analysis was conducted on Perkin Elmer 100 FTIR analyser where 15 mg of each sample was placed in an attenuated reflectance sample holder prior to a gentle force that was applied to the sample. Before data collection within the range of 400-4000 cm^{-1} the instrument was conditioned to correct the baseline from background noise that was subtracted from the spectra.

3.4.6. Brunauer-Emmett-Teller (BET)

N_2 adsorption via the Brunauer-Emmett-Teller analysis was used to measure the surface area of the synthesised fly ash based zeolite ZSM-5 products. This technique was conducted on Micrometrics ASAP 2020 instrument. During analysis, 500 mg of each sample was weighed and dried overnight at a temperature of 90 ^{0}C. The dried samples were then loaded in a sample tube before being inserted into the instrument. The instrument was set to degas the samples at 90 ^{0}C for 2 hours and then 400 ^{0}C for 4 hours so that the moisture trapped in the porous network of the catalysts can be removed. At this stage of the analysis, the BET analysis was conducted with N_2 at 77 K with the use of the surface area analyser of Micrometrics 2020.

3.4.7. Nuclear magnetic resonance (NMR)

The Nuclear magnetic resonance (NMR) spectroscopy was performed to investigate the framework and extra framework aluminium in the synthesised fly ash based zeolite ZSM-5 products and the commercial H-ZSM-5. During analysis, 50 mg of the sample was compressed in a 7-mm diameter NMR rotor before insertion into the instrument. This analysis was conducted on a Bruker Ultra shield 600 MHz/54 mm spectrometer. The same procedure was used to investigate the framework silica of the samples.

3.4.8. Inductive coupled plasma-optical emission spectroscopy (ICP-OES)

Inductive coupled plasma optical emission spectroscopy was used to determine the elemental composition of fused fly ash extract (FFAE). 0.25 g of the fused fly ash extract (FFAE) was mixed with 2 mL of concentrated sulphuric acid (98-99%) and 5 mL of aqua regia (HNO/HCl,

1:3) in a digestion vessel. The digestate was then placed in the oven that was set at 250 ^{0}C for 2 hours. After the time of the sample in the oven had elapsed, the digestate was removed and allowed to cool. The excess HF in the digestate was neutralised using 25 mL of boric acid (H_3BO_3) solution before filtration. The filtrate of the digestate was finally diluted with 50 mL of distilled water before being taken for elemental analysis using Varian 710-ES ICP-OES that was calibrated with the investigated elements. ICP-OES was also used to determine the elemental composition of the ion exchanging solution that was obtained from synthesised zeolite ZSM-5 samples and the commercial ZSM-5.

3.4.9. Gas Chromatography (GC)

A Gas Chromatographic technique was utilised to separate compounds of the methanol to hydrocarbons reaction over the synthesised fly ash based and commercial H-ZSM-5 so that each of the compounds can be separately analysed in terms of the peak size and the number of ions. The basis for the GC technique is that after injection of the analytes into the column, the compounds are made to flow between two different phases in contact i.e. the stationary and the mobile phase. The stationary phase was an RT-Q-BOND column bonded with a 100% divinyl benzene (inert compound) while the mobile phase was an inert carrier gas, namely N_2. When the analytes were carried across the column by the mobile phase, the various compounds achieve a different level of interaction with the stationary phase. Analytes with stronger interaction either had stronger Van der Waal forces or higher boiling points and thus a longer retention time before elution than other compounds. Thus smaller chain hydrocarbons were eluted before the longer chain hydrocarbons.

In the flame ionisation detector chamber, hydrocarbon samples are burnt in the presence of hydrogen and air and produced ions that are detected by a high voltage metal collector. Thus, the FID is a detector for carbon atoms. The response factor of carbon in hydrocarbons is almost the same no matter the type and size of the compound whereas calibration is needed with oxygenated hydrocarbon compounds.

Knowing from literature that the products synthesised from the methanol to hydrocarbons catalytic reactions consist primarily of C2, C3, C4, and higher hydrocarbons, the GC was standardised with these hydrocarbon compounds so that their resulting hydrocarbon peaks could be detected together with their retention times that could be used for product qualitative and quantitative analysis. Employing the use of a micropipette, 50 μl of C2, C3, and C4 hydrocarbons was pipetted from the as-received standard. Using a 10 μl syringe the mixture was then injected into the GC column for calibration. As a result of this process, retention times and area under the peak of each compound was observed and recorded. The same procedure was repeated for methanol and dimethyl. The size of the area under a peak after elution of a compound is directly proportional to the number of molecules of that compound present.

Methanol and dimethyl ether that were considered reactants to this process were used to standardise the G.C so that the conversion efficiency of the catalyst (H-FF2, H-FF3, and commercial H-ZSM-5) and the selectivity towards olefins (C2, C3, and C4 compounds) could be calculated using equation 3.1 to 3.8

CHAPTER 4
CHARACTERISATION OF FLY ASH, FUSED FLY ASH, FUSED FLY ASH EXTRACT AND THE SYNTHESISED FLY ASH BASED ZEOLITE ZSM-5 PRODUCTS

4.1. Introduction

This chapter presents the physical and chemical properties of the as-received Arnot fly ash (FA), fused fly ash (FFA), and fused fly ash extract (FFAE) using XRD, SEM, XRF, FTIR and ICP-OES analytical techniques. The obtained results were presented as basis for synthesis. It also highlights the physico-chemical properties of zeolite ZSM-5 samples that were synthesised from fused fly ash extract with the addition of small amounts of fumed silica using the synthesis formulation detailed in Table 3.3. The synthesised Na-FF1-TPBr, Na-FF2-TPBr, and Na-FF3-TPBr were ion exchanged to their acid form (H-form) by using a 1M NH_4NO_3 solution and a calcination process. Thereafter, the ion-exchanged supernatants of the ZSM-5 products were characterised using ICP-OES analytical technique. Finally, the synthesised H-ZSM-5 products were characterised and compared with the commercial H-ZSM-5 using the following analytical methods: XRD, SEM/EDS, NMR, FTIR, and N_2 BET methods. The GC results of hydrocarbons that were used to analysed products coming from the methanol to hydrocarbons reaction was also presented in this chapter.

4.2. Characterisation of the as-received Arnot fly ash (FA), fused fly ash (FFA) and fused fly ash extract (FFAE)

The XRD, SEM, and FTIR data of the as-received fly ash (FA), fused fly ash (FFA), and fused fly ash extract (FFAE) are presented and compared in this section. The XRF and ICP-OES data revealed the elemental composition of the as-received fly ash and fused fly ash extract (FFAE) respectively. Finally, the ion-exchanged supernatant of the synthesised zeolite ZSM-5 products were also analysed using the ICP-OES technique.

Figure 4.1 presents the XRD pattern of the as-received fly ash (FA), fused fly ash (FFA) and fused fly ash extract (FFAE)

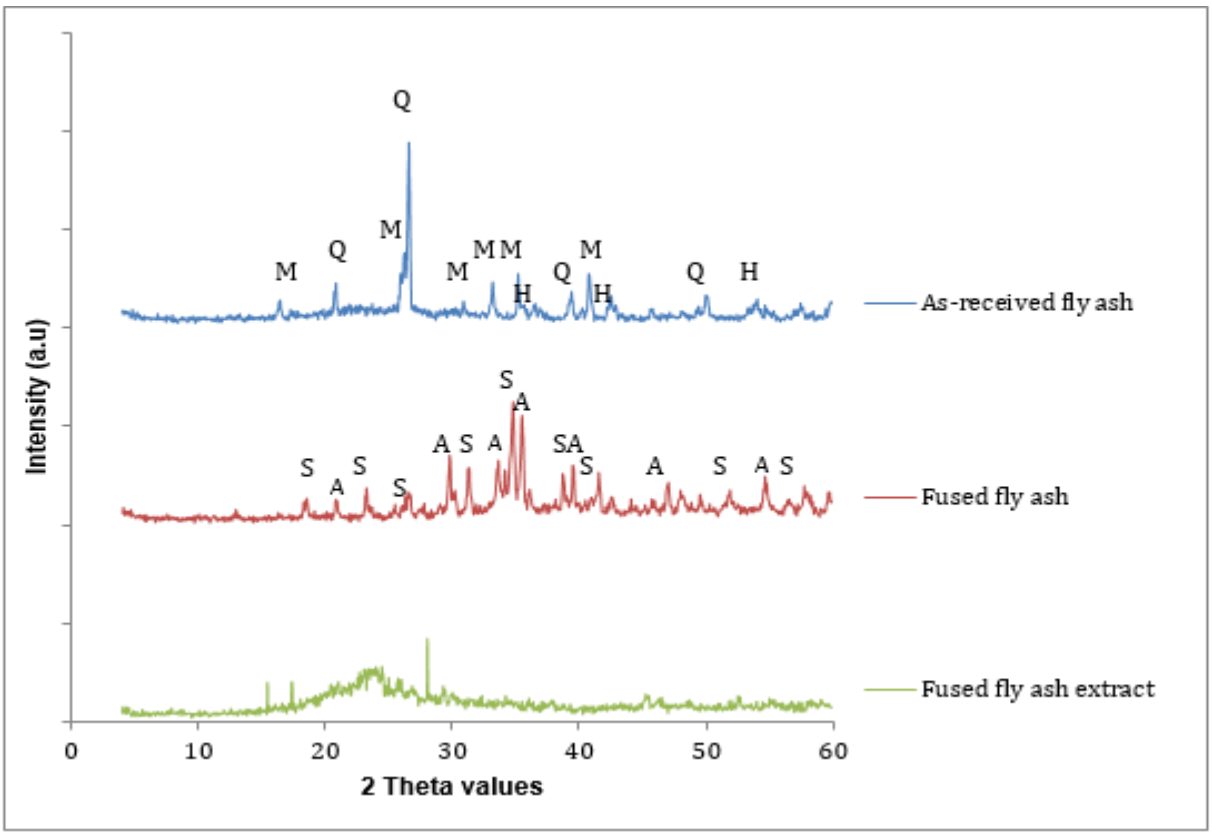

Figure 4. 1: Comparative XRD pattern of the as-received fly ash (FA), fused fly ash (FFA), and fused fly ash extract (FFAE) and Q, M, and H stands for quartz, mullite, and hematite phases respectively while S = sodium silicate and A = sodium aluminate

From the XRD results shown in Figure 4.1, it could be seen that the major crystalline phases of the as-received fly ash were identified to be quartz (SiO_2), mullite ($3Al_2O_3.SiO_2$), and lastly hematite (Fe_2O_3. The glassy amorphous material observed in the fly ash XRD spectra was apparent as an extensive low background hump between 18 and 36^0 2Theta and has been reported by other authors (Criado et al., 2007, Inada et al., 2005).

In the XRD spectra of fused fly ash (FFA), it was noticed that all the main quartz and mullite mineral phases of the raw fly ash were fully converted to Na-silicate or Na-aluminate. The occurrence of the new mineral phases in fused fly ash (FFA) was due to the solid-state reaction between the as-received fly ash (FA) and NaOH in the presence of heat (Ojha et al., 2004)

Finally, the XRD spectra of fused fly ash extract (FFAE) revealed that the extract was composed of mainly amorphous silica. This can identified by the hump that occurred between 18 and 36^o 2θ. Comparative XRD study of fused fly ash extract (FFAE) and the as-received fly ash showed that they had in common the hump that characterised the presence of amorphous silica. The fusion process of the as-received fly ash digested the quartz and mullite phases completely and it is noteworthy that the new formed sodium silicate and sodium aluminate lost all crystallinity after sulphuric acid treatment and the precipitate formed was fully amorphous.

This result was in agreement with the XRD pattern of amorphous silica that was reported by Rida and Harb, (2014). Figure 4.2 presents the structural analysis of the as-received fly ash (FA), fused fly ash (FFA), and fused fly ash extract (FFAE)

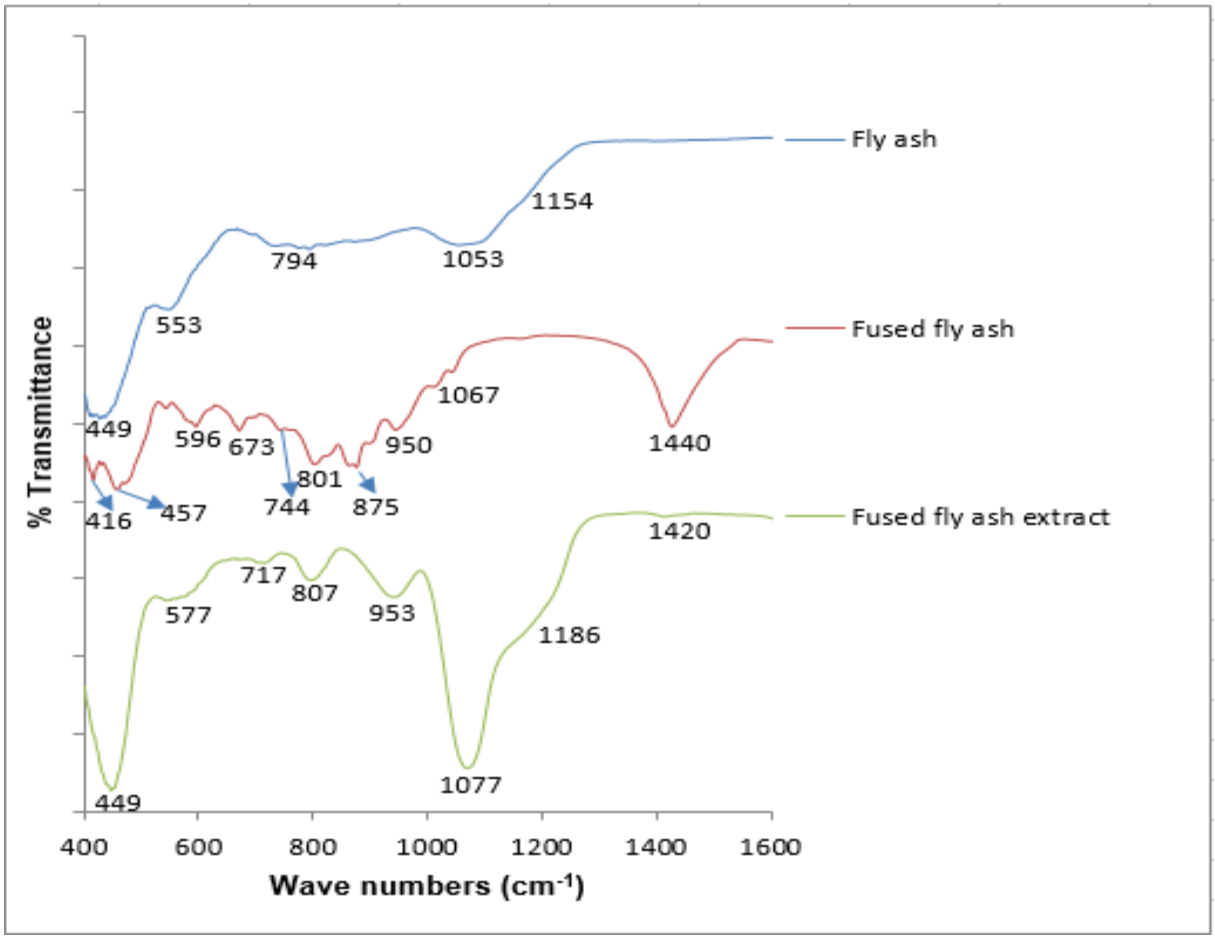

Figure 4. 2: FT-IR spectrum of the as-received fly ash (FA), fused fly ash (FFA) and fused fly ash extract (FFAE)

The FTIR data of the as-received Arnot fly ash presented in Figure 4.2 revealed three characteristic bands of either silica or alumina bonding to an oxygen atom. The band at 433 cm^{-1} could be assigned with the T-O bending vibrations (T= Al, Si). The characteristic bands that were noticed at 800 cm^{-1} were attributed to the symmetric stretching vibration of T-O (T=Si, Al) that indicates the presence of quartz. The band noticed at 1067 cm^{-1} was assigned to the asymmetric stretching vibrations of T-O (T= Si, Al). A less significant band that appeared at 1153 cm^{-1} was suggested by Ojha et al. (2004) to be a symmetrical and asymmetrical stretching vibrations of the Al-O-Si groups. Lastly the band appearing at 552 cm^{-1} could be assigned to the Al-O stretching for mullite.

According to Bass and Turner (1997) the FTIR data of fused fly ash showed vibrational bands of sodium silicate species between 700 cm^{-1} to 1240 cm^{-1} while glassy sodium silicate species were noticed below 600 cm^{-1}. In this study, these vibrational bands were noticed at 744 cm^{-1},

801 cm^{-1} and 1067 cm^{-1} while the intense peaks at 875 cm^{-1} and 950 cm^{-1} could be assigned to orthosilicates. The peak at 449 could be assigned to the vibration of T-O bending (Fernández-Jiménez and Palomo, 2005). Li et al. (2011) suggested that the peak at 875 cm^{-1} could be associated to tetrahedral aluminate ions while the peak at 1440 cm^{-1} could be attributed to the presence of carbonates in the fused fly ash (Zheng et al., 1997). The silicate vibrational bands in the as-received fly ash is noticed to be broad and diffuse due to different silicate vibrations from different minerals that are overlapping (Mollah et al., 1999).

The FTIR spectra of fused fly ash extract (FFAE) had Si-O-Si vibrations. The band at 499 cm^{-1} and 717 cm^{-1} could be attributed to Si-O-Si bending vibration or stretching vibration respectively (Rida and Harb, 2014). The band observed at 577 cm^{-1} could be assigned to Al-O stretch (Voll et al., 2002). The band noticed at 953 cm^{-1} could be attributed to the stretch of Si-O (Bass and Turner, 1997). The vibrational band for H-O-H water bending was noticed at 1420 cm^{-1} (Saikia and Parthasarathy, 2010). The band at 807 could also be attributed to Si-O-Si bond stretching vibration (Rida and Harb, 2014). The Band noticed at 1077 and 1186 could be assigned to asymmetric stretching vibrations (Tao et al., 2006). It was noteworthy that the FTIR spectra of fused fly ash extract (FFAE) did not show characteristic bands of the commercial ZSM-5 presented in Figure 4.2 hence no ZSM-5 phase was observed (as also complemented by its XRD spectra in Figure 4.1). Figure 4.3 presents the SEM micrographs of fly ash (FA), fused fly ash (FFA), and fused fly ash extract (FFAE)

a

b

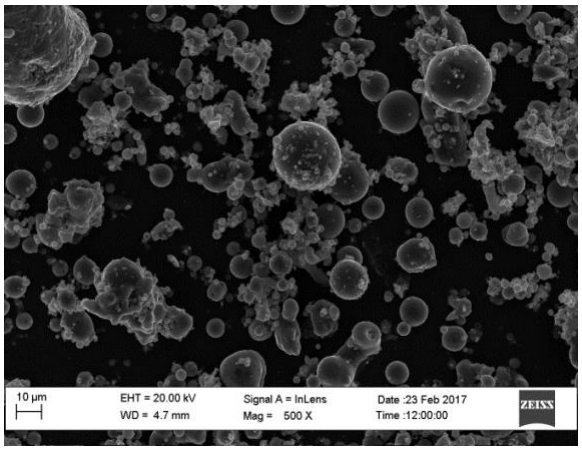

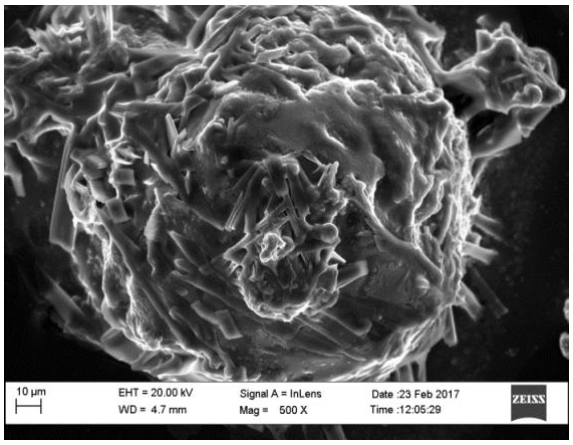

c

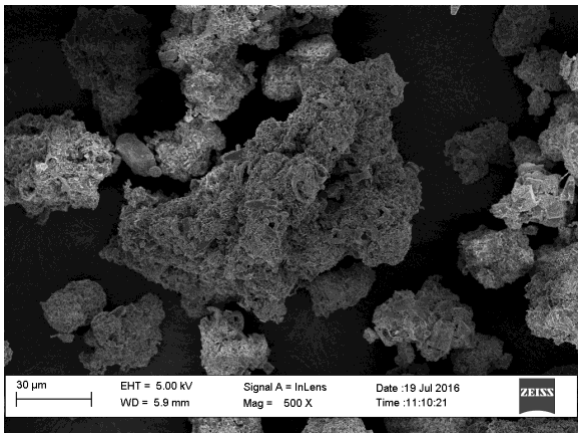

Figure 4. 3: SEM micrographs of a) Fly ash, b) fused fly ash and c) fused fly ash extract (silica extract)

When the morphology of the raw fly ash (in Figure 4.3 a) was observed, majority of the fly ash particles were smooth and spherical in shape. The spherical nature of the fly ash particles was due to fly ash solidification as suspended droplets cool down in flue gas (Lu et al., 2003). In addition, the smoothness of the fly ash particles can be attributed to the presence of amorphous molten glass phase covering the fly ash particles (Inada et al., 2005). Finally, it can also be noticed that though most of the fly ash particles size are less than 10 μm, there were some larger and indefinite shaped particles present. What was not easily identified on the as-received fly ash SEM micrograph were their mineral phases. This was because crystalline components are very small and intimately intermixed in the glass (Ward and French, 2005).

When the morphology of the Arnot fused fly ash (in Figure 4.3 b) was investigated, it was observed that there was a significant transformation from the spherical shaped particles of the raw fly ash to a porous mass of fused fly ash. This can be attributed to the solid-state reaction between NaOH and the as-received fly ash during fusion as detailed in section 3.3.2. The porous mass of material that was identified by the XRD technique to be a Na-aluminosilicate

phase had a green colour. In agreement with Shigemoto et al. (1993) and Musyoka et al. (2012), the amorphous phase in the fused fly ash is readily soluble in water and alkali solutions. One of the reasons NaOH was used during the fusion process of the as-received fly ash was that it acts as an additional source of Na^+ that plays an important role in stabilising the sub-building unit during the synthesis of zeolites from fly ash (Ojha et al., 2004). The OH group from NaOH also plays a critical role in breaking down the complex silicon content in the minerals into simpler form.

Figure 4.3 (c) showed that the obtained morphology of fused fly ash extract (also known as silica extract) was different from that of the as-received fly ash (FA) and fused fly ash (FFA). However, the morphology of fused fly ash extract was similar to the amorphous silica SEM micrograph that was reported by Abou Rider and Harb, (2014). Furthermore, the elemental composition of the as-received fly ash (FA) and fused fly ash extract (FFAE) were determined using XRF and ICP-OES respectively. During analysis, the XRF technique was carried out in triplicate on the same fly ash but fresh samples of the same batch. The standard deviation of the oxides in the fly ash sample was calculated based on their mean value.

Table 4.1 presents the elemental composition of the as-received Arnot fly ash (FA) on a volatile free basis.

Table 4. 1: Elemental compositions of the as-received Arnot coal fly ash (n=3) (F1 = first XRF analysis of fly ash, F2 = second XRF analysis of fly ash, F3 =third XRF analysis of fly ash of the same batch, Fav = average XRF analysis of fly ash, SD = standard deviation)

Mass %					
Element (oxide)	F1	F2	F3	F_{av}	SD
SiO_2	57.35	57.4	57.43	57.39	57.39±0.03
Al_2O_3	28.98	29.07	29.15	29.06	29.06±0.06
CaO	5.03	4.96	4.92	4.97	4.97±0.04
Fe_2O_3	5.31	5.23	5.2	5.24	5.24±0.04
MgO	1.09	1.08	1.06	1.07	1.07±0.01
TiO_2	1.1	1.1	1.1	1.1	1.10±0.00
K_2O	0.62	0.62	0.61	0.61	0.61±0.00
P_2O_5	0.37	0.37	0.36	0.36	0.36±0.00
Na_2O	0.09	0.08	0.1	0.09	0.09±0.00
MnO	0.05	0.05	0.05	0.05	0.05±0.00
SO_3	0.06	0.08	0.05	0.06	0.06±0.01
SUM	100.05	100.04	100.30	100.00	100±0.10
SiO_2 /Al_2O_3	1.97	1.97	1.97	1.97	

From the XRF results of the as-received fly ash reported in Table 4.1, it could be observed that the two main oxides detected in the sample were SiO_2 and Al_2O_3 that sum up to 83.33% of the total oxides in the sample. Other oxides that were detected in small percentages but were significantly more than others were CaO, Fe_2O_3, MgO, and TiO_2. The calculated standard deviation of the as-received fly ash was noticed to be very small and this indicated that the as-received fly ash was homogenous. It was reported by Querol et al. (2002) that fly ash can be utilised as a raw material towards the synthesis of zeolites such as FAU etc. due to its likeness to some volcanic material that are precursors of natural zeolites. On the contrary, the as-received fly ash was not suitable for the synthesis of zeolite ZSM-5 due to a Si/Al ratio far less than 10 (as shown in Table 4.1 to be 1.97). In order to boost up the Si/Al ratio in the as-received fly ash, the raw fly ash was fused with sodium hydroxide and mixed with deionised water to obtain a slurry that was filtered prior to treatment with concentrated sulphuric acid (98-99%) to extract silica (named fused fly ash extract). The elemental composition of fused fly ash extract (FFAE) is presented in Figure 4.4

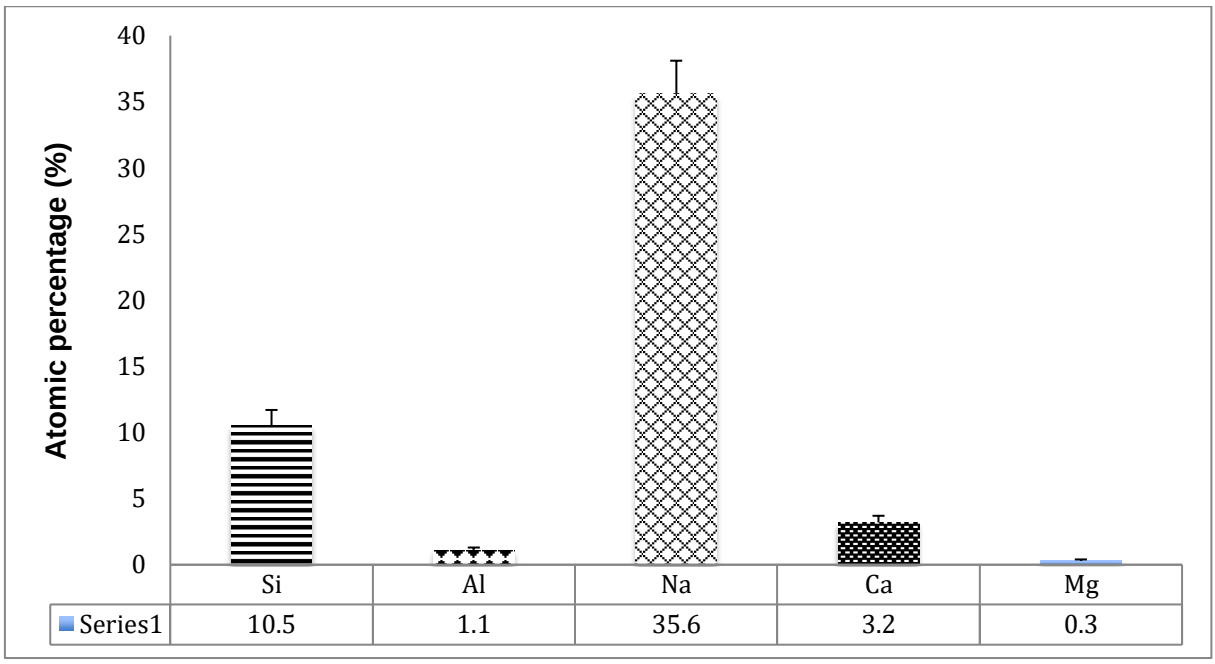

Figure 4. 4: Elemental composition of the Arnot fused fly ash extract (ICP-OES)

The elemental composition of fused fly ash extract (FFAE) reported in Figure 4.4 was presented in atomic percentage (%). It could be observed that the atomic percentage of oxygen in the fused fly ash extract was not reported given the fact that ICP-OES analytical technique could only quantify cations and metals. It was also noticed that the sodium content in the fused fly ash extract (FFAE) was the most abundant with an atomic percentage of 33.2%. This was sodium coming from the fusion process of fly ash with NaOH (fused fly ash). Silicon content was the second highest with an atomic percentage of 10.5 %, followed by calcium (3.2%), aluminium (1.1%), and magnesium (0.3%) respectively. When the Si/Al ratio of the fused fly ash extract was calculated based on the results in Figure 4.4, it was found to be 9.5. The obtained ratio was still not deemed siliceous enough for the synthesis of a highly siliceous zeolite such as ZSM-5. In order to synthesise zeolite ZSM-5 as suggested by Van der Gaag (1987), a Si/Al ratio above 10 is required and therefore to boost up the Si/Al ratio of fused fly ash extract (FFAE), 0.000, 0.250 g or 0.375 g of fumed silica was added to its synthesis gel (see Table 3.3 section 3.3.1). Thereafter, 1 g of tetrapropylammonium bromide (TPBr) as a structure-directing agent was also added to the synthesis gel prior to hydrothermal crystallisation as detailed in section 3.3.4. After hydrothermal crystallisation, the samples were washed, dried, detemplated, ion exchanged with a 1M NH_4NO_3 solution followed by calcination to transform the synthesised Na-ZSM-5 products (Na-FF1-TPBr, Na-FF2-TPBr, and Na-FF3-TPBr) to their H-form (H-FF1, H-FF2, and H-FF3). The ion exchanged solutions of Na-FF1, Na-FF2, Na-FF3 and the commercial Na-ZSM-5 were then analysed using ICP-OES technique as detailed in section 3.5.7 so that the concentration of various charge balancing cations such as sodium (Na), calcium (Ca), magnesium (Mg), potassium (K), iron (Fe), zinc (Zn), and copper (Cu) could be detected and quantified.

Figure 4.5 presents the concentration of cations exchanged from Na-FF1, Na-FF2, Na-FF3 and the commercial Na-ZSM-5

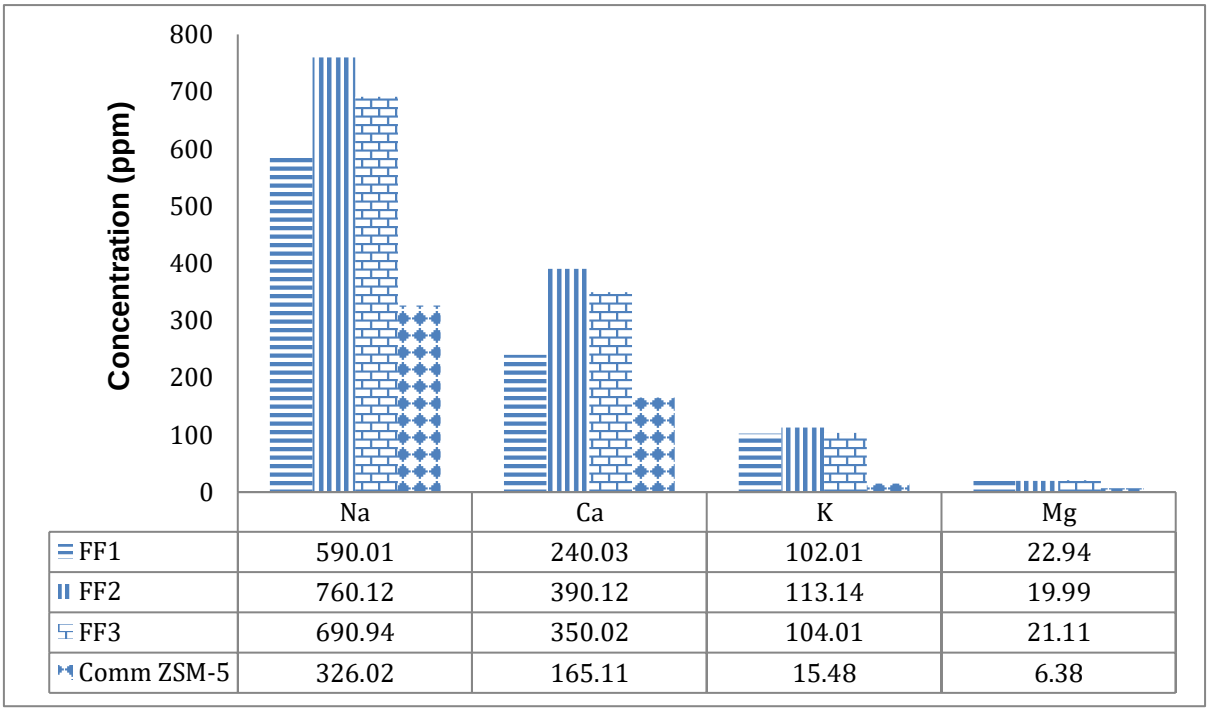

	Na	Ca	K	Mg
FF1	590.01	240.03	102.01	22.94
FF2	760.12	390.12	113.14	19.99
FF3	690.94	350.02	104.01	21.11
Comm ZSM-5	326.02	165.11	15.48	6.38

Figure 4. 5: Concentration (ppm) of cations exchanged or leached out from Na-FF1, Na-FF2, Na-FF3 and the commercial Na-ZSM-5 in 1 M NH_4NO_3 solution (10 mL of acid solution: 1 g of catalyst)

Figure 4.5 reported the concentration of exchangeable cations (Na^+, Ca^{2+}, $Mg^{2+,}$, K^+, Fe^{2+}, Cu^{2+}) in the ion exchanging solutions of Na-FF1, Na-FF2, Na-FF3 and commercial Na-ZSM-5. It could be observed that the most abundant cations exchanged out of the zeolites (Na-FF1, Na-FF2, Na-FF3, and com Na-ZSM-5) were sodium and calcium that followed a sequence of Na^+> Ca^{2+}> Mg^2 > $k^{+,}$ > Fe^{2+}> Cu^{2+}. This pattern could be attributed to the high capacity for sodium and magnesium to be replaced by the ammonium ion but some of the Na in the supernatant could possibly be remnants from Na used in fusion. The commercial zeolite contained the least charge balancing counterions as could be expected as it was provided in its Na-form. Metal ions in the synthesised fly ash based zeolite ZSM-5 products are related to their content in the fly ash based feedstock (Missengue et al., 2016). In this line of investigation, Kirov and Filizova (2012) studied the influence of the extra framework charge balancing cations such as Na^+, Ca^{2+}, and Mg^{2+} during the synthesis of zeolites and they concluded that Na^+, Ca^{2+}, and Mg^{2+}, influences the stability of the large channels in ZSM-5. This can be attributed to their capacity of hydration and where they could be situated in the channels (Kirov and Filizova, 2012), Meanwhile Petrik et al. (1995) reported that K^+ may cause problems during self-assembly of the precursor phase of zeolite ZSM-5 and therefor limits effective zeolitisation. The complex nature of the bulk composition of the as-received fly ash used in this study for the synthesis of

zeolite ZSM-5 products makes it very difficult to attribute any one component to a particular outcome.

The following section presents the physico-chemical properties of zeolite ZSM-5 samples that were synthesised from fused fly ash extract (FFAE) with the addition of small amounts of fumed silica.

4.3. Effect of fumed silica on the properties of zeolite ZSM-5 products synthesised from fused fly ash extract (FFAE)

H-FF1, H-FF2, and H-FF3 that were synthesised from fused fly ash extract (FFAE) with the addition of a silica source (named fumed silica) were characterised and compared with that of a commercial zeolite ZSM-5 purchased from Zeolyst. This was to determine the effect of fumed silica on the quality/purity, crystallinity, morphology, Si/Al ratio and N_2 BET surface area of the synthesised ZSM-5 products.

4.3.1. Mineralogical and relative crystallinity study of the synthesised zeolite ZSM-5 products and the commercial H-ZSM-5 by X-ray diffraction technique (XRD)

The effect of adding different small amounts of fumed silica into the synthesis mixture of fused fly ash extract (FFAE) on the mineralogy of ZSM-5 products was investigated. Figure 4.6 compares the X-ray diffraction patterns of the synthesised ZSM-5 products (H-FF1, H-FF2 and H-FF3) with that of a commercial H-ZSM-5 zeolite. As a reminder, H-FF1, H-FF2, or H-FF3 was synthesised when 0.000 or 0.250, or 0.375 g of fumed silica was added to the following compounds: 2.5 g of fused fly ash extract (FFAE), 40 mL of distilled water and 1 g of tetrapropylammonium bromide (template or structure directing agent). The hydrothermal synthesis condition was set at 165 ^{0}C for 72 hours. Thereafter crystallisation, Na-FF1-TPBr, Na-FF2-TPBr, and Na-FF3-TPBr were washed, dried, detemplated, and transformed to their acidic form (H-form) by ion exchange and calcination. Figure 4.6 presents a comparative XRD diffraction pattern of H-FF1, H-FF2, H-FF2 and the commercial H-ZSM-5.

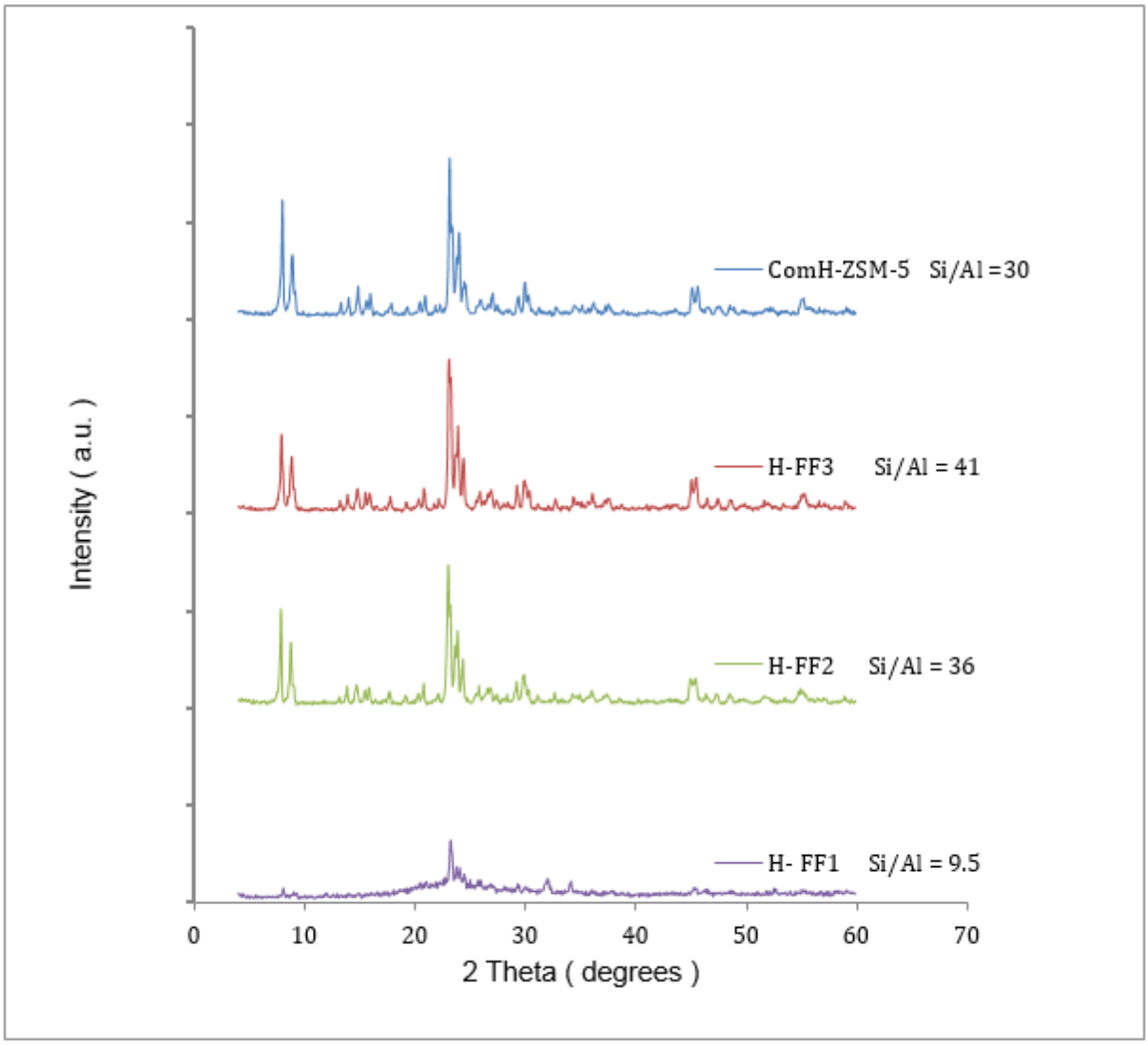

Figure 4. 6: Comparison of the XRD patterns of the synthesised fly ash based zeolite ZSM-5 products (H-FF1, H-FF2, H-FF3), with the commercial H-ZSM-5

Figure 4.6 XRD spectra showed that H-FF1 consisted mainly of amorphous silica phase with few ZSM-5 crystals formed (as complemented by the SEM results). This can be identified by the presence of a hump associated with low intensity ZSM-5 finger print peaks that occurred between 18 and 36^{o} 2 Theta. Partially crystalline H-FF1 was formed as a result of its low Si/Al ratio (Si/Al = 9.5). However, as the Si/Al ratio in the hydrothermal gel was adjusted above 10 (Si/Al = 36, and 41) by adding small amounts of fumed silica to the synthesis gel, the intensity of the ZSM-5 fingerprint peaks of H-FF2 and H-FF3 increased significantly. This indicated the complete formation of crystals and the absence of amorphous material after 72 hours at 165 ^{0}C. The absence of quartz and mullite phase in the synthesised ZSM-5 samples was as a result of the fusion process that digested both mineral phases in the fly ash (FA). It could also be observed that the X-ray diffraction (XRD) patterns of H-FF2 and H-FF3 were identical to the commercial H-ZSM-5. This was further proved by comparing the XRD patterns of the synthesised zeolite ZSM-5 products with the simulated XRD patterns for zeolite ZSM-5.

Traditionally, the synthesis of zeolite ZSM-5 directly from raw fly ash requires an excessive additional amount of silica source as reported by Kalyankar et al. (2011) and Chareonpanich et al. (2004) when zeolite ZSM-5 was synthesised from the Mae-Moh and Indian fly ash respectively. Unlike in the previous studies, the results presented in this section proved that the fusion step coupled with the extraction of silica (named FFAE) from fly ash led to the synthesis of high purity zeolite ZSM-5 products with small amounts of fumed silica added to the synthesis mixture. This method also digested the quartz and mullite phase observed by previous authors that hinders effective zeolitisation as well as crystallinity.

Figure 4.7 presents the calculated relative XRD crystallinity of H-FF1, H-FF2 and H-FF3 with the commercial H-ZSM-5 as a reference using Nicolaides equation (Nicolaides (1999)).

$$\text{Relative XRD Crystallinity} = \frac{Sum\ of\ peak\ intensity\ of\ sample}{Sum\ of\ peak\ intensity\ of\ standard} * 100 \quad \textbf{Equation 4. 1}$$

Based on Nicolaides equation, the peak intensities were measured using a software named Origin Pro 8 at the following peaks: 8.0, 8.8, 12.4, 13.7, 14.7, 15.9, 21.1, 23.2, 23.8, 24.5, 25.4, 29, 29.6, 44.7, and 45.5 ^{0} 2Theta on the XRD diffractogram

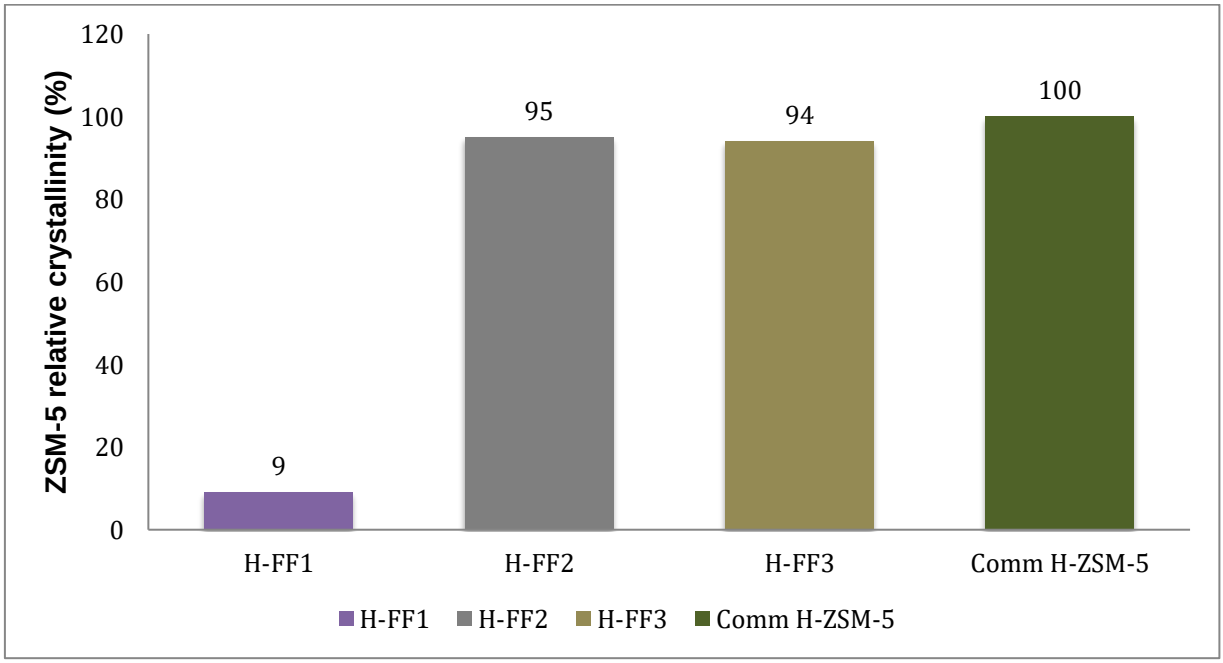

Figure 4. 7: Calculated relative XRD crystallinity of synthesised fly ash based zeolite ZSM-5 products (H-FF1, H-FF2 and H-FF3) compared with commercial H-ZSM-5

Figure 4.7 showed that the calculated XRD relative crystallinity of H-FF1, H-FF2, and H-FF3 were 9%, 95% and 94 % respectively relative to the commercial H-ZSM-5 zeolite that was 100%. H-FF1 had the lowest relative crystallinity since it was mostly made up of amorphous material. It could also be noticed that, the XRD relative crystallinity of H-FF2 to H-FF3 dropped

by 1 % when the Si/Al ratio increased from 36 to 41 % respectively. The 100 % relative crystallinity of the commercial H-ZSM-5 was due to high intensity of the ZSM-5 finger print peaks at 8.0 and 8.8. However, the XRD relative crystallinity of H-FF2 or H-FF3 was comparable to that of the commercial H-ZSM-5.

Figure 4.8 presents the SEM micrographs of H-FF1, H-FF2, H-FF3, and the commercial H-ZSM-5 in the following section

4.3.2. Morphological interpretation, elemental composition, and mean crystal size of the synthesised H-FF1, H-FF2, H-FF3 and the commercial H-ZSM-5 by using the SEM/EDS method

The effect of adding small amounts of fumed silica into the synthesis mixture of fused fly ash extract (FFAE) on the morphology and crystal size of zeolite ZSM-5 products (H-FF1, H-FF2, and H-FF3) was investigated by the SEM technique. During synthesis, FFAE (2.5 g) was mixed with 40 mL of deionised H_2O, (0.000, 0.250 or 0.375 g) of fumed silica, and 1 g of TPBr. The hydrothermal synthesis conditions were set at 165 ^{0}C for 72 h. Thereafter crystallisation, synthesised ZSM-5 products (Na-FF1-TPBr, Na-FF2-TPBr, or Na-FF3-TPBr) were filtered, washed, and dried in the oven set at 70 ^{0}C. Finally, Na-form of the synthesised ZSM-5 samples were then detemplated at 550 ^{0}C for 5 hours and transformed to their acidic form (H-form) using a 1 M NH_4NO_3 solution prior for calcination at 550 ^{0}C for 3 hours. The SEM micrographs of H-FF1, H-FF2 and H-FF3 were presented and compared to that of a commercial H-ZSM-5 zeolite as shown in Figure 4.8

Synthesised H-FF1

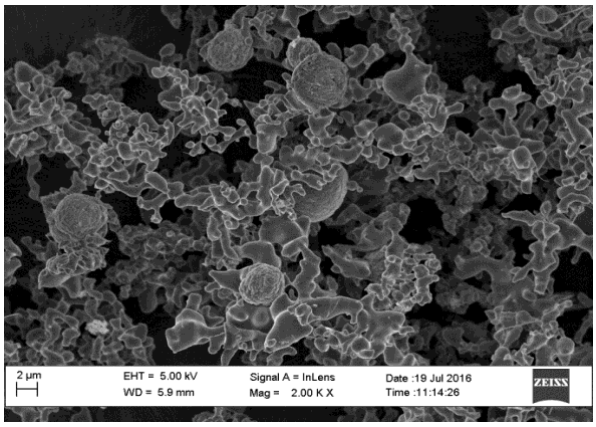

Synthesised H-FF2

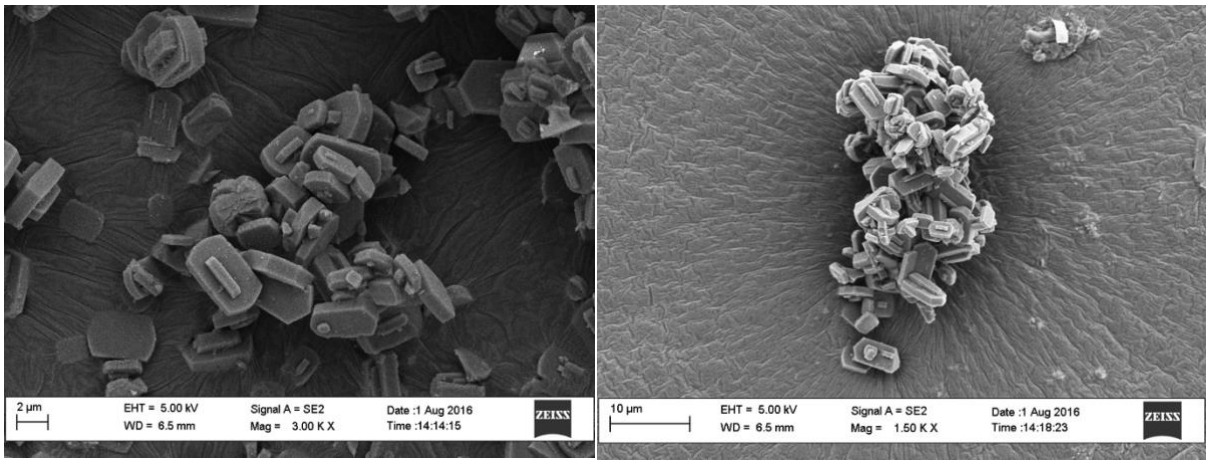

Synthesised H-FF3

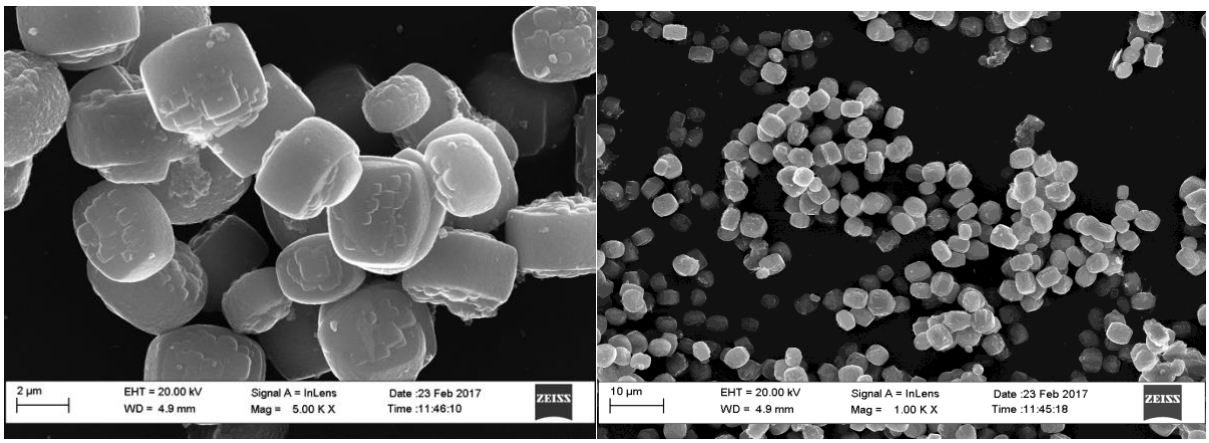

Commercial H-ZSM-5

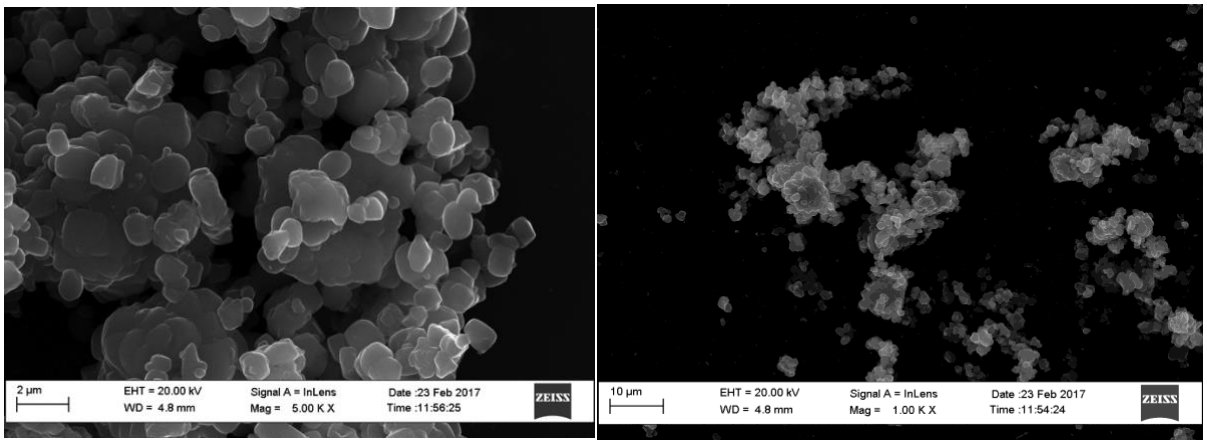

Figure 4. 8: SEM micrographs of H-FF1, H-FF2, H-FF3 and the commercial H-ZSM-5 (comm-ZSM-5)

Figure 4.8 SEM micrographs revealed that H-FF1 (Si/Al = 9.5) that was synthesised from fused fly ash extract (FFAE) without an additional silica source (0.000 g) was made up of mostly amorphous materials with few crystals formed (as complemented by the XRD technique).

However, H-FF2 and H-FF3 were made up of characteristic coffin shaped or cuboidal shaped crystals of ZSM-5 when the Si/Al was adjusted above 10. The commercial H-ZSM-5 was composed of characteristic spherulitic shaped crystals of ZSM-5. H-FF1, H-FF2, H-FF3 and the commercial H-ZSM-5 had different mean crystal length and width or crystal size (as proved in Figure 4.10). This may be attributed to their molar elemental composition or the Si/Al ratio of the hydrothermal gel used for their synthesis. Shirazi et al. (2008) reported that the morphology and crystal particles size of ZSM-5 depend mainly on the Si/Al ratio in the hydrothermal gel. Petrik et al. (1995) reported the synthesis of zeolite ZSM-5 products with similar Si/Al ratio but different morphologies by altering some of the synthesis parameters. These results corroborate the SEM results obtained in this study. Table 4.2 presents the elemental composition of the synthesised H-FF1, H-FF2, H-FF3 and the commercial H-ZSM-5 obtained from the SEM/EDS data.

Table 4. 2: Si/Al ratio of H-FF1, H-FF2, H-FF3 and commercial H-ZSM-5 (n=6, and spec=spectra)

H-FF1	EDS data
Elements (%)	Si/Al = 9.5
Al	
Si	
O	

H-FF2	EDS data						
Elements (%)	Spec 1	Spec 2	Spec 3	Spec 4	Spec 5	Spec 6	$Spec_{All}/6$
Al	0.86	0.81	0.72	0.79	0.81	0.84	0.80
Si	33.90	31.04	27.32	27.31	27.24	26.90	28.95
O	65.24	68.15	71.95	71.91	71.95	72.25	70.24
Si/Al ratio	36						

H-FF3	EDS data						
Elements (%)	Spec 1	Spec 2	Spec 3	Spec 4	Spec 5	Spec 6	$Spec_{All}/6$
Al	0.84	0.93	0.89	0.76	0.87	0.90	0.86
Si	35.22	34.98	33.80	33.15	37.52	35.48	35.02
O	63.94	64.09	65.32	66.10	61.61	63.62	64.11
Si/Al ratio	41						

Commercial H-ZSM-5	EDS data
Elements (%)	Si/Al = 30
Al	
Si	
O	

The procedure used during the elemental analysis on each ZSM-5 sample was that six different areas on each sample were targeted and analysed for silica, alumina, and oxygen. The obtained mean result of silica and alumina on each sample was used to establish the Si/Al ratio of that ZSM-5 sample. From Table 4.2, it could be noticed that the Si/Al ratio of the synthesised ZSM-5 samples increased from H-FF1<H-FF2<H-FF3 when the elemental composition of the synthesis gel was adjusted with different amounts of fumed silica. It was also observed that the Si/Al ratio of the commercial H-ZSM-5 was 30. Finally, the mean crystal length and width or crystal size of H-FF2, H-FF3 or the commercial H-ZSM-5 was determined using the image J software tool, the mean equation (4.2) and 20 crystal particles of each sample. The mean crystal length and width of H-FFI was difficult to analyse since the few crystals formed after hydrothermal crystallisation were intermixed in amorphous material. Moreover, its calculated XRD relative crystallinity and SEM results proved that H-FF1 was not a pure phase zeolite and hence was not further analysed.

Equation 4.2 and Figure 10 presents the mean equation and the mean crystal size of the ZSM-5 products

$$AM = \frac{1}{n}\sum_{i=1}^{n} a_i = \frac{1}{n}(a_1 + a_2 + \cdots + a_n) \ldots\ldots\ldots\ldots \text{(Equation 4.2)}$$

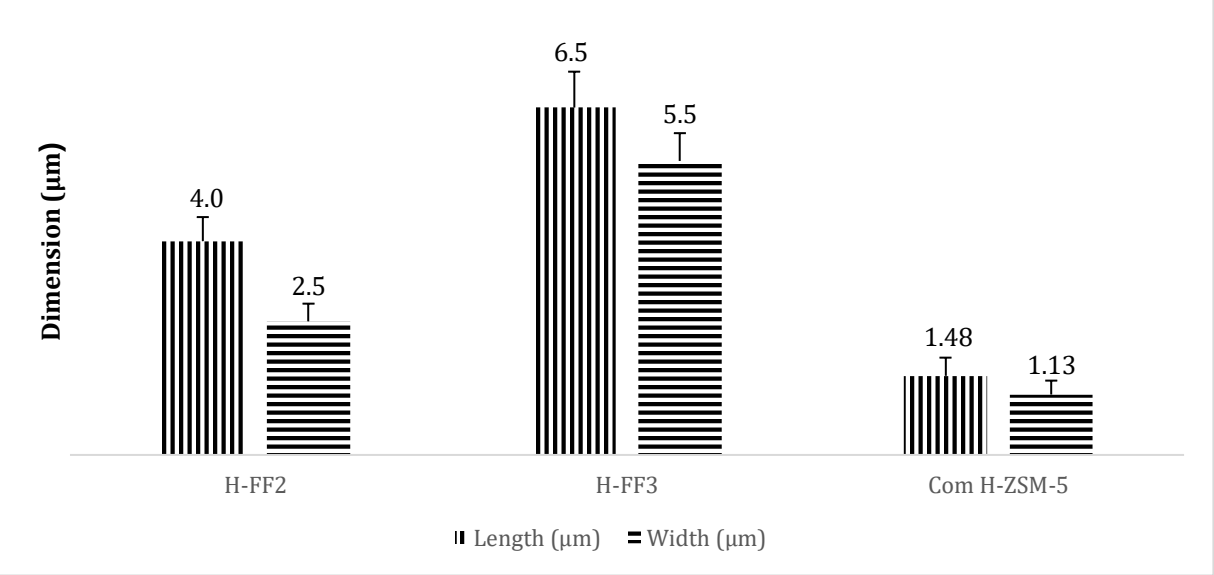

Figure 4. 9: Comparative mean ZSM-5 length and width of H-FF2, H-FF3, and commercial H-ZSM-5

It was observed from Figure 4.9 that the synthesised ZSM-5 mean crystal length and width increased from H-FF2 (4 ±0.45 by 2.5 ± 0.33 μm) to H-FF3 (6.5 ± 0.67 by 5.5 ± 0.52 μm) as the Si/Al ratio in the hydrothermal gel of fused fly ash extract (FFAE) increases from 36 to 41 respectively. The mean crystal length and width of the commercial H-ZSM-5 was found to be

(1.48± 0.34 by 1.13 ± 0.26 μm) with a Si/Al ratio of 30. Taking into consideration the error bars associated with H-FF2 or H-FF3 mean crystal length and width, the obtained results are in good agreement with Shirazi et al. (2008) who reported that the mean crystal size of zeolite ZSM-5 increased from 1 to 10 μm with an increase in the Si/Al ratio from 10 to 50. The framework and extra framework aluminium of H-FF1, H-FF2 and the commercial H-ZSM-5 were investigated and the results are presented in Figure 4.10

4.3.3. Analysis of aluminium and silica coordination of H-FF2, H-FF3 and the commercial H-ZSM-5 by ^{27}Al and ^{29}Si nuclear magnetic resonance (NMR)

The percentage of aluminium in the framework and extra-framework of the synthesised H-FF2 and H-FF3 was investigated and compared with that of a commercial H-ZSM-5 using their solid-state ^{27}Al NMR spectra as presented in Figure 4.10. During analysis, 0.1 M of $Al(NO_3)_3$ solution was used as a reference. In this study, Na-FF2-TPBr and Na-FF3-TPBr were synthesised from fused fly ash extract (FFAE), fumed silica (small amounts), deionised water, and TPBr as a structure-directing agent. Thereafter synthesis, Na-FF2-TPBr and Na-FF3-TPBr were transformed to their acidic form (H-form) by treatment with 1 M NH_4NO_3 solution (10 mL of acid solution: 1 g of catalyst) followed by calcination at 550 ^{0}C for 5 hours. Figure 4.11 presents the Solid-state ^{27}Al NMR results of the synthesised H-ZSM-5 samples and the commercial H-ZSM-5.

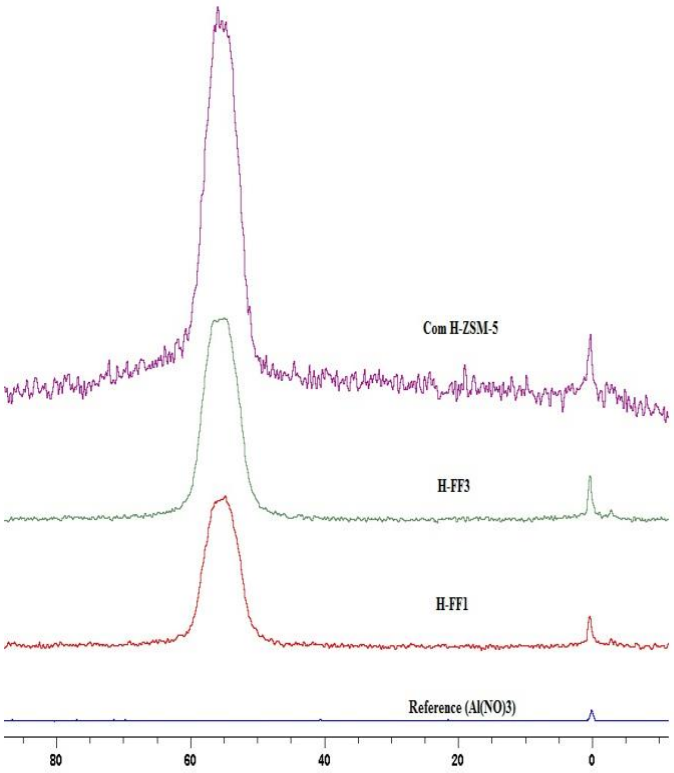

Figure 4. 10: ^{27}Al NMR of referenced $Al(NO_3)_3$, H-FF2, H-FF3, and commercial H-ZSM-5

The ^{27}Al NMR of H-FF2, H-FF3 and the commercial H-ZSM-5 are presented in figure 4.10. A characteristic strong signal with a chemical shift at 55 ppm is attributed to Al tetrahedrally co-ordinated with the SiO_4 framework (Triantafillidis et al., 1999). A small signal indicating octahedrally coordinated extra-framework Al atoms was observed for all ZSM-5 samples at a resonance corresponding to 0 ppm on the spectra. These results are in accordance with the results reported by Sazama et al. (2011). Triantafillidis et al. (1999) reported that the extra-framework aluminium that was displayed at resonance corresponding to 0 ppm does not exhibit any form of acidity in the zeolite. Previous authors such as Katada et al., (1997) also reported that aluminium atom pairs that appear as four-member rings are aluminium atoms that do not exhibit any form of acidity and hence are extra-framework aluminium. However, Katada et al. (1997) pointed out that the aluminium atom pairs that appear as a four-member ring may display some form of acidity if one of the aluminium atoms was blocked by sodium. From Figure 4.10 it was also noticed that the intensity of the peaks at 55 ppm was stronger in the commercial H-ZSM-5 than in the synthesised ZSM-5 samples. This can be attributed to a more significant well-arranged coordination of the framework aluminium as complemented by the XRD crystallinity. The percentage of framework and extra framework Al in H-FF2, H-FF3 or the commercial H-ZSM-5 was calculated based on equation 4.3

$$\% = \frac{Intergration_i}{\sum Intergration_i} * 100 \quad \text{.....Equation 4.3}$$

Table 4. 3: Percentage of framework and extra-framework aluminium in the reference $Al(NO_3)_3$, H-FF2, H-FF3 and the commercial H-ZSM-5

Samples	Framework tetrahedrally coordinated aluminium (%)	Extra framework octahedrally coordinated aluminium (%)
Reference $Al(NO_3)_3$	00.0	100.0
H-FF2	97.5	2.5
H-FF3	96.0	4.0
Commercial H-ZSM-5	96.5	3.5

It could be seen from Table 4.3 that the percentage of tetrahedrally coordinated Al (framework Al) or octahedrally coordinated Al (extra-frame work Al) of H-FF2, H-FF3 and commercial H-ZSM-5 were 97.5, 96, 96.5 or 2.5, 4.0, and 3.5 respectively. These results contradicted the XRD relative crystallinity results of H-FF2, H-FF3, and the commercial H-ZSM-5 that was 95,

94 and 100% respectively. Figure 4.12 presents the silica coordination in H-FF2, H-FF3 and the commercial H-ZSM-5 using the ^{29}Si nuclear magnetic resonance (NMR)

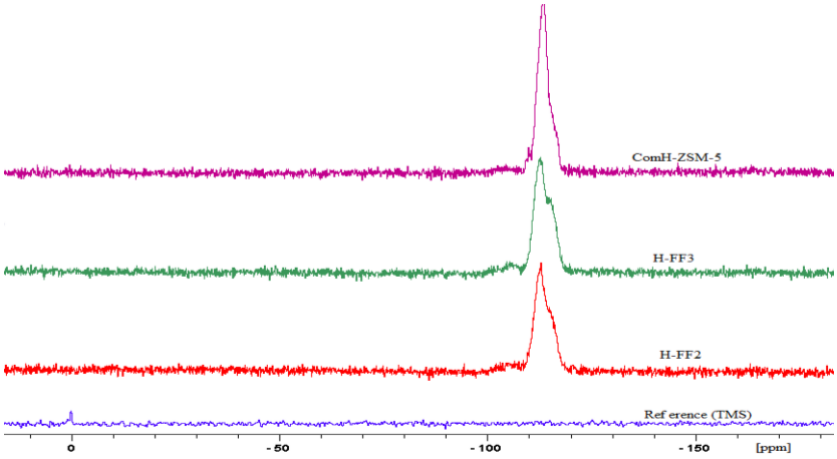

Figure 4. 11: Comparative 29Si NMR of synthesised H-FF2, H-FF3 with Com H-ZSM-5

From Figure 4.11, the large peak observed at -112 and the shoulder noticed at -115 can be attributed to $Si(OSi)_4$ unit. The peak at -105 can be assigned to $Si(OSi)_3$ unit.

4.3.4. Structural analysis of the synthesised ZSM-5 products (H-FF2 and H-FF3) and the commercial H-ZSM-5 by Fourier transformed infrared (FTIR)

Figure 4.13 presents the Fourier transformed infrared (FTIR) spectra of the synthesised H-FF2 and H-FF3 compared to that of the commercial H-ZSM-5. H-FF2 and H-FF3 were synthesised from fused fly ash extract (FFAE) using the procedure detailed in section 3.3.1. Thereafter, Na-FF2-TPBr and Na-FF3-TPBr were converted to H-FF2 and H-FF3 using a 1 M NH_4NO_3 solution. The Na-form of the commercial ZSM-5 was converted to its H-form using the same procedure (refer to section 3.3.1).

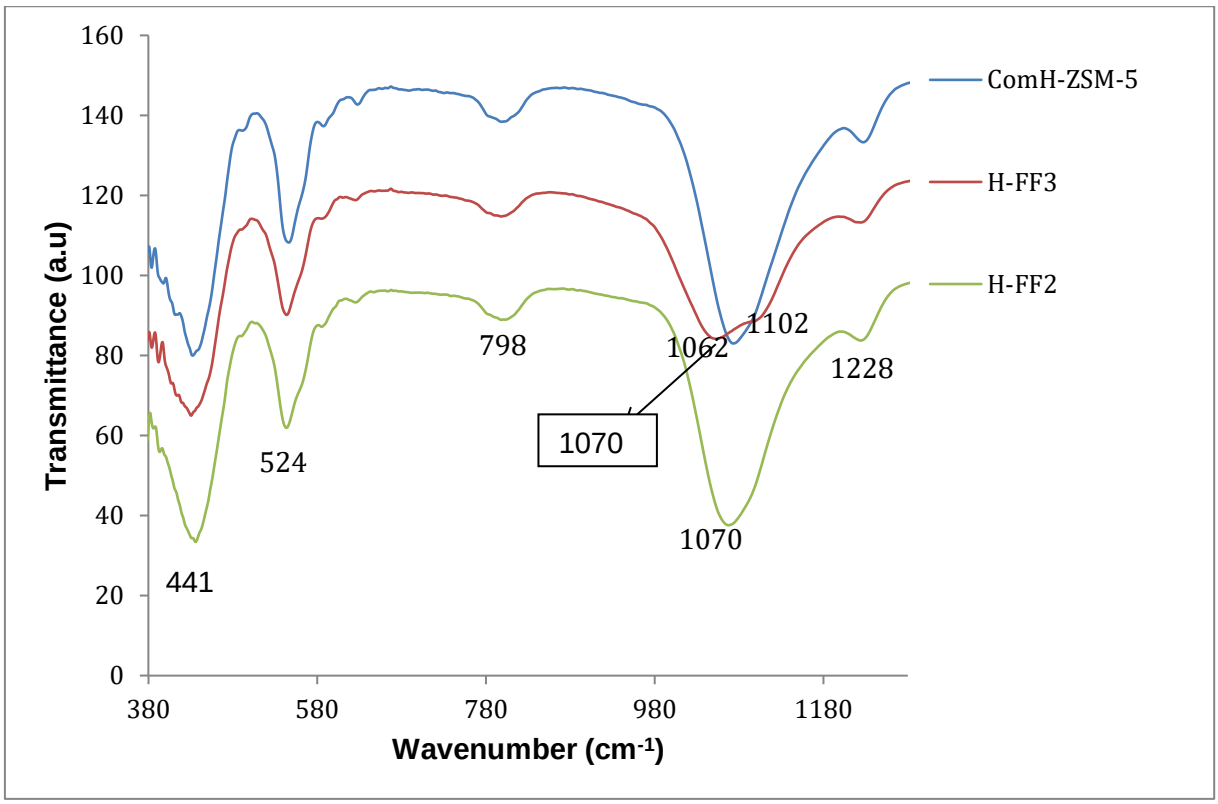

Figure 4. 12: FTIR spectra of H-FF2, H-FF3, and the commercial H-ZSM-5

From Figure 4.12, H-FF2 and H-FF3 presents characteristic bands of ZSM-5 at 441, 524, 798, (1070 for H-FF2 and commercial H-ZSM-5), (1062, 1102 for H-FF3), and 1228 cm^{-1}. The characteristic bands at 441 and 524 could be assigned to a Si-O bend and a double ring vibration respectively (Shirazi et al., 2008). The band observed at 798 cm^{-1} could be attributed to an external symmetric stretch. The characteristic ZSM-5 band that occurred at 1070 cm^{-1} and (1062, 1102) on the FTIR spectra could be attributed to Si-O internal asymmetric stretch (Ali et al., 2003). The shoulder on the spectra observed at 1228 cm^{-1} could be assigned to the external asymmetric stretch (Tao et al., 2006). The FTIR spectra of H-FF2, H-FF3 and the commercial H-ZSM-5 had similar bands at 441, 524, 798, and at 1228 cm^{-1}. However, the band that describes the Si-O stretch in H-FF2, H-FF3 and the commercial H-ZSM-5 was similar for H-FF2 and the commercial H-ZSM-5 but different for H-FF3 as seen on the FTIR spectra. This was due to a shift at higher wavelengths as the Si/Al ratio increases (Shirazi et al.,2008). The MFI double ring vibration for the ZSM-5 samples was observed to appear at 524 cm^{-1} on the spectra. The absence of the C-H band on the spectra indicated that the samples were adequately detemplated to drive away TPBr (that was used as a template). Furthermore, characteristic bands that were present in the FTIR spectra of the starting material (fly ash) at 552, 800, and 919 cm^{1} representing mullite vibration, quartz stretch T-O (T=Al, Si), and Al-O (AlO_4) stretch respectively were completely absent in the FTIR spectra of the synthesised ZSM-5 products. This indicated that the fusion of fly ash with NaOH digested the fly ash mineral phases prior to obtain FFAE that was used to synthesise zeolite ZSM-5 products. The surface

area analysis of H-FF2, H-FF3, and the commercial H-ZSM-5 were presented in the following section.

4.3.5. Surface area analysis of the synthesised fly ash based products (H-FF2, H-FF3) and the commercial H-ZSM-5

Table 4.4 and Figure 4.13 show the BET surface area and N_2 adsorption/desorption isotherms of H-FF2, H-FF3 and the commercial H-ZSM-5 respectively that were obtained by N_2 adsorption/desorption measurements investigated at 77.1 K. The ZSM-5 samples were degassed for 2 hours and 4 hours at 90 ^oC and 400 ^oC respectively prior to BET analysis as detailed in section 3.5.5. H-FF2 and H-FF3 were synthesised and transformed to their acid form as detailed in section 3.3.1 and 3.3.3. Table 4.4 presents the BET surface area of H-FF2, H-FF2, and the commercial H-ZSM-5

Table 4. 4: BET surface area of H-FF2, H-FF3 compared to the commercial H-ZSM-5 (Com-ZSM)

Properties		H-FF2	H-FF3	Comm H-ZSM-5
Surface area (m^2/g)	Micropore	70.21	62.53	88.08
	Mesopore	205.22	138.37	308.78
	Macropore	104.25	149.35	84.36
BET surface area (m2/g		379.68	350.25	481.22

The BET results and its N_2 adsorption/desorption isotherms of the synthesised ZSM-5 samples and the commercial H-ZSM-5 are discussed below.

Figure 4.13 present the N_2 adsorption/desorption isotherm of H-ZSM-5 samples

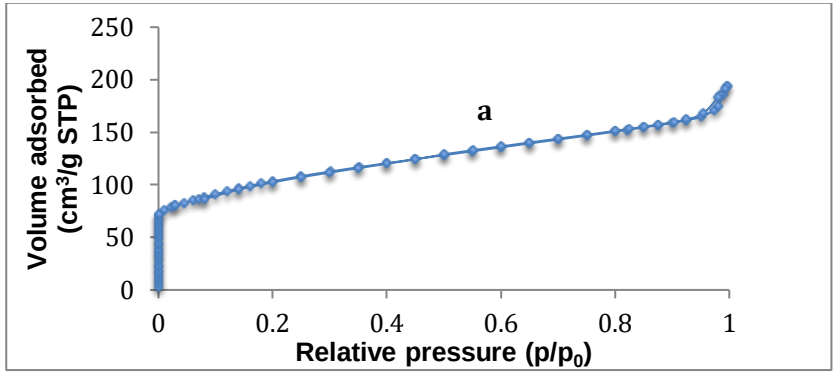

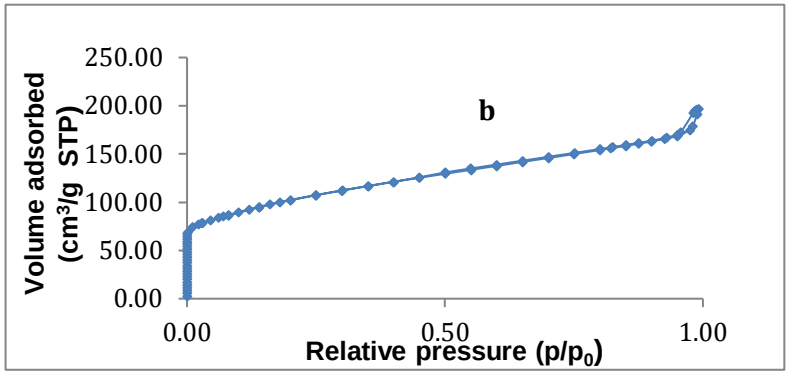

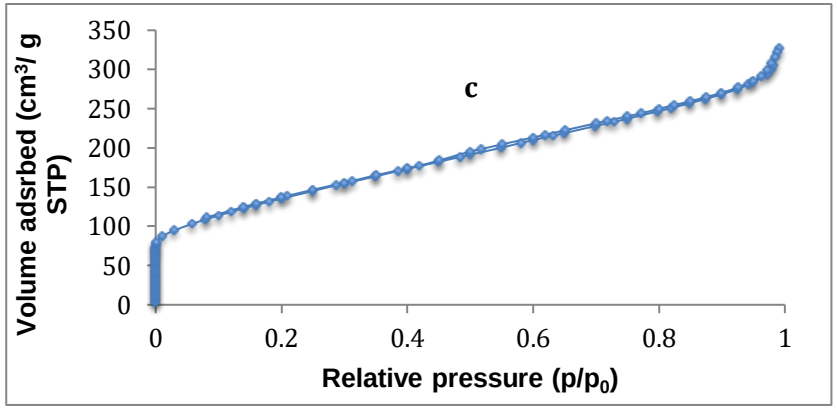

Figure 4. 13: N_2 adsorption/desorption isotherm of a) H-FF2, b) H-FF3 and (C) Commercial H-ZSM-5. All measured at 77.41 K

It was observed from Figure 4.13 that the adsorption/desorption isotherms of H-FF2, H-FF3, and the commercial H-ZSM-5 were that of type IV. The presence of mesopores in the ZSM-5 samples was described by the presence of a small hysteresis loop (Lowell et al., 2004). The surface area of H-FF2, H-FF3 and the commercial H-ZSM-5 were 379.68, 350.25, and 481.22 m^2/g respectively. These results proved that a pure phase zeolite ZSM-5 that have textural properties similar to the commercial ZSM-5 could be synthesised from fused fly ash extract with the addition of a small silica source. It could also be seen that as the Si/Al ratio of the synthesised ZSM-5 products increases from H-FF2=36 to H-FF3=41, the N_2 BET surface area decreases. However, the obtained BET results contradicted the BET results of Shirazi et al. (2008) who reported that the BET surface area of ZSM-5 products synthesised from $Al_2(SO_4)$, Na_2SiO_3 and TPBr increased with an increase in their Si/Al ratio (10, 25, 40 and 60) in the synthesis mixture. In this line of investigation, it would be difficult to compare the surface area findings of Shirazi et al. (2008) to that of the present study since their synthetic formulation and starting materials were different. Table 4.5 presents a summary of the physico-chemical properties of H-FF2, H-FF3, and the commercial H-ZSM-5.

Table 4. 5: Summary of the Physico-chemical properties of H-FF2, H-FF3, and Commercial H-ZSM-5

Properties		H-FF2	H-FF3	Comm H-ZSM-5
Surface area (m^2/g)	Micropore	70.21	62.53	88.08
	Mesopore	205.22	138.37	308.78
	Macropore	104.25	149.35	84.36
BET surface area (m^2/g)		379.68	350.25	481.22
Si/Al ratio		36	41	30
Relative crystallinity (%)		95	94	100
Framework aluminium (%)		96.5	94.5	97.0
Extra framework Al (%)		3.5	5.5	3.0
Crystal size (µm)	Length	(4.0 ±0.45)	(6.5 ± 0.67)	(1.48±0.34)
	Width	(2.5 ± 0.33)	(5.5 ± 0.52)	(1.13±0.26)

Table 4.5 shows that pure phase zeolite ZSM-5 products were synthesised from a South African fused fly ash extract (FFAE) when small amounts of fumed silica (0.000 or 0.250, or 0.375 g), was added to the hydrothermal gel of fused fly ash extract (FFAE). It could be seen that H-FF2 and H-FF3 had a significant level of macroporous area associated with their BET surface area unlike the commercial H-ZSM-5 that was highly mesoporous. The porous distribution in H-FF2 and H-FF3 may have a negative effect in converting methanol to hydrocarbons (MTH). This is because macroporous area lacks the effect of shape selectivity in zeolites. It is also important to note that the large crystal size of H-FF2 and H-FF3 might not favour their catalytic efficiency, as many of their micropores and mesopores may not be easily accessible. However, H-FF2 with smaller particle size and high BET surface area may have a better catalytic activity than H-FF3 with larger crystal size and low BET surface area. Overall, the commercial H-ZSM-5 with smaller crystal size and high BET surface area was predicted to have an excellent conversion capability together with high stability on stream. Furthermore, it is noteworthy that the Si/Al ratio of the samples was directly proportional to their mean crystal size and inversely proportional to their BET surface area. The next section introduces the Gas Chromatography results of the hydrocarbon compounds that were used to standardise the GC (Agilent 7890A) for product detection.

4.4. Gas Chromatography Standard analysis of hydrocarbons

From literature, it was revealed that the products that are commonly targeted from the methanol to hydrocarbon reaction over H-ZSM-5 catalyst are C2 (ethylene), C3 (propylene), and C4 (butane) hydrocarbons. With this in mind, the GC (Agilent 7890A) was calibrated with these hydrocarbon compounds so that their retention times and area under the peak can be accurately identified for product analysis. The method that was used in this process was detailed in section 3.3.6. Table 4.6 shows the temperature program for Agilent 7890A Gas Chromatograph.

Table 4. 6: Temperature program for Agilent 7890A during analysis of C2, C3, and C4 hydrocarbons

Agilent 7890A			
Rate (^{0}C/min)	Temp (^{0}C)	Hold time (min)	Run time (min)
	100	0	0
5	260	2	34

Figure 4.14 presents a typical chromatograph for the GC (Agilent 7890A) analysis of C2 and C3 hydrocarbons as well as their retention times (injected volume of components = 1 µm)

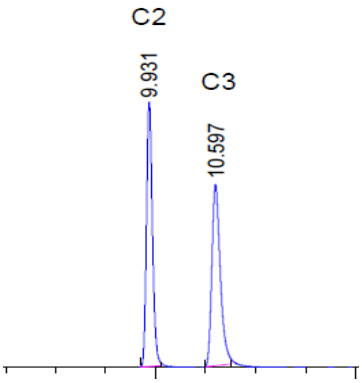

Figure 4. 14: GC chromatograph of C2 (ethylene) and C3 (propylene)

The retention times and area under the peak for C2 and C3 hydrocarbons after elution are presented in Table 4.7

Table 4. 7: Retention times and area under the peak for ethylene and propylene

Component	Symbol	Retention time	Area
Ethene	C2	9.931	116.339
Propene	C3	10.597	116.367

From Table 4.7, It was noticed that C2 eluted with a lesser retention time than C3 due to its lower boiling point. It is also noteworthy that during analysis of the methanol to hydrocarbon products, C2 is expected to elute earlier than C3 as indicated on Table 4.7. A typical GC chromatograph of a C4 hydrocarbon (injected volume = 1 µm) as well as its retention time and area under the peak was presented in Figure 4.15 and Table 4.8

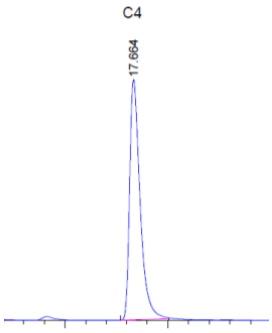

Figure 4. 15: Gas chromatograph of C4 (butane)

Retention time and area under the peak for C4 (butene) hydrocarbon is presented in Table 4.8

Table 4. 8: Retention time and area under the peak for butene (C4) compound

Component	Symbol	Retention time	Area
Butene	C4	12.664	119.45

As noticed, C4 had a higher retention time than C2 and C3 due to its higher boiling point. The area under the peak for C2, C3 and C4 were similar due to thesame concentration that was used to prepare their standards. It is also important to note that methanol and dimethyl ether that were considered as reactants in the probe reaction were already detected by the GC using the same temperature program.

4.5. Summary of Chapters 3 and 4

Crystalline fly ash based zeolite ZSM-5 products (H-FF2 and H-FF3) were synthesised when the Si/Al ratio of fused fly ash extract (FFAE) was adjusted above 10 by adding small amounts of fumed silica into the synthesis mixture. Partially crystalline H-FF1 was formed as a result of using FFAE without adjusting its Si/Al that was 9.5 to be above 10. This study has successfully utilised fly ash that was a waste material (from burning coal) in the synthesis of highly siliceous zeolite ZSM-5 products. The GC was also successfully standardised with C2 (ethylene), C3 (propylene) and C4 (butylene) so that hydrocarbon products coming from the conversion of methanol over the synthesised ZSM-5 catalysts can be detected and quantified.

The following chapter (5) presents the results obtained during the conversion of methanol to hydrocarbons over H-FF2, H-FF3, and the commercial H-ZSM-5

CHAPTER 5
APPLICATION OF ZEOLITE ZSM-5 SYNTHESISED FROM SOUTH AFRICAN FLY ASH IN THE CONVERSION OF METHANOL TO HYDROCARBONS

5.1. Introduction

The application of the synthesised fly ash based zeolite ZSM-5 catalyst in the conversion of methanol to other valuable hydrocarbons was demonstrated in this study and discussed in this chapter (Chapter 5). The performance of the synthesised H-FF1 and H-FF2 was compared with that of the commercial H-ZSM-5 in terms of conversion and selectivity towards C2, C3 and C2-C4 olefins. The motivation that led to the utilisation of the synthesised ZSM-5 products in the methanol to hydrocarbons (MTH) reaction was based on the fact that they were synthesised from the South African coal fly ash (that was a waste material) and their physico-chemical properties can be easily correlated to their performance on stream.

5.2. Methanol to Hydrocarbons (MTH) Conversion and selectivity

The conversion of methanol to other valuable hydrocarbons was conducted in a fixed bed quartz tube reactor. As a brief reminder, the fly ash based zeolite ZSM-5 products were synthesised as detailed in section 3.3.4. Thereafter crystallisation, the obtained crystals were allowed to cool, washed, dried, detemplated followed by ion exchange to their H-form using a 1M NH_4NO_3 solution as detailed in section 3.3.6 and calcination set at 550 ^oC for 5 hours. Subsequently H-FF2, H-FF3 and the commercial H-ZSM-5 were used as solid catalysts to run the methanol to hydrocarbons reaction. After each MTH reaction run, the conversion of methanol and the selectivity towards C2, C3, and C2-C4 products were calculated based on equation 3.2 to 3.9 respectively as highlighted in chapter 3.

5.2.1. Methanol to hydrocarbons (MTH) conversion and selectivity over H-FF2 and H-FF3 and the commercial H-ZSM-5 using different temperatures

During the synthesis of C2, C3 and C2-C4 hydrocarbons from methanol over H-FF2, H-FF3, and the commercial H-ZSM-5, two different temperatures at 350 ^oC and 400 ^oC were used to optimise the MTH reaction run of H-FF2. The temperature that had the best conversion efficiency and selectivity of methanol over H-FF2 was selected to run the MTH reaction of H-FF3 and the commercial H-ZSM-5.

Figure 5.1, 5.2, and 5.3 presents the performance of H-FF2 in the conversion of methanol to hydrocarbons at 350 ^oC and 400 ^oC respectively.

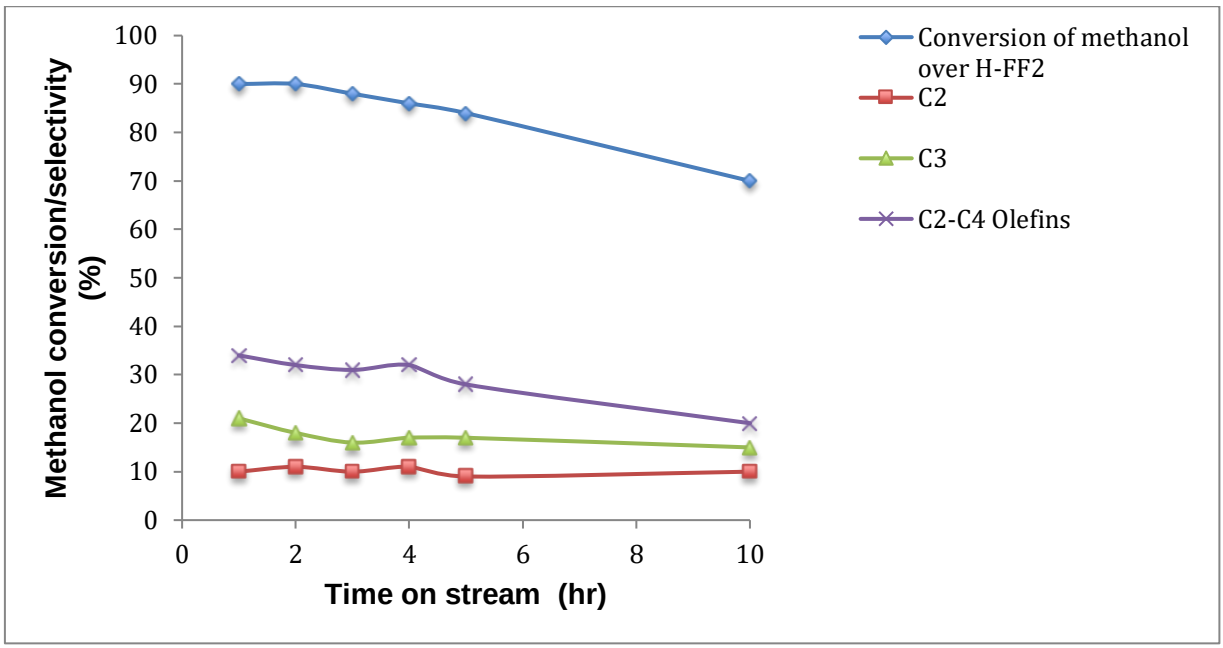

Figure 5. 1 : MTH Conversion and selectivity towards C2 (ethylene), C3 (propylene), and C2-C4 Olefins, over H-FF2 (temperature 350 °C, catalyst loading 0.5 g, WHSV = $2h^{-1}$ and atmospheric pressure)

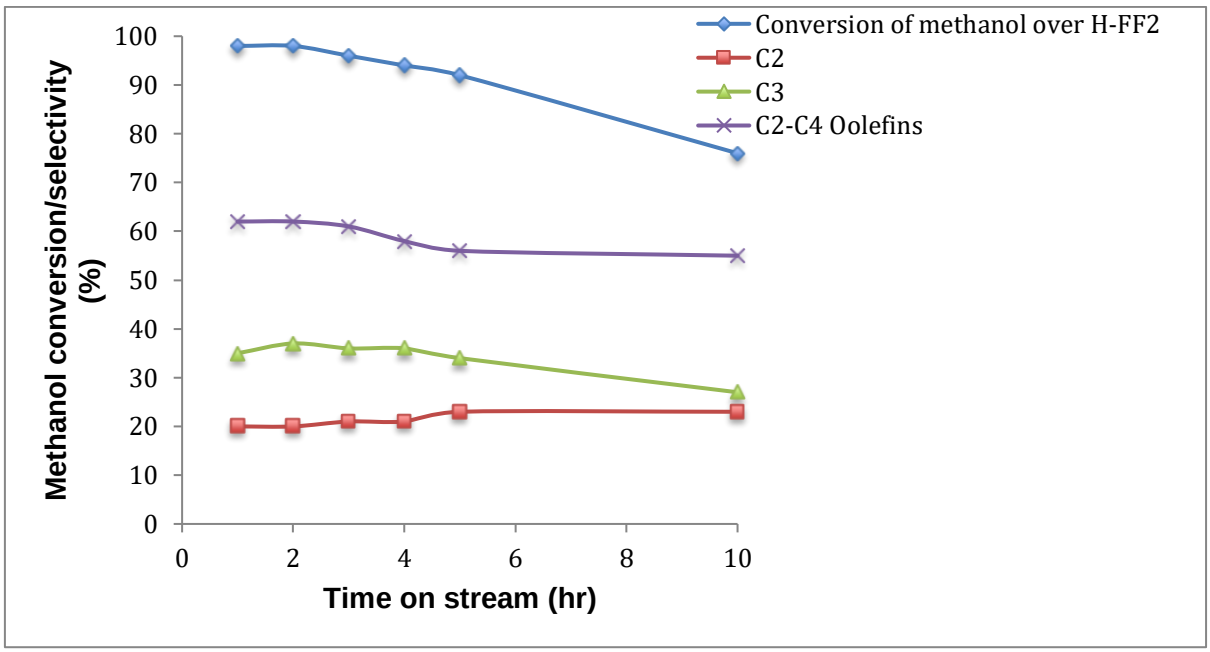

Figure 5. 2: Conversion of methanol and selectivity towards C2 (ethylene), C3 (propylene), and C2-C4 Olefins, over H-FF2 (temperature 400 ^{o}C, catalyst loading 0.5 g, WHSV = $2h^{-1}$ and atmospheric pressure)

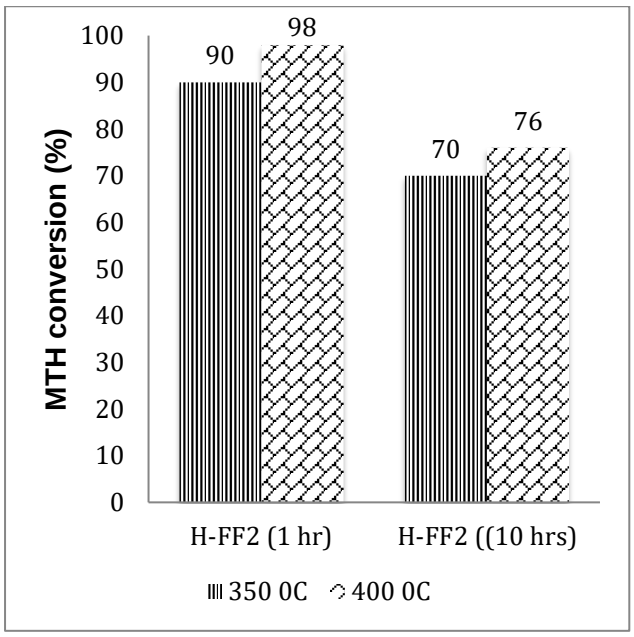

Figure 5. 3: Performance of H-FF2 in the conversion of methanol to hydrocarbons

Figure 5.1, 5.2 and 5.3 demonstrate the conversion and selectivity of H-FF2 at 350 ^{o}C and 400 ^{o}C. At a temperature of 400 ^{o}C, the initial conversion of methanol to hydrocarbons was 98 % after an hour of time on stream (TOS) that later decreased to 76 % after 10 hours of time on stream. At a temperature of 350 ^{o}C, the initial conversion of methanol to hydrocarbons was 90 % that later decreased to 70 % as the reaction proceed to 10 hours of time on stream (TOS). The high conversion of methanol at 400 ^{o}C could be attributed to the fact that the active sites of the catalyst acquired more energy to dehydrate more molecules of methanol and its formed intermediate (dimethyl ether) to form products than at a temperature of 350 ^{o}C. However, the rate of deactivation of the catalyst at both temperatures (350 ^{o}C and 400 ^{o}C) were similar even though H-FF2 (at 350 ^{o}C) had a lower conversion at the end of the MTH reaction. This was because the formation of oligomers at a lower temperature balances up the formation of coke at a higher temperature that therefore deactivates the catalyst at both temperatures in a similar profile. It could also be observed that the selectivity towards C3 and C2-C4 olefins at both temperatures was higher than that towards C2, however as the time on stream of the catalyst at both temperatures moved towards 10 hours of time on stream (TOS), the synthesis of C2 from methanol increased while that of C3 and C2-C4 decreased. This phenomenon can be justified based on the fact that as the time on stream (TOS) of the catalyst increased, the deposition of carbonaceous material (coke) at 400 ^{0}C and the formation of oligomers at 350 ^{o}C tend to increase and that slowly blocks the pores of the active sites thereby allowing the diffusional path of smaller light olefin (ethylene). It is noteworthy that the catalyst (H-FF2) that was used in the probe reaction was synthesised from the South African Arnot fused fly ash extract (FFAE) and its performance could be affected by some undesired insignificant framework cations coming from fly ash. Chen et al., (2015) reported that the impregnation of H-ZSM-5 (Si/Al = 38) with different loadings of magnesium interacted with strong acid sites

and generated new medium strong acid sites that enhanced the synthesis of propylene from methanol while Zhang et al also reported on the enhanced conversion of methanol to olefins after modifying ZSM-5 with calcium. In this line of investigation, the fused fly ash extract (FFAE) that was utilised in the synthesis of the ZSM-5 products initially contained some of these elements (Ca, Mg) as indicated in Figure 4.4. Eventhough these elements were not detected by the EDS analysis after three ion exchanged of the synthesised ZSM-5 products, they may still be present in the synthesised catalysts and may influence the MTH reaction.

Based on the fact that the temperature at 400 ^{o}C had a higher methanol conversion efficiency than at a temperature of 350 ^{o}C over H-FF2, the synthesised H-FF3 and the Commercial H-ZSM-5 was tested at 400 ^{o}C to study their performance. Figure 5.2 was repeated in 5.4 for a comparative purpose.

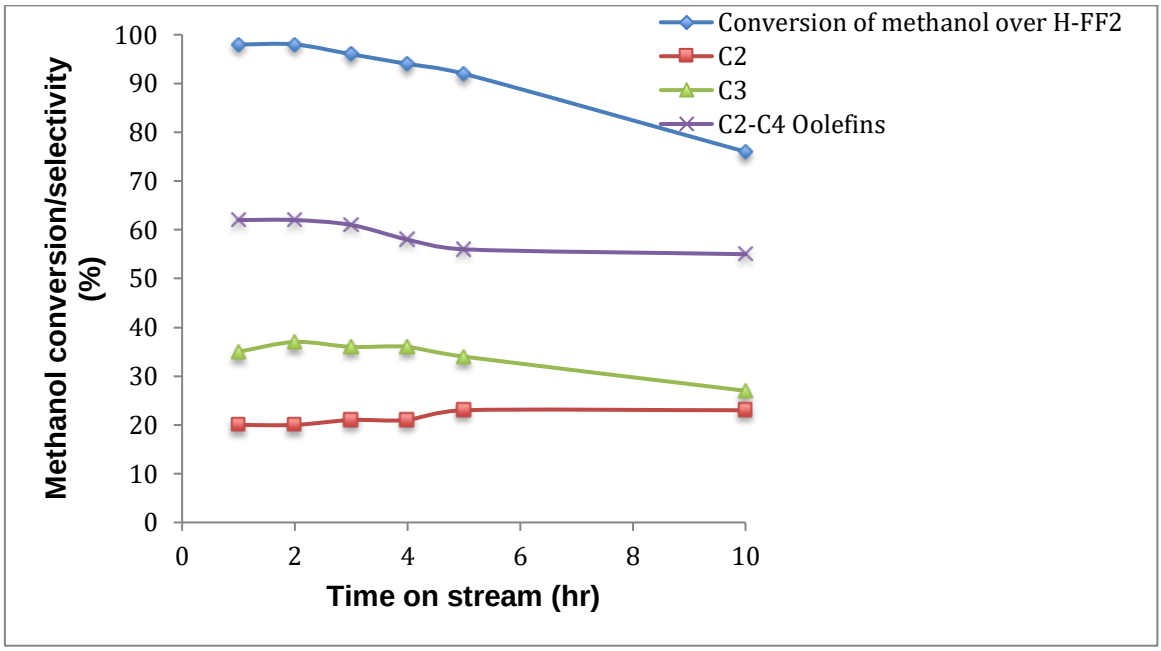

Figure 5. 4: Conversion of methanol and selectivity towards C2 (ethylene), C3 (propylene), and C2-C4 Olefins, over H-FF2, (temperature 400 ^{o}C, catalyst loading 0.5 g, WHSV = 2h^{-1} and atmospheric pressure)

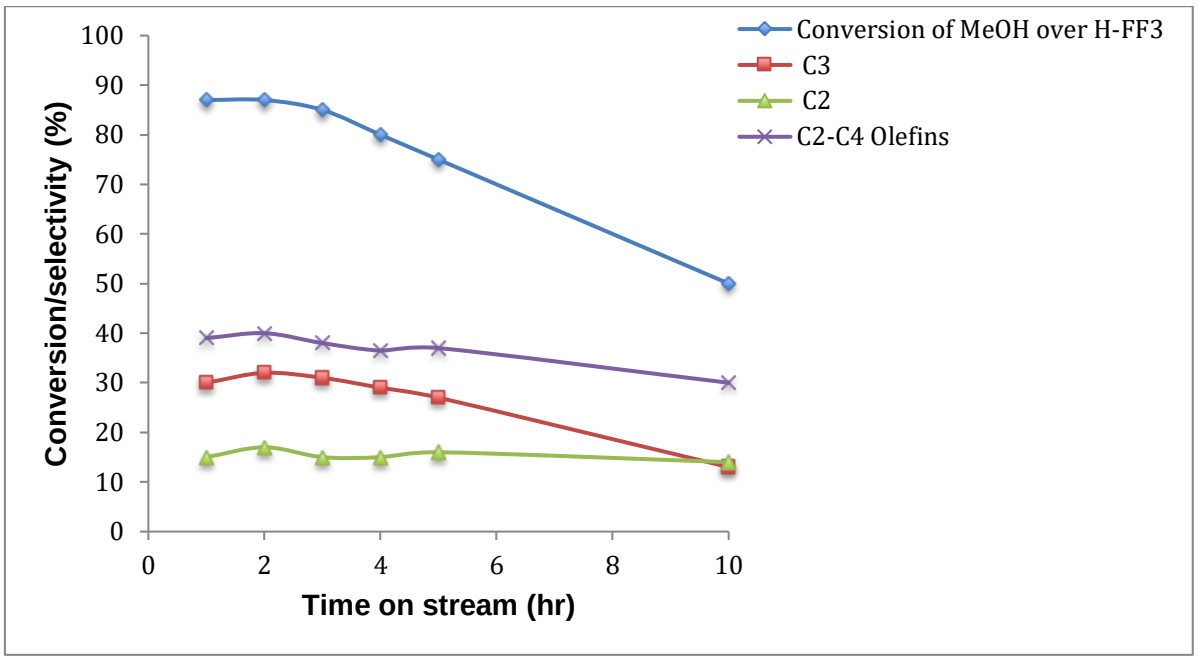

Figure 5. 5: Conversion of methanol and selectivity towards C2 (ethylene), C3 (propylene), and C2-C4 Olefins, over H-FF3, (temperature 400 ^{o}C, catalyst loading 0.5 g, WHSV = 2h^{-1} and atmospheric pressure)

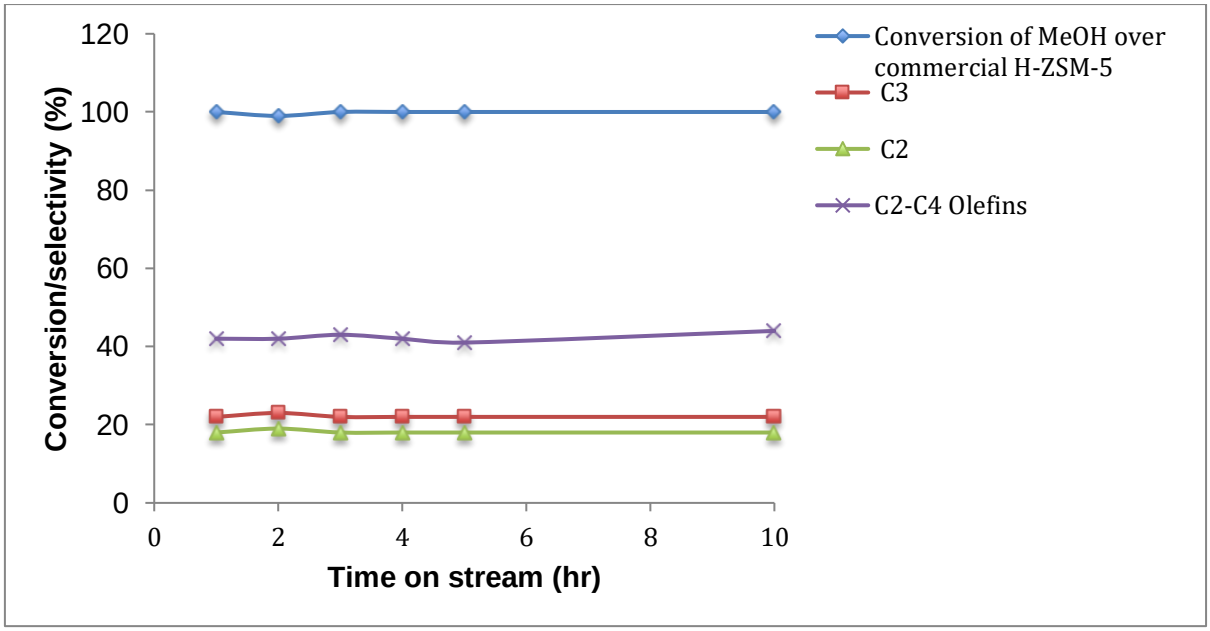

Figure 5. 6: Conversion of methanol and selectivity towards C2 (ethylene), C3 (propylene), and C2-C4 Olefins, over the commercial H-ZSM-5, (temperature 400 ^{o}C, catalyst loading 0.5 g, WHSV = 2h^{-1}and atmospheric pressure)

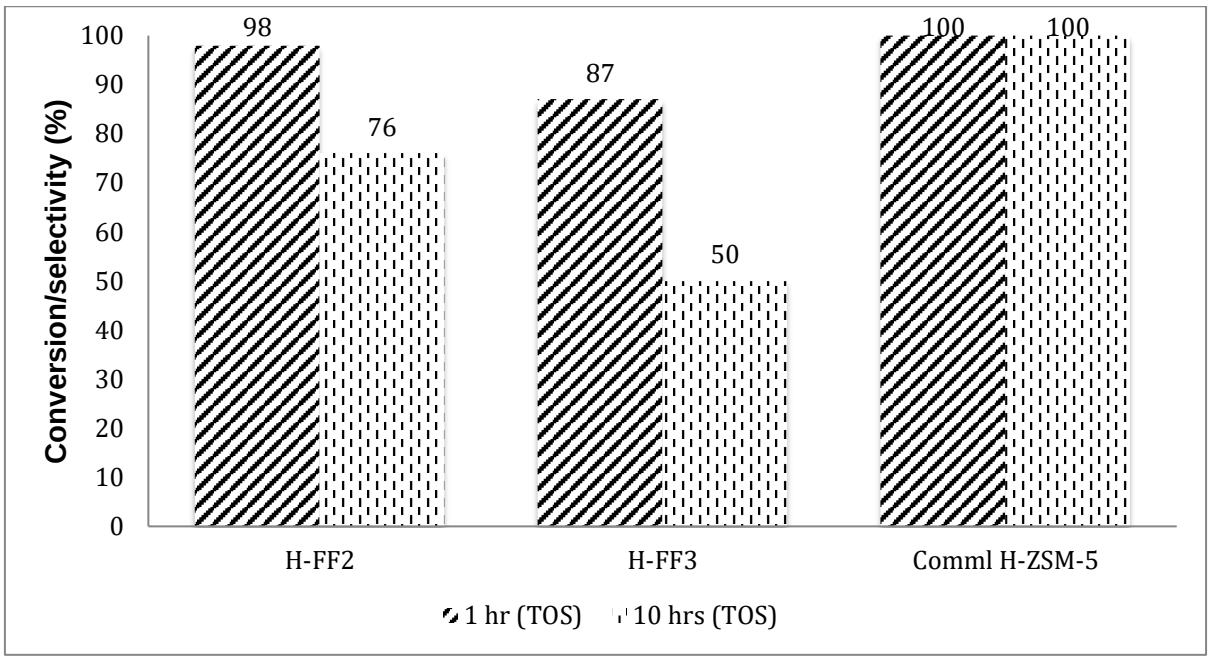

Figure 5. 7: Conversion efficiency of H-FF2, H-FF3, and the Commercial H-ZSM-5 at 400 ^{o}C from the initial and final time on stream (TOS)

Figure 5.4, 5.5, 5.6 and 5.7 showed the conversion and selectivity of methanol to ethylene, propylene, and C2-C4 olefins at 400 ^{o}C over H-FF2 (Si/Al=36), H-FF3 (Si/A =46) and the commercial H-ZSM-5 (Si/Al =30). Their MTH conversion was 98, 87, and 100% respectively after an hour of time on stream (TOS). Thereafter the methanol to hydrocarbons conversion efficiency of H-FF2 and H-FF3 decreased steadily to 76 and 50 % respectively after 10 hours of time on stream (TOS). It was noteworthy that H-FF2 and H-FF3 deactivated faster when compared with the commercial H-ZSM-5 that maintained a 100% conversion even after 10 hours of time on stream (TOS). However, with regard to the synthesised zeolite ZSM-5 catalysts, H-FF3 deactivated faster than H-FF2 as the reaction proceeds to 10 hours of time on stream (TOS).

In this study, there were some parameters that were directly related to the catalytic activity of the synthesised zeolite ZSM-5 (H-FF2 and H-FF3) and the commercial zeolite ZSM-5, which are the crystal size, and the BET surface area. As the crystal size decreased from H-FF3 (length=6.5 μm $\pm$ 0.67 by width=5.5 $\pm$ 0.52 μm)> H-FF2 (length=4.0 $\pm$0.45 by width=2.5 $\pm$ 0.33 μm)> commercial H-ZSM-5 (length=1.48 μm $\pm$ 0.34 by width=1.13 μm $\pm$ 0.26) (refer to Figure 4.9) the conversion efficiency was inversely proportional to the crystal size. However, the BET surface area of H-FF2, H-FF3, and the commercial H-ZSM-5 that was 379.68, 350.25, and 481.22 m^2/g respectively was directly proportional to the methanol to hydrocarbons (MTH) conversion efficiency. This can be attributed to the fact that, a decrease in the crystal size with an increased surface area enhances the accessibility of reactants to the active sites by shortening the diffusion path length, thus decreases the formation of coke, decreasing the deactivation rate, and increasing the conversion efficiency of the catalyst. In this same line of

investigation, Mohammadparast et al. (2015) and Wan et al. (2013) reported that an increased methanol conversion was observed when the ZSM-5 crystal size was reduced while Chen et al. (2012) reported that small crystal particles of ZSM-5 experience a long life catalytic activity (Petrik et al., 1995). Furthermore Liu et al. (2015) investigated and reported the role of the BET surface area during the conversion of methanol to hydrocarbons (MTH) reaction by loading different amount of MoO_3 onto zeolite ZSM-5. The author observed that the BET surface area decreased with increasing metal loading that subsequently decreased the conversion efficiency of methanol. The above stated facts on the effects of the crystal size and the BET surface area explained the reasons why H-FF3 deactivated faster than H-FF2 after 10 hours of time on stream (TOS) and why the commercial H-ZSM-5 sample still had a 100% conversion after 10 hours of time on stream (TOS). It is noteworthy that adjusting the Si/Al of the synthesis gel to synthesise H-FF3 (Si/Al = 41) was not necessary. This was because that led to an increase in crystal size, a decrease in the BET surface area, faster coke formation, faster deactivation rate (after 10 hours of time on stream), less conversion efficiency of methanol, and an increase in cost during synthesis. It was also noticed that the activity of H-FF2 in the MTH reaction initially competed with that of the commercial H-ZSM-5 (obtained from Zeolyst) that later lost its activity due to diffusional constraints by their pore structure and coke formation. It is also noteworthy that the commercially synthesised zeolites such as zeolite ZSM-5 that was utilised in this study are often formulations of active zeolite, binder and other additives hence making the comparison with the synthesised zeolites (H-FF2 and H-FF3) difficult and often inconclusive.

This study has successfully transformed a waste material (fly ash) into an active, high silica zeolite ZSM-5, however, the synthesis parameters should be further optimised and tailored in order to increase the microporous and mesoporous nature of the catalyst which had more significant effect than the Si/Al.

5.3. Chapter 5 summary

In summary, Chapter 5 confirmed that the synthesised H-FF2 and H-FF3 from fused fly ash extract (FFAE) could be utilised as a solid catalyst in the methanol to hydrocarbon (MTH) conversion. An increase in the Si/Al ratio by adjusting the elemental composition of H-FF2 and H-FF3, led to an increase in the crystal growth and the reduction of the BET surface area. This led to a faster deactivation of the larger crystal particles as compared to the smaller crystal particles of the commercial ZSM-5. The increase in the Si/Al ratio of H-FF3 (Si/Al = 41) did not improve its performance on stream when compared to H-FF2 and the commercial H-ZSM-5 (with Si/Al = 36 and Si/Al = 30 respectively). H-FF1 was not utilised in the MTH reaction because its XRD, calculated XRD relative crystallinity, and its SEM micrograph proved that the

sample was partially crystalline and had a low relative crystallinity hence making the catalysts inactive.

Chapter 6 of the present study will provide detailed information of the general findings found in chapter 4 and 5.

CHAPTER 6
GENERAL CONCLUSION AND RECOMMENDATIONS

6.1. Introduction

This chapter reappraises the aims and objectives of this study that were laid out in chapter one based on the gaps found in literature. It further highlights the findings reported in chapter 4 and 5 and outlines recommendations for future study.

6.2. General findings

The main aim of this research was to synthesise zeolite ZSM-5 from South African fused fly ash extract and compare its performance in the methanol to hydrocarbon (MTH) reaction with that of commercial ZSM-5. Zeolite. The synthesis of zeolite ZSM-5 directly from the as-received fly ash requires the addition of an excessive amount of silica to the synthesis mixture. However, the experimental approach that was utilised in this study for the synthesis of zeolite ZSM-5 products from the South African fly ash (FA), minimised the amount of silica added to the synthesis mixture. In this study, coal fly ash from the Arnot power station in the Mpumalanga province (South Africa) was used as a raw material (as-received fly ash) because of its initial source of Si and Al that can be used for zeolite synthesis. The as-received coal fly ash was analysed using various analytical techniques such as XRD, SEM, FTIR, and XRF. These analyses show that quartz, mullite and the amorphous phase was the major phases in the as received coal fly ash (CFA). The XRF technique revealed that the major oxides in the as-received coal fly ash was SiO_2 (57.35), and Al_2O_3 (28.98) that accounts for 86.33 % of the as-received coal fly ash composition with a SiO_2/ Al_2O_3 ratio of 1.97. Based on this fact, the as-received fly ash was classified as a class F fly ash (SiO_2 and Al_2O_3 was above 70 %). The SEM results revealed that the as-received coal fly ash was composed of spherical shaped particles. Conventionally the synthesis of zeolite ZSM-5 requires a Si/Al ratio that is greater than 10. However, the Si/Al ratio in the as-received fly ash used in this study was 1.97, which was not deemed enough for the synthesis of zeolite ZSM-5.

In this study, the method that was investigated to synthesise zeolite ZSM-5 from the as-received coal fly ash raised the Si/Al ratio above 10. This method involves the precipitation of silica in a fused fly ash filtrate using concentrated H_2SO_4 (98-99%) (Si/Al = 9.5) before raising the Si/Al ratio in the synthesis mixture using varied amount of fumed silica (0.000 g, 0.250 g, or 0.375 g). It was noticed that the Si/Al ratio in the hydrothermal gel was directly proportional to the amount of fumed silica added to the synthesis mixture. Finally, tetrapropylamonium bromide (TPBr) as a template was added to the synthesis mixture before hydrothermal crystallisation set at 165 ^{0}C for 72 hours. Thereafter crystallisation, the synthesised zeolite

ZSM-5 products (Na-FF1-TPBr, Na-FF2-TPBr, and Na-FF3-TPBr) were washed, dried, detemplated and transformed to their H-form using a 1 M solution of NH_4NO_3 followed by calcination.

The obtained H-form of the synthesised ZSM-5 products (H-FF1, H-FF2, H-FF3) were characterised using the following analytical techniques, which are: XRD, SEM/EDS, Image J NMR, FTIR, and BET. The XRD analytical technique proved that pure phase zeolite ZSM-5 products were synthesised from fly ash with a relative crystallinity of H-FF2 = 95 %, and H-FF3 = 94 % that was comparable to the commercial H-ZSM-5 = 100 %. However, H-FF1 had a relative crystallinity of 9 % indicating that the few crystals formed were covered in amorphous material. The XRD results also showed the absence of quartz and mullite phase in the samples. The SEM results showed that the effect of adding different amounts of fumed silica to the synthesis mixture tailored the morphology of the synthesised ZSM-5 products and increased the mean crystal size as the Si/Al ratio increases. It also showed that the amorphous material in the fused fly ash extract was completely transformed into hexagonal and cuboidal shaped crystals in H-FF2 and H-FF3 respectively. However, the crystals in H-FF1 sample were intimately intermixed in amorphous material hence difficult to analyse its morphology and mean crystal size. H-FF1 was proved by the XRD and SEM results to be an inactive solid catalyst and hence was not further analysed. The BET surface area of H-FF2 and H-FF3 were 385 and 350 respectively that was inversely proportional to their crystal size. The ^{27}Al NMR results showed that H-FF2, H-FF3 and the commercial H-ZSM-5 had octahedrally extra framework aluminium that did not take part during the MTH catalytic application.

The Methanol to hydrocarbon (MTH) reaction was the probe reaction that was utilised in this research to study the performance of zeolite ZSM-5 products that were synthesised from fused fly ash extract (FFAE). The effect of adding different amounts of fumed silica into the hydrothermal gel of FFAE on the performance of H-FF2 and H-FF3 was investigated by comparing the methanol to hydrocarbons (MTH) conversion and selectivity towards C2, C3, and C2-C4 olefins. The performance of H-FF3 in the MTH reaction was lower than that of H-FF2 because of its larger crystal size and high macroporous BET surface area that did not take part in the MTH reaction. Therefore, it was worthless to add 0.375 g of fumed silica to the synthesis gel of H-FF3, because that led to an increase in crystal growth (during hydrothermal synthesis) and faster deactivation rate during the MTH reaction. This finding further reduced the amount of fumed silica added to the synthesis mixture and established the addition of 0.250 g of fumed silica to the synthesis mixture was an optimum condition for synthesis. However, both catalysts (H-FF2 and H-FF3) deactivated from the 3rd hour of time on stream (TOS) to the 10th hour of TOS (with a steeper slope for H-FF3) while the commercial H-ZSM-5 was as stable as the first hour. This suggested that H-FF2 initially competed with the commercial H-ZSM-5 during the MTH reaction but lost activity due to diffusional constraints by their pore structure

and coke formation. It is noteworthy that it is very important to create a mesoporous network system in the zeolite particles that consist of secondary mesopores so that the effect of diffusional constraints of molecules do not impact upon the efficiency of the catalysts and therefore improve its catalytic activity.

It is important to note that the synthesis formulation used in this study successfully synthesised zeolite ZSM-5 products from the South African fly ash that can be used as solid catalysts, however some of the parameters used for synthesis needs to be optimised.

6.3. Recommendations for future studies

This research has shown that the Arnot fly ash from the Mpumalanga province can be successfully transformed to zeolite ZSM-5 using the proposed synthesis formulation. The study has also shown that the synthesised catalysts were active in the methanol to hydrocarbon (MTH) reaction, however most of the synthesis parameters and the parameters used to run the MTH reaction still needs to be optimised and as follows:

- Optimisation of the amount of concentrated H_2SO_4 used for treating the fused fly ash extract to raise the Si/Al ratio of the synthesis gel

- The synthesised H-FF2 had higher conversion efficiency than H-FF3 and initially competed with the commercial H-ZSM-5. This was because it was less subjected to diffusional constraints and had a smaller mean crystal size and higher mesoporous area compared to H-FF3. Therefore, creating much smaller crystal size, with sufficient microporous and mesoporous network could limit the effect of diffusional constraints and loss of catalytic activity. A synthetic formulation that would create highly microporous and mesoporous network could be applied by optimising the process parameters that were constant during the synthesis of zeolite ZSM-5 or the use of a porous directing agent could also be applied during synthesis.

- Further optimise the WHSV and temperature used to run the methanol to hydrocarbon reaction (MTH) reaction

REFERENCES

Adamczyk, B. & Bialecka, B. 2005. Hydrothermal Synthesis of Zeolites from Polish Coal Fly Ash. *Polish Journal of Environmental Studies,* 14.

Adriano, D., Page, A., Elseewi, A., Chang, A. & Straughan, I. 1980. Utilization and disposal of fly ash and other coal residues in terrestrial ecosystems: a review. *Journal of Environmental Quality,* 9**,** 333-344.

Ahmaruzzaman, M. 2010. A review on the utilization of fly ash. *Progress in Energy and Combustion Science,* 36**,** 327-363.

Akinyemi, S. A. 2011. *Geochemical and mineralogical evaluation of toxic contaminants mobility in weathered coal fly ash: as a case study, Tutuka dump site, South Africa.* University of the Western Cape.

Amber, I., Folayan, C., Suleiman, R. & Atta, A. Y. 2013. Application Of Synthesised Zeolite A From Kankara Kaolin For Solar Adsorption Refrigeration. *Journal of Mechanical Engineering and Technology (JMET),* 5.

Atta, A., Ajayi, O. & Adefila, S. 2007. Synthesis of faujasite zeolites from Kankara kaolin clay. *J Appl Sci Res,* 3**,** 1017-1021.

Attfield, M. P. 2002. Microporous materials. *Science Progress,* 85**,** 319-345.

Auerbach, S. M., Carrado, K. A. & Dutta, P. K. 2003. *Handbook of zeolite science and technology*, Marcel Dekker, Inc., New York.

Babajide, O., Musyoka, N., Petrik, L. & Ameer, F. 2012. Novel zeolite Na-X synthesized from fly ash as a heterogeneous catalyst in biodiesel production. *Catalysis Today,* 190**,** 54-60.

Barrer, R., Baynham, J., Bultitude, F. & Meier, W. 1959. 36. Hydrothermal chemistry of the silicates. Part VIII. Low-temperature crystal growth of aluminosilicates, and of some gallium and germanium analogues. *Journal of the Chemical Society (Resumed)***,** 195-208.

Bass, J. L. & Turner, G. L. 1997. Anion distributions in sodium silicate solutions. Characterization by 29Si NMR and infrared spectroscopies, and vapor phase osmometry. *The Journal of Physical Chemistry B,* 101**,** 10638-10644.

Barzetti, T., Selli, E., Moscotti, D. & Forni, L. 1996. Pyridine and ammonia as probes for FTIR analysis of solid acid catalysts. *Journal of the Chemical Society, Faraday Transactions,* 92**,** 1401-1407.

Bekkum, H. V., Jansen, J. & flanigen, E. 1991. Introduction to zeolite science and practice.

Belviso, C., Cavalcante, F. & Fiore, S. 2010. Synthesis of zeolite from Italian coal fly ash: differences in crystallization temperature using seawater instead of distilled water. *Waste Management,* 30**,** 839-847.

Belviso, C., Cavalcante, F., Lettino, A. & Fiore, S. 2009. Zeolite synthesised from fused coal fly ash at low temperature using seawater for crystallization. *Coal Combustion and Gasification Products,* 1**,** 8-1.

Bhanarkar, A., Gavane, A., Tajne, D., Tamhane, S. & Nema, P. 2008. Composition and size distribution of particules emissions from a coal-fired power plant in India. *Fuel,* 87**,** 2095-2101.

Bibby, D. & Dale, M. 1985. Synthesis of silica-sodalite from non-aqueous systems. *Nature,* 317**,** 157-158.

Bleken, F. L., Chavan, S., Olsbye, U., Boltz, M., Ocampo, F. & Louis, B. 2012. Conversion of methanol into light olefins over ZSM-5 zeolite: Strategy to enhance propene selectivity. *Applied Catalysis A: General,* 447**,** 178-185.

Boltz, M., Losch, P., Louis, B., Rioland, G., Tzanis, L. & Daou, T. J. 2014. MFI-type zeolite nanosheets for gas-phase aromatics chlorination: a strategy to overcome mass transfer limitations. *RSC Advances,* 4**,** 27242-27249.

Bonilla, G., Díaz, I., Tsapatsis, M., Jeong, H.-K., Lee, Y. & Vlachos, D. G. 2004. Zeolite (MFI) crystal morphology control using organic structure-directing agents. *Chemistry of Materials,* 16**,** 5697-5705.

Byrappa, K. & Yoshimura, M. 2001. Handbook OF Hydrothermal Technology A technology for Crystal Growth and Materials Processing,(2001). Noyes Publications/William Andrew Publishing, LLC, New York.

Cejka, J., van Bekkum, H., Corma, A., Schuth, F. (2007), Introduction to zeolite science and practice. 3rd Edition Elsevier, Oxford.

Chal, R., Gerardin, C., Bulut, M. & Van Donk, S. 2011. Overview and industrial assessment of synthesis strategies towards zeolites with mesopores. *ChemCatChem,* 3**,** 66-81.

Chareonpanich, M., Namto, T., Kongkachuichay, P. & Limtrakul, J. 2004. Synthesis of ZSM-5 zeolite from lignite fly ash and rice husk ash. *Fuel processing Technology,* 85**,** 1623-1634.

Chen, D., Moljord, K. & Holmen, A. 2012. A methanol to olefins review: Diffusion, coke formation and deactivation on SAPO type catalysts. *Microporous and Mesoporous Materials,* 164**,** 239-250.

Chester, A. W. & Derouane, E. G. 2009. *Zeolite characterization and catalysis*, Springer.

Chunfeng, W., Jiansheng, L., XIA, S., Lianjun, W. & Xiuyun, S. 2009. Evaluation of zeolites synthesized from fly ash as potential adsorbents for wastewater containing heavy metals. *Journal of Environmental Sciences,* 21**,** 127-136.

Colella, C. & Gualtieri, A. F. 2007. Cronstedt's zeolite. *Microporous and Mesoporous Materials,* 105**,** 213-221.

Crelling, J. C., Hagemann, H. W., Sauter, D. H., Ramani, R. V., Vogt, W., Leininger, D., KRZACK, S., Meyer, B., OrywaL, F. & Reimert, R. 1986. Coal. *Ullmann's encyclopedia of industrial chemistry*.

Criado, M., Fernández-jiménez, A., De La Torre, A., Aranda, M. & Palomo, A. 2007. An XRD study of the effect of the SiO 2/Na 2 O ratio on the alkali activation of fly ash. *Cement and Concrete Research,* 37**,** 671-679.

Csicsery, S. 1983. Shape-selective catalysis in zeolites. *Prepr. Pap.-Am. Chem. Soc., Div. Fuel Chem.;(United States),* 28.

Csicsery, S. M. 1986. Catalysis by shape selective zeolites-science and technology. *Pure and Applied Chemistry,* 58**,** 841-856.

Cubillas, P. & Anderson, M. W. 2010. Synthesis mechanism: crystal growth and nucleation. *Zeolites and Catalysis: Synthesis, Reactions and Applications***,** 1-55.

Cundy, C. S. & Cox, P. A. 2005. The hydrothermal synthesis of zeolites: Precursors, intermediates and reaction mechanism. *Microporous and Mesoporous Materials,* 82**,** 1-78.

Davini, P. 1996. Investigation of the SO2 adsorption properties of Ca (OH) 2-fly ash systems. *Fuel,* 75**,** 713-716.

Davis, M. E. 2002. Ordered porous materials for emerging applications. *Nature,* 417**,** 813-821.

Devadas, M. (2006), Selective catalytic reduction (SCR) of nitrogen oxides with ammonium over Fe-ZSM-5, PhD thesis, Swiss Federal Institute of Technology, Zurich.

Eary, L., Rai, D., Mattigod, S. & Ainsworth, C. 1990. Geochemical factors controlling the mobilization of inorganic constituents from fossil fuel combustion residues: II. Review of the minor elements. *Journal of Environmental Quality,* 19**,** 202-214.

Eisler, R. 2012. *The Fukushima 2011 Disaster*, CRC Press Taylor & Francis Group, London.

Fernández-Jiménez, A. & Palomo, A. 2005. Mid-infrared spectroscopic studies of alkali-activated fly ash structure. *Microporous and Mesoporous Materials,* 86**,** 207-214.

Flanigen, E. M., Broach, R. W. & WILSON, S. T. 2010. Introduction. *Zeolites in Industrial Separation and Catalysis***,** 1-26.

Foner, H., Robl, T., Hower, J. & Graham, U. 1999. Characterization of fly ash from Israel with reference to its possible utilization. *Fuel,* 78**,** 215-223.

Friedel, G. 1896. New experiments on zeolites. *Bull. Soc. Fr. Minéral. Cristallogr,* 19**,** 363-390.

Gilson, J.-P., Marie, O., Mintova, S. & Valtchev, V. 2011. Emerging Applications of Zeolites.*Zeolites and Ordered Porous Solids***,** 245.

Grandjean, F. 1910. Optical study of the absorption of the heavy vapors by certain zeolites. *CR Acad. Sci,* 149**,** 866-868.

Gupta, A. K., Singh, R. P., Ibrahim, M. H. & LEE, B.-K. 2012. Fly ash for agriculture: implications for soil properties, nutrients, heavy metals, plant growth and pest control. *Agroecology and Strategies for Climate Change.* Springer.

Gupta, G. & Torres, N. 1998. Use of fly ash in reducing toxicity of and heavy metals in wastewater effluent. *Journal of Hazardous Materials,* 57**,** 243-248.

Guth, J.-L. & Kessler, H. 1999. Synthesis of aluminosilicate zeolites and related silica-based materials. *Catalysis and Zeolites.* Springer.

Hay, R. L. & Sheppard, R. A. 2001. Occurrence of zeolites in sedimentary rocks: An overview. *Reviews in Mineralogy and Geochemistry,* 45**,** 217-234.

Herrmann, R., Schwieger, W., Scharf, O., Stenzel, C., Toufar, H., Schmachtl, M., Ziberi, B. & GRILL, W. 2005. In situ diagnostics of zeolite crystallization by ultrasonic monitoring. *Microporous and Mesoporous Materials,* 80**,** 1-9.

Holler, H. & Wirsching, U. 1985. Zeolite formation from fly-ash. *Fortschritte der mineralogie,* 63**,** 21-43.

Hudec, P. FCC catalyst–key element in refinery technology. 45th International Petroleum Conference, 2011.

Hunger, M. 1997. Br⊘nsted Acid Sites in Zeolites Characterized by Multinuclear Solid-State NMR Spectroscopy. *Catalysis Reviews,* 39**,** 345-393.

Inaba, M., Murata, K., Saito, M. & Takahara, I. 2006. Ethanol conversion to aromatic hydrocarbons over several zeolite catalysts. *Reaction Kinetics and Catalysis Letters,* 88**,** 135-141.

Inada, M., Tsujimoto, H., Eguchi, Y., Enomoto, N. & Hojo, J. 2005. Microwave-assisted zeolite synthesis from coal fly ash in hydrothermal process. *Fuel,* 84**,** 1482-1486.

Ismail, M., Eltayeb, M. & Maged, S. 2013. Elimination of heavy metals from aqueous solutions using Zeolite LTA synthesized from sudanese clay. *Res. J. Chem. Sci,* 3**,** 93-8.

Jacob, B. 1998. A comparative study of medium and large pore zeolites in Alkylation reactions.

Jennings, W., Mittlefehldt, E. & Stremple, P. 1997. *Analytical gas chromatography*, Academic Press.

Jha, B. & Singh, D. 2011. A review on synthesis, characterization and industrial applications of flyash zeolites. *Journal of Materials Education,* 33**,** 65.

Kalyankar, A., Choudhari, A. & Joshi, A. 2011. Low Frequency Dielectric properties of Fly ash based zeolite ZSM-5.

Kalyoncu, R. S. & Olson, D. W. 2001. *Coal combustion products*, US Department of the Interior, US Geological Survey.

Karge, H. G. & Robson, H. 2001. Verified syntheses of zeolitic materials. *Characterization by IR spectroscopy. Berlin, Germany: Fritz-Haber-Institut der Max-Planck-Gesellschaft*.

Katada, N., Igi, H., Kim, J.-H. & Niwa, M. 1997. Determination of the acidic properties of zeolite by theoretical analysis of temperature-programmed desorption of ammonia based on adsorption equilibrium. *The Journal of Physical Chemistry B,* 101**,** 5969-5977.

Kirov, G. & Filizova, L. 2012. Cationic hydration impact on zeolite formation and properties: A review and discussion. *Geochem. Miner. Petrol. Sofia,* 49**,** 65-82.

Kitaev, L., Kolesnikova, E., Biryukova, E., Kolesnichenko, N. & Khadzhiev, S. 2013. Formation of superacid centers in the structure of zeolite ZSM-5. *Russian Journal of Physical Chemistry A,* 87**,** 668-673.

Klamrassamee, T., Pavasant, P. & Laosiripojana, N. 2010. Synthesis of zeolite from coal fly ash: its application as water sorbent. *Engineering Journal,* 14.

Koukouzas, N., Hämäläinen, J., Papanikolaou, D., Tourunen, A. & Jäntti, T. 2007. Mineralogical and elemental composition of fly ash from pilot scale fluidised bed combustion of lignite, bituminous coal, wood chips and their blends. *Fuel,* 86**,** 2186-2193.

Krüger, J. 2003. South African fly ash: A cement extender. *A South Coal Fly Ash Association publication*.

Kutchko, B. G. & Kim, A. G. 2006. Fly ash characterization by SEM–EDS. *Fuel,* 85**,** 2537-2544.

Kuwahara, Y., Ohmichi, T., Kamegawa, T., Mori, K. & Yamashita, H. 2010. A novel conversion process for waste slag: synthesis of a hydrotalcite-like compound and zeolite from blast furnace slag and evaluation of adsorption capacities. *Journal of Materials Chemistry,* 20**,** 5052-5062.

Lercher, J. A. & Jentys, A. 2011. Basic concepts in zeolite acid-base catalysis. *Zeolites and ordered porous solids***,** 181.

Li, X., Wang, D., Zhou, Q., Liu, G. & Peng, Z. 2011. Concentration variation of aluminate ions during the seeded precipitation process of gibbsite from sodium aluminate solution. *Hydrometallurgy,* 106**,** 93-98.

Liu, B., France, L., Wu, C., Jiang, Z., Kuznetsov, V. L., Al-Megren, H. A., Al-kinanY, M., Aldrees, S. A., Xiao, T. & Edwards, P. P. 2015. Methanol-to-hydrocarbons conversion over MoO 3/H-ZSM-5 catalysts prepared via lower temperature calcination: a route to tailor the distribution and evolution of promoter Mo species, and their corresponding catalytic properties. *Chemical Science,* 6**,** 5152-5163.

Losch, P., Boltz, M., Bernardon, C., Louis, B., Palčić, A. & Valtchev, V. 2016. Impact of external surface passivation of nano-ZSM-5 zeolites in the methanol-to-olefins reaction. *Applied Catalysis A: General,* 509**,** 30-37.

Louis, B., Ocampo, F., Yun, H.-S., Tessonnier, J.-P. & Pereira, M. M. 2010. Hierarchical pore ZSM-5 zeolite structures: From micro-to macro-engineering of structured catalysts. *Chemical Engineering Journal,* 161**,** 397-402.

Lowell, S., Shields, J., Thomas, M. & Thommes, M. 2004. Characterization of Porous Solids and Powders: Surface Area, Pore Size and Density, 2004. *The Netherlands: Kluwer Academic Publishers*.

Lowell, S., Shields, J. E., Thomas, M. A. & Thommes, M. 2012. *Characterization of porous solids and powders: surface area, pore size and density*, Springer Science & Business Media.

Lu, R., Tangbo, H., Wang, Q. & Xiang, S. 2003. Properties and characterization of modified HZSM-5 zeolites. *Journal of Natural Gas Chemistry,* 12**,** 56-62.

Madzivire, G., Gitari, W. M., Vadapalli, V. K., Ojumu, T. V. & Petrik, L. F. 2011. Fate of sulphate removed during the treatment of circumneutral mine water and acid mine drainage with coal fly ash: Modelling and experimental approach. *Minerals Engineering,* 24**,** 1467-1477.

Madzivire, G., Petrik, L. F., Gitari, W. M., Ojumu, T. V. & Balfour, G. 2010. Application of coal fly ash to circumneutral mine waters for the removal of sulphates as gypsum and ettringite. *Minerals Engineering,* 23**,** 252-257.

Maier, S. M., Jentys, A. & Lercher, J. A. 2011. Steaming of zeolite BEA and its effect on acidity: A comparative NMR and IR spectroscopic study. *The Journal of Physical Chemistry C,* 115**,** 8005-8013.

Manz, O. E. 1999. Coal fly ash: a retrospective and future look. *Fuel,* 78**,** 133-136.

Marcilly, C. 1986. Les zéolithes: structures, synthèse et modifications. *Petrole et Techniques,* 328**,** 12-18.

Martínez, C. & Pérez-pariente, J. 2011. Zeolites and ordered porous solids. *3rd FEZA School on Zeolites: fundamentals and applications".* Editorial Universitat Politecnica de Valencia Valencia.

Meier, W. & Baerlocher, C. 1999. Zeolite type frameworks: connectivities, configurations and conformations. *Structures and Structure Determination.* Springer.

Millini, R. 2011. Zeolites in refining and petrochemistry", 5th International FEZA Conference, 3rd FEZA School on Zeolites, Valence, Spain, pp. 211-243

Google Patents. Milton, R.M. (1959), Molecular sieve adsorbents, US Patent 2,882,243

Missengue, R. N., Musyoka, N. M., Madzivire, G., Babajide, O., Fatoba, O. O., Tuffin, M. & Petrik, L. F. 2016. Leaching and antimicrobial properties of silver nanoparticles loaded onto natural zeolite clinoptilolite by ion exchange and wet impregnation. *Journal of Environmental Science and Health, Part A,* 51**,** 97-104.

MohammadparasT, F., Halladj, R. & Askari, S. 2015. The crystal size effect of nano-sized ZSM-5 in the catalytic performance of petrochemical processes: a review. *Chemical Engineering Communications,* 202**,** 542-556.

Moliner, M. 2012. Direct synthesis of functional zeolitic materials. *ISRN Materials Science,* 2012.

Moliner, M., González, J., Portilla, M. T., Willhammar, T., Rey, F., Llopis, F. J., Zou, X. & Corma, A. 2011. A new aluminosilicate molecular sieve with a system of pores between those of ZSM-5 and beta zeolite. *Journal of the American Chemical Society,* 133**,** 9497-9505.

Mollah, M., Promreuk, S., Schennach, R., Cocke, D. & Güler, R. 1999. Cristobalite formation from thermal treatment of Texas lignite fly ash. *Fuel,* 78**,** 1277-1282.

Murphy, T. E., Christensen, P. A., Behrns, R. J. & Jaquier, D. R. 1984. Fly ash analysis by complementary atomic absorption spectrometry and energy dispersive X-ray spectrometry. *Analytical Chemistry,* 56**,** 2534-2537.

Musyoka, N. M. 2009. *Hydrothermal synthesis and optimisation of zeolite Na-P1 from South African coal fly ash.*

Musyoka, N. M., Missengue, R., Kusisakana, M. & Petrik, L. F. 2014. Conversion of South African clays into high quality zeolites. *Applied Clay Science,* 97**,** 182-186.

Musyoka, N. M., Petrik, L. & Hums, E. Synthesis of zeolite A, X and P from a South African coal fly ash. Advanced Materials Research, 2012. Trans Tech Publ, 1757-1762.

Nagy, J., Bodart, P., Hannus, I. & Kiricsi, I. 1998. Characterization and Use of Zeolitic Microporous Materials. *Deagen, Szeged*.

Narayanan, S., Sultana, A., Krishna, K., Mériaudeau, P. & Naccache, C. 1995. Synthesis of ZSM-5 type zeolites with and without template and evaluation of physicochemical properties and aniline alkylation activity. *Catalysis Letters,* 34**,** 129-138.

Nicolaides, C. 1999. A novel family of solid acid catalysts: substantially amorphous or partially crystalline zeolitic materials. *Applied Catalysis A: General,* 185**,** 211-217.

Nyale, S. M., Babajide, O. O., Birch, G. D., Böke, N. & Petrik, L. F. 2013. Synthesis and characterization of coal fly ash-based foamed geopolymer. *Procedia Environmental Sciences,* 18**,** 722-730.

Öhrman, O. 2005. *Structured MFI film catalysts and adsorbents.* Luleå tekniska universitet.

Ojha, K., Pradhan, N. C. & Samanta, A. N. 2004. Zeolite from fly ash: synthesis and characterization. *Bulletin of Materials Science,* 27**,** 555-564.

Pecharsky, V. K. & ZavaliJ, P. Y. 2009. *Fundamentals of powder diffraction and structural characterization of materials*, Springer.

Petrik, L. 2009. The influence of cation, anion and water content on the rate of formation and pore size distribution of zeolite ZSM-5. *South African Journal of Science,* 105**,** 251-257.

Petrik, L., O'connor, C. & Schwarz, S. 1995. The influence of various synthesis parameters on the morphology and crystalsize of ZSM-5 and the relationship between morphology and crystal size and propene oligomerization activity. *Studies in Surface Science and Catalysis,* 94**,** 517-524.

Petrik, L. F., White, R. A., Klink, M. J., Somerset, V. S., Burgers, C. L. & Fey, M. V. Utilization of South African fly ash to treat acid coal mine drainage, and production of high quality zeolites from the residual solids. Proceedings of the Ash Utilization Symposium, Lexington, KY, USA, 2003.

Querol, X., Moreno, N., Umaña, J. T., Alastuey, A., Hernández, E., Lopez-Soler, A. & Plana, F. 2002. Synthesis of zeolites from coal fly ash: an overview. *International Journal of Coal Geology,* 50**,** 413-423.

Ramasamy, K. K. & Wang, Y. 2013. Catalyst activity comparison of alcohols over zeolites. *Journal of Energy Chemistry,* 22**,** 65-71.

Reanvattana, N. 2005. *Two-Stage Synthesis of High Purity Zsm-5 Zeolite from Coal Fly Ash and Rice Husk Ash*, Kasetsart University.

Rida, M. A. & Harb, F. 2014. Synthesis and characterization of amorphous silica nanoparitcles from aqueous silicates uisng cationic surfactants. *Journal of Metals, Materials and Minerals,* 24.

Saikia, B. J. & Parthasarathy, G. 2010. Fourier transform infrared spectroscopic characterization of kaolinite from Assam and Meghalaya, Northeastern India. *Journal of Modern Physics,* 1**,** 206.

Sani-Souna-SIDO, A., Chassaing, S., Pale, P. & Sommer, J. 2008. Behavior of arylvinylketones in zeolites: A systematic study. *Applied Catalysis A: General,* 336**,** 101-108.

Sazama, P., Wichterlova, B., Dedecek, J., Tvaruzkova, Z., Musilova, Z., Palumbo, L., Sklenak, S. & Gonsiorova, O. 2011. FTIR and 27 Al MAS NMR analysis of the effect of framework Al-and Si-defects in micro-and micro-mesoporous H-ZSM-5 on conversion of methanol to hydrocarbons. *Microporous and Mesoporous Materials,* 143**,** 87-96.

Scheetz, B. E. & Earle, R. 1998. Utilization of fly ash. *Current Opinion in Solid State and Materials Science,* 3**,** 510-520.

Shcherban, S., Pevzner, I. & Rayzman, V. 1995. Technologies of coal fly ash processing into metallurgical and silicate chemical products. American Chemical Society, Washington, DC (United States).

Shigemoto, N., Hayashi, H. & Miyaura, K. 1993. Selective formation of Na-X zeolite from coal fly ash by fusion with sodium hydroxide prior to hydrothermal reaction. *Journal of Materials Science,* 28**,** 4781-4786.

Shirazi, L., Jamshidi, E. & Ghasemi, M. 2008. The effect of Si/Al ratio of ZSM-5 zeolite on its morphology, acidity and crystal size. *Crystal Research and Technology,* 43**,** 1300-1306.

Skousen, J. G. & ZIEMKIEWICZ, P. F. 1995. *Acid mine drainage control and treatment*, West Virginia University Morgantown.

Somerset, V., Petrik, L. & Iwuoha, E. 2008. Alkaline hydrothermal conversion of fly ash precipitates into zeolites 3: the removal of mercury and lead ions from wastewater. *Journal of Environmental Management,* 87**,** 125-131.

Somerset, V., Petrik, L., White, R., Klink, M., Key, D. & Iwuoha, E. 2004. The use of X-ray fluorescence (XRF) analysis in predicting the alkaline hydrothermal conversion of fly ash precipitates into zeolites. *Talanta,* 64**,** 109-114.

Speight, J. G. 2015. *Handbook of coal analysis*, John Wiley & Sons.

Subotic, B. & Bronic, J. 2003. Theoretical and practical aspects of zeolite crystal growth. *Handbook of Zeolite Science and Technology,* 129.

Szostak, R. 1998. Molecular Sieves, Principles of Synthesis and Identification, Blackie Academic & Professional. *New York, NY*.

Takahashi, G. 2015. Sample preparation for X-ray fluorescence analysis. *Rigaku Journa,* 31**,** 26-30.

Tao, Y., Kanoh, H. & Kaneko, K. 2006. Developments and structures of mesopores in alkaline-treated ZSM-5 zeolites. *Adsorption,* 12**,** 309-316.

Triantafillidis, C. S., Evmiridis, N. P., Nalbandian, L. & Vasalos, I. A. 1999. Performance of ZSM-5 as a fluid catalytic cracking catalyst additive: effect of the total number of acid sites and particle size. *Industrial & Engineering Chemistry Research,* 38**,** 916-927.

Tsuchiai, H., Ishizuka, T., Ueno, T., Hattori, H. & Kita, H. 1995. Highly active absorbent for SO2 removal prepared from coal fly ash. *Industrial & Engineering Chemistry Research,* 34**,** 1404-1411.

Ural, S. 2005. Comparison of fly ash properties from Afsin–Elbistan coal basin, Turkey. *Journal of Hazardous Materials,* 119**,** 85-92.

Vadapalli, V. R., Gitari, W. M., Ellendt, A., Petrik, L. F. & Balfour, G. 2010. Synthesis of zeolite-P from coal fly ash derivative and its utilisation in mine-water remediation. *South African Journal of Science,* 106**,** 62-68.

Valtchev, V., Majano, G., Mintova, S. & Pérez-Ramírez, J. 2013. Tailored crystalline microporous materials by post-synthesis modification. *Chemical Society Reviews,* 42**,** 263-290.

Van Der Gaag, F. J. 1987. ZSM-5 type zeolites: Synthesis and use in gasphase reactions with ammonia.

Viraraghavan, T. Ash utilization in water-quality management. Abstracts of papers of the American Chemical Society, 1993. Amer chemical SOC 1155 16TH ST, NW, Washington, DC 20036, 61-Fuel.

Voll, D., Angerer, P., Beran, A. & Schneider, H. 2002. A new assignment of IR vibrational modes in mullite. *Vibrational Spectroscopy,* 30**,** 237-243.

Wan, Z., Wang, C., Yang, H. & Zhang, D. 2013. Effect of crystal size of ZSM-5 on its catalytic activity for methanol to gasoline conversion. *Chemeca 2013: Challenging Tomorrow***,** 885.

Wang, J., Groen, J. C., Yue, W., Zhou, W. & Coppens, M.-O. 2008. Facile synthesis of ZSM-5 composites with hierarchical porosity. *Journal of Materials Chemistry,* 18**,** 468-474.

Wang, S. & Wu, H. 2006. Environmental-benign utilisation of fly ash as low-cost adsorbents. *Journal of hazardous materials,* 136**,** 482-501.

Ward, C. R. & French, D. 2005. Relation between coal and fly ash mineralogy, based on quantitative X-ray diffraction methods. *World Coal Ash (WOCA), April***,** 11-15.

Weigel, O. & STeinhoff, E. 1925. Adsorption of organic liquid vapors by chabazite. *Z. Kristallogr,* 61**,** 125-154.

Weitkamp, J., Ernst, S. & Puppe, L. 1999. Shape-selective catalysis in zeolites. *Catalysis and Zeolites.* Springer.

Williams, D. B., Carter, C. B. & Veyssiere, P. 1998. *Transmission electron microscopy: a textbook for materials science*, Springer.

Wilson, S. T., LOK, B. M., Messina, C. A., Cannan, T. R. & Flanigen, E. M. 1982. Aluminophosphate molecular sieves: a new class of microporous crystalline inorganic solids. *Journal of the American Chemical Society,* 104**,** 1146-1147.

Wright, P. A. & Lozinska, M. 2011. Structural Chemistry and Properties of zeolites. *Zeolites and ordered porous solids***,** 1.

Yilmaz, b. & müller, u. 2009. catalytic applications of zeolites in chemical industry. *topics in catalysis,* 52**,** 888-895.

Yao, Z., Xia, M., Sarker, P. & Chen, T. 2014. A review of the alumina recovery from coal fly ash, with a focus in China. *Fuel,* 120**,** 74-85.

Yilmaz, B. & Müller, U. 2009. Catalytic applications of zeolites in chemical industry. *Topics in Catalysis,* 52**,** 888-895.

Zhang, W., Xin, H., Yu, Y. & He, H. 2014. Oxalic Acid Treating of ZSM-5 Zeolite for the Enhanced Photocatalytic Activity of TiO2/HZSM-5. *Journal of Advanced Oxidation Technologies,* 17**,** 359-364.

Zhao, X., Lu, G. & Zhu, H. 1997. Effects of ageing and seeding on the formation of zeolite Y from coal fly ash. *Journal of Porous Materials,* 4**,** 245-251.

Zheng, K., Gerson, A. R., Addai-Mensah, J. & Smart, R. S. C. 1997. The influence of sodium carbonate on sodium aluminosilicate crystallisation and solubility in sodium aluminate solutions. *Journal of Crystal Growth,* 171**,** 197-208.

October 2007